National Library of Canada

Cataloguing Branch
Canadian Theses Division

Ottawa, Canada
K1A 0N4

Bibliothèque nationale du Canada

Direction du catalogage
Division des thèses canadiennes

NOTICE

The quality of this microfiche is heavily dependent upon the quality of the original thesis submitted for microfilming. Every effort has been made to ensure the highest quality of reproduction possible.

If pages are missing, contact the university which granted the degree.

Some pages may have indistinct print especially if the original pages were typed with a poor typewriter ribbon or if the university sent us a poor photocopy.

Previously copyrighted materials (journal articles, published tests, etc.) are not filmed.

Reproduction in full or in part of this film is governed by the Canadian Copyright Act, R.S.C. 1970, c. C-30. Please read the authorization forms which accompany this thesis.

THIS DISSERTATION
HAS BEEN MICROFILMED
EXACTLY AS RECEIVED

AVIS

La qualité de cette microfiche dépend grandement de la qualité de la thèse soumise au microfilmage. Nous avons tout fait pour assurer une qualité supérieure de reproduction.

S'il manque des pages, veuillez communiquer avec l'université qui a conféré le grade.

La qualité d'impression de certaines pages peut laisser à désirer, surtout si les pages originales ont été dactylographiées à l'aide d'un ruban usé ou si l'université nous a fait parvenir une photocopie de mauvaise qualité.

Les documents qui font déjà l'objet d'un droit d'auteur (articles de revue, examens publiés, etc.) ne sont pas microfilmés.

La reproduction, même partielle, de ce microfilm est soumise à la Loi canadienne sur le droit d'auteur, SRC 1970, c. C-30. Veuillez prendre connaissance des formules d'autorisation qui accompagnent cette thèse.

LA THÈSE A ÉTÉ
MICROFILMÉE TELLE QUE
NOUS L'AVONS REÇUE

DYNAMIC ANALYSIS OF TAPERED STIFFNESS STRUCTURES

Mahmoud Osama Ahmed Mahmoud

A Dissertation
in the
Faculty of Engineering

© Mahmoud Osama Ahmed Mahmoud 1977

Presented in Partial Fulfillment of the Requirements
for the Degree of Master of Engineering
at
Concordia University
Montreal, Quebec, Canada

September, 1977

ABSTRACT

DYNAMIC ANALYSIS OF TAPERED STIFFNESS STRUCTURES

Mahmoud Osama Ahmed Mahmoud

The seismic analysis of tall structures requires the natural frequencies and mode shapes to be known. This work presents the dynamic analysis of a class of tall structures which are modelled as uniform mass and tapered stiffness beams, in flexure or in shear. The effect of stiffness taper on modal frequencies, mode shapes, and beam stresses is investigated.

The seismic behaviour of this class of structure is studied using the response spectrum technique. A comparison between tapered flexural and tapered shear beams for the behaviour in terms of both base shear and overturning moment is made. The effect of stiffness taper on the base moment reduction factor is also investigated.

ACKNOWLEDGEMENTS

My most warm and lively thanks to all those who have helped me in different ways.

Of the persons to whom I am deeply indebted I would like to mention particularly my supervisor, Dr. O.A. Pekau, for initiating the point of investigation, providing all sorts of assistance and his continuous encouragement and guidance.

Thanks are likewise extended to Mr. R. Blackwell for his assistance in writing some of the computer programs required for this investigation. Thanks are dedicated to my father and my late mother for giving the inspiration, and to my wife for her patience and encouragement.

Thanks are due to Ann Harding, Department of Civil Engineering for typing the text.

TABLE OF CONTENTS

		Page
Abstract		i
Acknowledgements		ii
List of Figures		v
List of Tables		viii
Nomenclature		ix
CHAPTER I	INTRODUCTION	1
1.1	The Problem	1
1.2	Literature Review	1
1.3	Scope of Present Study	3
CHAPTER II	REVIEW OF AVAILABLE METHODS OF ANALYSIS	6
2.1	Introduction	6
2.2	Rayleigh-Ritz Method	6
2.3	Myklestad-Prohl Method	8
2.4	Stodola Method	9
2.5	Modified Rayleigh-Ritz Method	10
CHAPTER III	EIGEN ANALYSIS OF TAPERED STIFFNESS STRUCTURES	15
3.1	Flexural Beams	15
3.2	Shear Beams	25
3.3	Convergence of the Solution	27
3.3.1	Convergence Criteria	27
3.3.2	Convergence of Modal Response parameters	28

		Page
CHAPTER IV	DERIVATION OF SEISMIC RESPONSE PARAMETERS	31
4.1	Base Shear and Overturning Moment	31
4.2	Moment Reduction Factor	38
CHAPTER V	RESULTS AND DISCUSSION	40
5.1	Effect of Taper on Modal Frequencies	40
5.2	Effect of Taper on Mode Shapes	41
5.3	Effect of Taper on Distribution of Modal Strains	41
5.4	Effect of Taper on Base Shear	42
5.5	Effect of Taper on Overturning Moment	44
5.6	Base Shear and Overturning Moment for Tapered Hybrid Beam	45
5.7	Effect of Taper on Moment Reduction Factor	45
CHAPTER VI	CONCLUSIONS	47
FIGURES AND TABLE		49
REFERENCES		80
APPENDIX I	VIBRATIONS OF UNIFORM SLENDER CANTILEVER BEAMS	81
APPENDIX II	GOVERNING EQUATIONS FOR TAPERED STIFFNESS BEAMS	83
APPENDIX III	ORTHOGONALITY CONDITIONS FOR NON-UNIFORM BEAMS	86
APPENDIX IV	DERIVATION OF MODAL BASE SHEAR AND MODAL BASE OVERTURNING MOMENT EXPRESSIONS	88
APPENDIX V	EVALUATION OF INTEGRALS	90
APPENDIX VI	RESULTS OF TESTS FOR CONVERGENCE	100

LIST OF FIGURES

Figure		Page
1	DISTRIBUTED MASS AND STIFFNESS	49
2	PROPERTIES OF VARIABLE STIFFNESS CANTILEVER BEAM	50
3	STATIC SEISMIC LOADING [REF. 4]	51
4	FLEXURAL STIFFNESS TAPER AND MODAL FREQUENCIES	52
5	SHEAR STIFFNESS TAPER AND MODAL FREQUENCIES	54
6	FLEXURAL STIFFNESS TAPER AND MODE SHAPES	56
7	SHEAR STIFFNESS TAPER AND MODE SHAPES	57
8	FLEXURAL STIFFNESS TAPER AND FIRST DERIVATIVE OF MODE SHAPES	58
9	FLEXURAL STIFFNESS TAPER AND SECOND DERIVATIVE OF MODE SHAPES	59
10	SHEAR STIFFNESS TAPER AND FIRST DERIVATIVE OF MODE SHAPES	60
11	FLEXURAL STIFFNESS TAPER AND BEAM SHEAR	61
12	SHEAR STIFFNESS TAPER AND BEAM SHEAR	62
13	FLEXURAL STIFFNESS TAPER AND MODAL SHEAR COEFFICIENTS	63
14	FLEXURAL STIFFNESS TAPER AND TOTAL BASE SHEAR (SRSS)	65
15	SHEAR STIFFNESS TAPER AND MODAL SHEAR COEFFICIENTS	66
16	SHEAR STIFFNESS TAPER AND TOTAL BASE SHEAR (SRSS)	68
17	EFFECT OF TAPER ON TOTAL BASE SHEAR	69
18	FLEXURAL STIFFNESS TAPER AND MODAL OVERTURNING MOMENT COEFFICIENTS	70

Figure		Page
19	FLEXURAL STIFFNESS TAPER AND TOTAL OVERTURNING MOMENT (SRSS)	72
20	SHEAR STIFFNESS TAPER AND MODAL OVERTURNING MOMENT COEFFICIENTS	73
21	SHEAR STIFFNESS TAPER AND TOTAL BASE OVERTURNING MOMENT (SRSS)	75
22	FLEXURAL STIFFNESS TAPER AND MOMENT REDUCTION FACTOR	76
23	SHEAR STIFFNESS TAPER AND MOMENT REDUCTION FACTOR	77
24	MOMENT REDUCTION FACTOR FOR TAPERED HYBRID BEAMS	78
V1-1	RATE OF CONVERGENCE OF FUNDAMENTAL MODE FREQUENCY	101
V1-2	RATE OF CONVERGENCE OF SECOND MODAL FREQUENCY	102
V1-3	RATE OF CONVERGENCE OF THIRD MODAL FREQUENCY	103
V1-4	RATE OF CONVERGENCE OF FOURTH MODAL FREQUENCY	104
V1-5	RATE OF CONVERGENCE OF FUNDAMENTAL MODE SHAPE	105
V1-6	RATE OF CONVERGENCE OF SECOND MODE SHAPE	106
V1-7	RATE OF CONVERGENCE OF THIRD MODE SHAPE	107
V1-8	RATE OF CONVERGENCE OF FOURTH MODE SHAPE	108
V1-9	RATE OF CONVERGENCE OF FIRST MODAL BASE SHEAR	109
V1-10	RATE OF CONVERGENCE OF FIRST MODAL OVERTURNING MOMENT	110
V1-11	RATE OF CONVERGENCE OF SECOND MODAL BASE SHEAR	111
V1-12	RATE OF CONVERGENCE OF SECOND MODAL OVERTURNING MOMENT	112
V1-13	RATE OF CONVERGENCE OF THIRD MODAL BASE SHEAR	113

Figure		Page
V1-14	RATE OF CONVERGENCE OF THIRD MODAL OVERTURNING MOMENT	114
V1-15	RATE OF CONVERGENCE OF FOURTH MODAL BASE SHEAR	115
V1-16	RATE OF CONVERGENCE OF FOURTH MODAL OVERTURNING MOMENT	116

LIST OF TABLES

Page

Table 1 Summary of Modal Shear Coefficients 79

NOMENCLATURE

Symbols are defined when they first appear in this text, those which appear frequently are listed below for reference.

A,B,C,D	numerical coefficients;
E	Young's modulus;
$C_V^{(r)}$	rth modal base shear coefficient;
$C_M^{(r)}$	rth modal base overturning moment coefficient;
g	acceleration of gravity;
H	height of cantilever structure;
i,j	subscripts designating displacement functions;
I(x)	moment of inertia of the area of a horizontal cross section of the structure about its central axis;
I_o	moment of inertia at the base of beam;
J	moment reduction factor;
k(x)	stiffness in shear;
k_o	shear stiffness at the base of beam;
L	length of beam;
m	mass per unit length;
M	overturning moment;
M_o	overturning moment due to code static loading;
n	total number of displacement functions;
S_v	velocity response spectrum;

S_a	acceleration response spectrum;
r,s	subscripts designating modes of non-uniform structures;
t	time, in seconds;
V	base shear;
V_o	base shear due to code static loading;
x	height variable;
y	coordinate perpendicular to the axial direction;
$\phi(x)$	displacement function;
$\overline{\phi}(x)$	mode shape of non-uniform structure;
ω_r	angular frequency of the rth mode, in radians per second;
β_r	eigenvalue of the rth mode;
Γ_r	modal participation factor of the rth mode; and
τ_k	stiffness taper in flexural or shear beams

CHAPTER I

INTRODUCTION

1.1 The Problem

A tall structure (tower or highrise building), which has equal floor weights and where the stiffness decreases towards the top of the structure, can be idealized as a cantilever beam with uniform distribution of mass and linear taper in stiffness. The seismic response of such a structure depends on its dynamic properties. Once the dynamic properties are known, the seismic response of the structure can be evaluated for given earthquake excitation.

The lateral deformation of the cantilever can be classified into three main types; namely, flexure, shear and combined flexure and shear. The actual structural system determines to which class the particular structure belongs. In this study, the combined or hybrid type is represented by an idealized cantilever with seismic characteristics equal to the average of those for shear deflecting and moment deflecting cantilevers.

1.2 Literature Review

The problem of linearly tapered structures acting in flexure was studied by Housner and Keightley [1]*

---

* Numbers in square brackets refer to references listed at the end of this text.

who determined the natural frequency and mode shapes of the first three modes of vibration of tapered cantilever beams for twelve different tapers. They considered both rectangular and conical shell beams. Tables and graphs to determine mode shapes and frequencies for different values of taper were produced.

Salvadori and Heer [2] calculated the periods of shear, bending, rocking and translation of a cantilever beam with linearly varying shear and flexural rigidities and with or without concentrated mass at the top. A formula for the approximate evaluation of periods of framed structures was suggested. Relations and tables were given for the periods of the cantilever for different types of behaviour for modes one to five.

Humar and Wright [3] studied the distribution of seismic forces and overturning moments throughout the height of building structures by using a simplified uniform hybrid cantilever beam. They examined the effect of building slenderness on the distribution of both the horizontal shear and the seismic overturning moment. Results in the form of tables and curves for the shear coefficients, moment response for shear deflecting structures, and moment reduction factor for uniform cantilevers were presented.

Heidebrecht [4] presented a procedure for evaluation of the dynamic shear and moment relationship and the overturning moment reduction factor for a class of uniform shear wall-

frame buildings subjected to earthquake excitation. He used spectrum analysis to determine the maximum values of specific response parameters. The results of this analysis, together with code specified static base shear and overturning moment were employed to determine moment reduction factor. Results were given for the fundamental mode shapes for shear-wall frame structures, and for the moment reduction or the spectra recommended in the 1975 National Building Code of Canada [9], and a constant spectrum. Reduction factors for the first five modes were obtained.

Finally, Pekau [5] studied beams of uniform mass and variable stiffness in shear. The solution, presented in that study, is a closed form solution expressed in terms of Bessel functions. In this study, the effect of stiffness taper on beam mode shapes, beam frequencies, beam modal masses, modal base shear coefficients and total base shear coefficients was investigated. Results were represented in the graphical form to indicate the importance of stiffness taper.

The work proposed in the following section attempts to provide similar data for flexural instead of shear type systems.

1.3 Scope of Present Study

As mentioned in Sec. 1.1, tall structures which have uniform mass distribution and stiffness decreasing from bottom to top can be idealized as cantilever beams with uniform mass and linearly tapered stiffness. Since dynamic analysis of

this class of structures to resist ground shocks or wind induced vibrations requires the knowledge of dynamic properties, such as modal frequencies for example, the problem of cantilever beams with constant mass and linearly variable stiffness in flexure will be investigated.

A continuous cantilever model has been adopted for this study similar to the one proposed by Pekau (5). Using this model will allow for comparison of results for flexural and shear systems. The choice of this continuous model is feasible for the problem under consideration because it lends itself to description in terms of simple parameter, whereas a discrete or lumped parameter model would require a more complex set of parameters for its definition.

The structural model considered in this study is a cantilever structure with uniform mass distribution m, length L, and flexural stiffness EI_o at the base. The flexural stiffness varies linearly along the beam length and the flexural stiffness taper τ_k defines the ration of base to top stiffness.

The method which will be used in the analysis for dynamic properties can be classified as modified Rayleigh-Ritz method. Generalized mass and stiffness of the tapered stiffness beam are first evaluated for a set of assumed displacement shapes, then the eigenvalue problem is formulated. The non-trivial solution of the eigenvalue problem gives the eigenvalues and eigenvectors which represent the natural frequencies and the mode shape coefficients of the tapered beam. The mode shape of

the tapered beam is obtained from the superposition of the modal displacement functions of the corresponding uniform beam multiplied by appropriate coefficients or generalized eigenvectors.

The effect of the flexural stiffness taper on the base shear and the overturning moment of the beam is evaluated using the response spectrum technique. The moment reduction factor is investigated to determine the importance of structural taper on this important seismic response parameter.

CHAPTER II

REVIEW OF AVAILABLE METHODS OF ANALYSIS

2.1 Introduction

This chapter presents a brief review of the various methods which could be employed to study the dynamic properties of non-uniform cantilever structures. The solution of the same problem for uniform beams vibrating in flexure could be obtained for certain end conditions, and by substituting the end conditions in the general solution of the differential equation of equilibrium, the frequency equation for any set of end conditions can be determined (See Appendix I). For non-uniform cantilever structures where the cross-sectional dimensions are functions of the axial co-ordinate x, with the exception of some special cases, closed form solutions of the vibration problem do not exist. In this case the alternative is an approximate method of analysis. These methods became available by means of digital computers, with an accuracy adequate for practical and design purposes.

2.2 Rayleigh-Ritz Method

This method [6] is based on the fact that a closer approximation to the exact mode shapes can be obtained by using the superposition of more than one function as used in Rayleigh's method. Upon making a good choice of functions, it allows the calculation of higher mode shapes and frequencies in addition

to a closer approximation to the exact first mode frequency.

The deflection $w(x)$ of any beam can be expressed in terms of n functions $\phi_i(x)$, $i=1,\ldots,n$, in the form

$$w(x) = C_1\phi_1(x) + C_2\phi_2(x) + C_3\phi_3(x) + \ldots + C_n\phi_n(x) \qquad (2.1)$$

the determination of the coeffiecients $C_1, C_2, \ldots, C_n$ takes place so that the superposed functions furnish the best approximation to the natural modes. This can be achieved by adjusting the coefficients to have stationary frequency at the natural modes which conforms with Rayleigh's principle. This can be done by using the Rayleigh frequency equation

$$w^2 = \frac{\int_0^L EI(x)\,[w''(x)]^2\,dx}{\int_0^L m(x)\,w^2(x)\,dx} \qquad (2.2)$$

together with Eq. (2.1) and differentiating the resulting expression partially with respect to each of the coefficients. These partial derivatives are set to zero to form a set of n homogeneous equations as follows

$$\left.\begin{aligned} \frac{\partial w^2}{\partial C_1} &= 0 \\ \frac{\partial w^2}{\partial C_2} &= 0 \\ &\vdots \\ \frac{\partial w^2}{\partial C_n} &= 0 \end{aligned}\right\} \qquad (2.3)$$

This is a set of linear, homogeneous algebraic equations in the coefficients of the mode shape functions which contain ω^2 as the unknown. This set defines an eigenvalue problem. The solution of this problem provides the eigenvalues and the eigenvectors as well. Each of the n eigenvectors contains n components in the C's. These components when inserted in Eq. (2.1) determine the best approximation to the rth natural mode $\bar{\phi}_r(x)$. Thus,

$$\bar{\phi}_r(x) = C_1^{(r)} \phi_1(x) + C_2^{(r)} \phi_2(x) + \ldots + C_n^{(r)} \phi_n(x) \qquad (2.4)$$

2.3 Myklestad-Prohl Method

This method [1] is a well known numerical procedure for the solution of the Bernoulli-Euler equation

$$(EIy'')'' + \rho A\ddot{y} = 0 \qquad (2.5)$$

where : y = beam lateral displacement, A = cross.sectional area of the beam, E = modulus of elasticity of beam material, I = moment of inertia of beam, and ρ = mass density of material.

Consider a cantilever beam vibrating freely in a classical mode of circular frequency ω with zero damping. If the beam is divided into segments with the mass for each is concentrated at the points of division, the shear and moment at the base of the beam plus the inertial forces at the concentrated masses m will produce the shear and the moment diagrams.

At any section n, the shear V_n, the moment M_n, the inclination of tangent θ_n and the deflection y_n can be expressed in terms of the corresponding characteristics at the base of the beam and the masses, the segment length Δx, the moment of inertia I, and Young's modulus of elasticity E of the beam.

In general the shear and moment at the free end of the beam will be expressed by corresponding terms at the base of the beam multiplied by four constants (2 each for shear and moment). To satisfy the boundary conditions of the cantilever beam at the free end, the determinant of the four constants should vanish. This requirement specifies the correct value of ω which can be determined by successive trials. Upon determining the value of ω for which the determinant is equal or sufficiently close to zero, the corresponding mode shape is determined by computing the deflected shape of the beam.

2.4 Stodola Method

This is another numerical procedure [1] for the solution of the Bernoulli-Euler equation given by Eq. (2.5). Consider the same beam as discussed in the preceding section vibrating in a classical normal mode of circular frequency ω with zero damping. From beam theory the shear V, the bending moment M, the slope angle θ and the deflection y for such a cantilever beam can be obtained. Therefore four integrations of $(\rho A\omega^2 y)/(EI)$ reproduce the deflection curve y if y is the exact mode shape. If, instead, $\rho Ay/EI$ is integrated four times

in the same manner, the resulting function is y/ω^2. To find the exact mode shape, a trial function y_T is assumed. In expanded form in terms of the exact mode shapes, y_T will take the form

$$y_T = a_1 y_1 + a_2 y_2 + \ldots\ldots + a_i y_i \qquad (2.6)$$

in which a_i is constant and y_i is the exact shape of mode i. If the expression $\rho A y_T/EI$ is integrated four times, a derived function y_{d_1} will be produced. Another derived function y_{d_2} can be obtained using y_{d_1} as a trial function. In each advanced cycle the power of ω in the denominator is increased by two. The values of ω for higher modes are larger than those for lower modes, so the first term in the derived function will dominate after a sufficient number of repetitions, and the process will converge to the first mode. The frequency of the lowest mode is the quotient of the second last to the last derived functions.

The higher modes of vibrations can be obtained by the same procedure with the application of the property of orthogonality of the modes.

2.5 Modified Rayleigh-Ritz Method

This method [6] provides results identical to those resulting from the analysis using Rayleigh-Ritz. This is why it is identified in this manner, although it does not follow the same reasoning. It is based on transformation to generalized

coordinates of the natural coordinates and solution of the eigenvalue problem in this transformed system.

Consider a system with distributed mass m(x) and stiffness EI(x), such as the cantilever beam of Fig. 1.

To find the expression for generalized mass, define a set of functions $\phi_i(x)$ and corresponding coordinates q_i $(i = 1, \ldots, n)$. The displacement at any point on the beam can be expressed as

$$w(x,t) = \sum_i \phi_i(x)\ q_i(t) \tag{2.7}$$

Taking the first derivative with respect to time and using the dot to denote this type of differentiation, Eq. (2.7) becomes

$$\dot{w}(x,t) = \sum_i \phi_i(x)\ \dot{q}_i \tag{2.8}$$

The square of the velocity $\dot{w}(x,t)$ is given by

$$\dot{w}^2(x,t) = \sum_i \sum \phi_i(x)\ \phi_j(x)\ \dot{q}_i \dot{q}_j \tag{2.9}$$

The kinetic energy for the distributed mass system can be written as

$$T = \frac{1}{2}\int m(x)\ \dot{w}^2(x,t)dx \tag{2.10}$$

The integration of the above expression extends over the length of the beam.

Substituting Eq. (2.9) in (2.10), the kinetic energy expression will be

$$T = \frac{1}{2} \int_0^L m(x) \left(\sum_{ij} \phi_i(x) \phi_j(x) \dot{q}_i \dot{q}_j \right) dx \tag{2.11}$$

Interchanging the order of summation and integration and rearranging the expression to have the mass function beside the mode shape functions ϕ_i and ϕ_j, Eq. (2.11) becomes

$$T = \frac{1}{2} \sum_{ij} \dot{q}_i \dot{q}_j \int_0^L m(x) \phi_i(x) \phi_j(x) dx \tag{2.12}$$

or

$$T = \frac{1}{2} \sum_{ij} m_{ij} \dot{q}_i \dot{q}_j \tag{2.13}$$

in which

$$m_{ij} = \int_0^L m(x) \phi_i(x) \phi_j(x) dx \tag{2.14}$$

The previous expression defines the generalized mass in terms of the distributed mass function $m(x)$, and the displacement functions $\phi_i(x)$ and $\phi_j(x)$ corresponding to generalized coordinates q_i and q_j.

To find the expression for generalized stiffness, displacement $w(x,t)$ of Eq. (2.7) is first differentiated twice with respect to x. Using primes to denote this differentiation, Eq. (2.7) gives

$$w''(x,t) = \sum_i \phi_i''(x) q_i \tag{2.15}$$

The square of the second derivative w (x) is given by

$$(w''(x,t))^2 = \sum_{ij}\sum \phi_i''(x)\ \phi_j''(x)\ q_i q_j \qquad (2.16)$$

The strain energy for a beam of length l in pure bending and with distributed stiffness function EI(x) is given by

$$u = \frac{1}{2}\int_0^L EI(x)\ (w''(x,t))^2 dx \qquad (2.17)$$

Substituting Eq. (2.16) into (2.17), the strain energy expression will be

$$u = \frac{1}{2}\int_0^L EI(x)\ \left(\sum_{ij}\sum \phi_i''(x)\ \phi_j''(x) q_i q_j\right) dx \qquad (2.18)$$

After interchanging the order of summation and integration and rearranging, Eq. (2.18) becomes

$$u = \frac{1}{2}\sum_{ij}\sum q_i q_j \int_0^L EI(x)\,\phi_i''(x)\,\phi_j''(x)\,dx \qquad (2.19)$$

Using Castigliano's first theorem, the generalized force Q_i related to mode i can be expressed as

$$Q_i = \frac{\partial u}{\partial q_i} \qquad (2.20)$$

or

$$Q_i = \sum_j q_j \int_0^L EI(x)\,\phi_i''(x)\,\phi_j''(x)\,dx \qquad (2.21)$$

The relation between the generalized force Q_i and the generalized displacements q_j can be written as

$$Q_i = \sum_j k_{ij} q_j \qquad (2.22)$$

The right hand terms of Eqs. (2.21) and (2.22), when compared term by term, give the resulting relationship

$$k_{ij} = \int_0^L EI(x) \phi_i''(x) \phi_j''(x) dx \qquad (2.23)$$

which is the generalized stiffness k_{ij} expressed in terms of the bending stiffness modulus $EI(x)$ and the modal shape derivatives $\phi_i(x)$ and $\phi_j(x)$ corresponding to generalized co-ordinates q_i and q_j, respectively.

Finally, in the generalized q coordinate system the classical eigenvalue problem is obtained as

$$-([k] - \omega^2 [M]) \{q\} = \{0\} \qquad (2.24)$$

where matrices [k] and [M] are defined by Eqs. (2.14) and (2.23), respectively.

Following standard procedures [6], the solution of Eq. (2.24) yields eigenvalues ω_r and eigenvectors $q_i^{(r)}$, $r = 1, \ldots, n$.

Using Eq. (2.7), the rth mode shape of the beam becomes

$$\bar{\phi}_r(x) = \sum_{i=1}^{n} q_i^{(r)} \phi_i(x) \qquad (2.25)$$

CHAPTER III

EIGEN ANALYSIS OF TAPERED STIFFNESS STRUCTURES

This chapter presents the formulation of the eigenvalue analysis for non-uniform structures using the modified Rayleigh Ritz method described in Sec. 2.5. Both flexural as well as shear systems having uniformly distributed mass and linear taper in stiffness are treated.

3.1 Flexural Beams

Selection of Displacement Function - Vibrations of the beam of Fig. 2 having uniformly distributed mass and linearly variable stiffness over height is governed by a linear differential equation of the fourth order (See Appendix II). Since a closed form solution could not be found for this equation, the modified Rayleigh-Ritz method described in Section 2.5 was adopted. The choice of this method was based upon the fact that it is convenient for treating systems having non-uniform mass and stiffness distributions in terms of a finite number of degrees of freedom.

The flexural stiffness EI(x) of the beam in Fig. 3 is a linear function of x. This function can be expressed in terms of the base stiffness EI_0, the ratio of base to top stiffness r_k, and the overall height L. It can be written in the form

$$EI(x) = EI_o\left[1 - \frac{(\tau_k - 1)}{\tau_k L} x\right] \tag{3.1a}$$

where

$$EI_o = EI(o) = \text{flexural stiffness at the base} \tag{3.1b}$$

$$\tau_k = \frac{EI(o)}{EI(L)} = \text{ratio of base to top flexural stiffness} \tag{3.1c}$$

Displacement functions $\phi(x)$ for use in Eq. (2.7) may be selected as the mode shapes for a cantilever beam of uniform mass and stiffness. These have the form [6]

$$\phi(x) = A_1 \text{ Sin } (\beta x) + B_1 \text{ Cos } (\beta x) + C_1 \text{ sinh } (\beta x) + D_1 \text{ Cosh } (\beta x) \tag{3.2}$$

where

$$B^4 = \frac{\omega^2 m}{EI_o} \tag{3.3a}$$

$$A_1 = -0.50\ (\cosh(\beta L)+\cos(\beta L))/\sinh(\beta L)\ \text{Cos}(\beta L)-\text{Cosh}(\beta L)\text{Sin}(\beta L) \tag{3.3b}$$

$$B_1 = 0.50\ (\sinh(\beta L)+\text{Sin}(\beta L))/(\text{Sinh}(\beta L)\ \text{Cos}(\beta L)-\text{Cosh}(\beta L)\text{Sin}(\beta L)) \tag{3.3c}$$

$$C_1 = -A_1 \tag{3.3d}$$

$$D_1 = -B_1 \tag{3.3e}$$

The function $\phi(x)$ satisfies both the geometric and the natural boundary conditions. The geometric boundary conditions state that displacement and slope are zeros at the base of the beam; namely,

$$\phi(o) = 0 \tag{3.4a}$$

$$\phi'(o) = 0 \tag{3.4b}$$

The corresponding natural boundary conditions require that bending moment and shear vanish at the free end of the beam; namely,

$$\phi''(L) = 0 \tag{3.5a}$$

$$\phi'''(L) = 0 \tag{3.5b}$$

Because of these conditions [6], the uniform beam mode shapes represent desirable choices for displacement functions $\phi_i(x)$ (and $\phi_j(x)$).

Generalized Mass and Stiffness Matrices. The generalized mass m_{ij}, expressed in terms of the distributed mass function $m(x)$ and the displacement functions $\phi_i(x)$ and $\phi_j(x)$ corresponding to generalized coordinates q_i and q_j, can be written in the form

$$m_{ij} = \int_0^L m(x)\ \phi_i(x)\ \phi_j(x)\ dx \tag{3.6}$$

For uniformly distributed mass, Eq. (3.6) takes the form

$$m_{ij} = m \int_0^L \phi_i(x)\ \phi_j(x)\ dx \tag{3.7}$$

or, alternatively

$$m_{ij} = m \cdot M_{ij}$$

where

$$M_{ij} = \int_0^L \phi_i(x)\ \phi_j(x)\ dx \qquad (3.8)$$

The displacement function $\phi_i(x)$ for the coordinate q_i can be written, from Eq. (3.2), in the form

$$\phi_i(x) = A_i \text{ Sin } \beta_i x + B_i \text{ Cos } \beta_i x + C_i \text{ Sinh } \beta_i x + D_i \text{ Cosh } \beta_i x \qquad (3.9)$$

The displacement function $\phi_j(x)$ has the same form.

The integral for M_{ij} can be expanded, using Eq. (3.9), in the form

$$\begin{aligned} M_{ij} = &\int_0^L (A_i A_j \text{ Sin } \beta_i(x) \text{ Sin } \beta_j(x)\ dx) \\ &+ \int_0^L (B_i A_j \text{ Cos } \beta_i(x) \text{ Sin } \beta_j(x)\ dx) \\ &+ \int_0^L (C_i A_j \text{ Sinh } \beta_i(x) \text{ Sin } \beta_j(x)\ dx) \\ &+ \int_0^L (D_i A_j \text{ Cosh } \beta_i(x) \text{ Sin } \beta_j(x)\ dx) \\ &+ \int_0^L (A_i B_j \text{ Sin } \beta_i(x) \text{ Cos } \beta_j(x)\ dx) \\ &+ \int_0^L (B_i B_j \text{ Cos } \beta_i(x) \text{ Cos } \beta_j(x)\ dx) \end{aligned}$$

$$+ \int_0^L (C_i B_j \text{ Sinh } \beta_i(x) \text{ Cos } \beta_j(x)\, dx)$$

$$+ \int_0^L (D_i B_j \text{ Cosh } \beta_i(x) \text{ Cos } \beta_j(x)\, dx)$$

$$+ \int_0^L (A_i C_j \text{ Sin } \beta_i(x) \text{ Sinh } \beta_j(x)\, dx)$$

$$+ \int_0^L (B_i C_j \text{ Cos } \beta_i(x) \text{ Sinh } \beta_j(x)\, dx)$$

$$+ \int_0^L (C_i C_j \text{ Sinh } \beta_i(x) \text{ Sinh } \beta_j(x)\, dx)$$

$$+ \int_0^L (D_i C_j \text{ Cosh } \beta_i(x) \text{ Sinh } \beta_j(x)\, dx)$$

$$+ \int_0^L (A_i D_j \text{ Sin } \beta_i(x) \text{ Cosh } \beta_j(x)\, dx)$$

$$+ \int_0^L (B_i D_i \text{ Cos } \beta_i(x) \text{ Cosh } \beta_j(x)\, dx)$$

$$+ \int_0^L (C_i D_j \text{ Sinh } \beta_i(x) \text{ Cosh } \beta_j(x)\, dx)$$

$$+ \int_0^L (D_i D_j \text{ Cosh } \beta_i(x) \text{ Cosh } \beta_j(x)\, dx) \qquad (3.10)$$

Each of the sixteen terms between brackets was evaluated separately and then added to form the generalized mass. The integrals of Eq. (3.10) are listed in Appendix V.

The orthogonality of the mode shape functions with respect to constant mass yields

$$M_{ij} = 0 \quad , \quad \text{for } i \neq j$$
$$= M_i \quad , \quad \text{for } i = j \qquad (3.11)$$

where M_i = generalized mass for the coordinate q_i.

The generalized stiffness k_{ij} expressed in terms of the distributed stiffness function $EI(x)$ and the displacement functions $\phi_i(x)$ and $\phi_j(x)$, can be written as

$$k_{ij} = \int_0^L EI(x)\ \phi_i''(x)\ \phi_j''(x)\ dx \qquad (3.12)$$

where

$$\phi_i''(x) = \beta_i^2\ (-A_i \text{ Sin } \beta_i(x) - B_i \text{ Cos } \beta_i(x) +$$
$$+ C_i \text{ Sinh } \beta_i(x) + D_i \text{ Cosh } \beta_i(x)) \qquad (3.13)$$

and $\phi_j''(x)$ has the same form.

If Eq. (3.1) is written in the form

$$EI(x) = a - bx \qquad (3.14a)$$

where

$$a = EI_o \text{ or flexural stiffness at the base} \qquad (3.14b)$$

$$b = \left(\frac{\tau_k - 1}{\tau_k L}\right) EI_o \qquad (3.14c)$$

or

$$bL = \left(\frac{\tau_k - 1}{\tau_k}\right) EI_o \qquad (3.14d)$$

Eq. (3.12) can be rearranged in the form

$$k_{ij} = \int_0^L a\ \phi_i''(x)\ \phi_j''(x)\ dx - \int_0^L b\ \phi_i''(x)\ \phi_j''(x)\ x\ dx$$

$$= a \int_0^L \phi_i''(x)\ \phi_j''(x)\ dx - b \int_0^L \phi_i''(x)\ \phi_j''(x)\ x\ dx \qquad (3.15)$$

$$= a\ I_c - bL \cdot I_v$$

in which I_c denotes the stiffness for a beam with uniform flexural stiffness EI_o, I_v represents the effect of the stiffness taper τ_k.

When expressions of I_c are written in expanded form some terms will be similar to corresponding terms of M_{ij}, with equal or opposite signs. For the second part, I_v may also be expanded to give

$$I_{v_{ij}} = \int_0^L (A_i A_j \text{ Sin } \beta_i(x) \text{ Sin } \beta_j(x)\ x\ dx)$$

$$+ \int_0^L (B_i A_j \text{ Cos } \beta_i(x) \text{ Cos } \beta_j(x)\ x\ dx)$$

$$- \int_0^L (C_i A_j \text{ Sinh } \beta_i(x) \text{ Sin } \beta_j(x)\ x\ dx)$$

$$- \int_0^L (D_i A_j \text{ Cosh } \beta_i(x) \text{ Sin } \beta_j(x)\ x\ dx)$$

$$+ \int_0^L (A_i B_j \text{ Sin } \beta_i(x) \text{ Cos } \beta_j(x)\ x\ dx)$$

$$+ \int_0^L (B_i B_j \text{ Cos } \beta_i(x) \text{ Cos } \beta_j(x)\ x\ dx).$$

$$
\begin{aligned}
&- \int_0^L (C_i B_j \text{ Sinh } \beta_i(x) \text{ Cos } \beta_j(x) \text{ x dx}) \\
&- \int_0^L (D_i B_j \text{ Cosh } \beta_i(x) \text{ Cos } \beta_j(x) \text{ x dx}) \\
&- \int_0^L (A_i C_j \text{ Sin } \beta_i(x) \text{ Sinh } \beta_j(x) \text{ x dx}) \\
&- \int_0^L (B_i C_j \text{ Cos } \beta_i(x) \text{ Sinh } \beta_j(x) \text{ x dx}) \\
&+ \int_0^L (C_i C_j \text{ Sinh } \beta_i(x) \text{ Sinh } \beta_j(x) \text{ x dx}) \\
&+ \int_0^L (D_i C_j \text{ Cosh } \beta_i(x) \text{ Sinh } \beta_j(x) \text{ x dx}) \\
&- \int_0^L (A_i D_i \text{ Sin } \beta_i(x) \text{ Cosh } \beta_j(x) \text{ x dx}) \\
&- \int_0^L (B_i D_i \text{ Cos } \beta_i(x) \text{ Cosh } \beta_j(x) \text{ x dx}) \\
&+ \int_0^L (C_i D_j \text{ Sinh } \beta_i(x) \text{ Cosh } \beta_j(x) \text{ x dx}) \\
&+ \int_0^L (B_i D_j \text{ Cosh } \beta_i(x) \text{ Cosh } \beta_j(x) \text{ x dx}) \qquad (3.16)
\end{aligned}
$$

The integrals of Eq. (3.16) are listed in Appendix V.

Similar to the case of generalized mass, the second derivatives of the shape functions are orthogonal only with respect to the constant part of the stiffness function and

not for the variable part which concerns the taper. Thus, for the tapered stiffness beam, the usual orthogonality conditions for uniform beams

$$k_{ij} = 0, \quad \text{for } i \neq j$$
$$= k_{ii}, \quad \text{for } i = j \tag{3.17}$$

do not apply, and the generalized stiffness matrix [k] will not be diagonal. The orthogonality conditions which are applicable to non-uniform flexural beams are available in Appendix III.

To specialize the generalized mass and stiffness matrices for a beam having particular values of τ_k, L, m, and EI_o it is convenient to denote the specialized beam generalized stiffness and mass matrices as quantities indicated by bars. Thus,

$$[\bar{k}] = EI_o L[k] \tag{3.18}$$

and

$$[\bar{M}] = mL[M] \tag{3.19}$$

With these notations, Eq. (2.24) becomes

$$([\bar{k}] - \omega^2[\bar{M}])\ \{q\} = \{0\}, \tag{3.20}$$

The solution of this eigenvalue problem was obtained in this study using subroutine NROOT [7] at the Concordia University Computer Centre. This subroutine computes the eigenvalues and eigenvectors of a real non-symmetric dynamical matrix of the form $[\bar{M}]^{-1}[\bar{k}]$.

Substituting Eqs. (3.18) and (3.19) into Eq. (3.20) yields

$$EI_o L\left([k] - \omega^2 \frac{m}{EI_o}[M]\right)\{q\} = \{0\} \tag{3.21}$$

For non-trivial solution of Eq. (3.21), the determinant vanishes; hence,

$$\left|\left([k] - \omega^2 \frac{m}{EI_o}[M]\right)\right| = 0 \tag{3.22}$$

Letting

$$\beta^4 = \frac{\omega^2 m}{EI_o} \tag{3.23a}$$

gives

$$(\beta L)^4 = \omega^2 \frac{mL^4}{EI_o} \tag{3.23b}$$

and, employing this notation, the circular frequency may be expressed as

$$\omega = (\beta L)^2 \sqrt{\frac{EI_o}{mL^4}} \tag{3.23c}$$

Using the substitution

$$a = \sqrt{\frac{EI_o}{m}} \tag{3.24a}$$

Eq. (3.23c) becomes

$$\omega = (\beta L)^2 \frac{a}{L^2} \tag{3.24b}$$

Once the eigenvalue solution has been obtained, in the form of ω_r and $\{q_i^{(r)}\}$, r = 1, ..., n, the rth mode shape for the tapered structure is obtained from Eq. (2.25), which is repeated here as

$$\bar{\phi}_r(x) = \sum_{i=1}^{n} q_i^{(r)} \phi_i(x) \qquad (3.25)$$

3.2 Shear Beams

The dynamic properties of uniform as well as non-uniform shear beams have been reported extensively in the literature [2,5]. Thus only a summary version of the shear beam analysis is presented here.

The analysis of linearly tapered shear beams was performed using, as employed in this study, the same method as used for linearly tapered flexural beams, i.e. the modified Rayleigh-Ritz method.

The rth mode shape $\phi_r(x)$ can be expanded using Eq. (2.25) with the displacement function $\phi_i(x)$ assumed as

$$\phi_i(x) = \text{Sin } (2i-1) \frac{\pi x}{2L} \qquad (3.25)$$

These functions represent the mode shapes for a cantilever shear beam which has uniformly distributed mass and stiffness.

The generalized mass is obtained from Eq. (2.14) for this displacement shape and, after integration, the elements of the mass matrix are [12]

$$m_{ii} = \frac{mL}{2} \qquad (3.26a)$$

$$m_{ij} = 0 \qquad (3.26b)$$

The mass matrix can be written in the form [12]

$$[M] = \frac{mL}{2} [I] \tag{3.27}$$

where [I] is the identity matrix.

The generalized stiffness of the beam can be written in the form [12]

$$k_{ij} = \int_0^L k(x)\ \phi_i'(x)\ \phi_j'(x)\ dx \tag{3.28}$$

where $\phi_i'(x)$, $\phi_j'(x)$ are the first derivatives of the displacement functions, and

$$k(x) = k_o \left[1 - \frac{(\tau_k - 1)}{\tau_k L} x \right] \tag{3.29a}$$

where

$$k_o = k(o) = \text{shear stiffness at the base} \tag{3.29b}$$

$$\tau_k = \frac{k(o)}{k(L)} = \text{ratio of base to top shear stiffness} \tag{3.29c}$$

After integration has been performed, Eq. (3.28) leads to the elements of the stiffness matrix expressed as [12]

$$k_{ii} = k_o \left\{ \frac{1}{2} \left(\frac{n^2\pi^2}{8} + 0.5 \right) \frac{1}{16\tau_k} (n^2\pi^2 - 4) \right\} \tag{3.30}$$

Eq. (3.30) prescribes the general form for the diagonal terms of the stiffness matrix. The similar form for the off diagonal terms of the stiffness matrix is expressed as [12]

$$k_{ij} = k_o\left[\left(\frac{1}{\tau_k} - 1\right)\frac{(nm)}{2}\left\{\frac{1}{(n-m)^2}\left(-1^{\frac{(n-m)}{2}} - 1\right)\right.\right.$$

$$\left.\left. + \frac{1}{(n+m)^2}\left(-1^{\frac{(n+m)}{2}} - 1\right)\right\}\right] \qquad (3.31)$$

where $n = 2i-1$, and $m = 2j-1$.

With the generalized mass and stiffness matrices as defined above, the solution of the eigenvalue problem was obtained, as for the flexural beam of the preceding section, by using subroutine NROOT.

3.3 Convergence of the Solution

Since the dynamic properties of the tapered stiffness beams were determined as a sum of a series of terms, it is important to investigate the convergence of the solution.

Definition - The series

$$u_1 + u_2 + u_3 + \ldots\ldots\ldots + u_n \qquad (3.32)$$

is said to be convergent when the sum of the terms approaches a finite limit, as the number of terms is indefinitely increased [10]. When this sum does not approach a finite limit, the series is divergent.

3.3.1 Convergence Criteria

To select the required number of terms to be used in a series which is related to one of the dynamic properties of the tapered stiffness beam, it is known [6] that the accuracy of the solution improves with increasing numbers of terms and, that

the use of a finite number of terms results in an approximate representation. In practice, the required number of natural modes is finite. To compose the required highest mode functions having the general characteristics of all sought modes must be included. Still, it is desirable to include functions corresponding to higher modes as this will improve accuracy.

3.3.2 Convergence of Modal Response Parameters

The convergence of the eigenvalue solution giving dynamic properties was examined in order to determine number of terms to be considered in Eq. (2.25).

Since it is known that natural frequencies are stationary with respect to assumed mode shape, convergence of frequency does not provide the number of terms that are required to achieve adequate accuracy for other dynamic properties, such as the mode shapes, for example. Convergence of beam mode shapes in addition to frequency, was therefore examined. Convergence test consisted of plotting the ordinate of the first mode shape at mid height (an arbitrary point) and the peak ordinates for the following three mode shapes resulting from Eq. (2.25) with number of terms, n, varied from two to six.

The results of the test for convergence are summarized in Appendix VI. Figures VI-1 to VI-4 present the test results with respect to modal frequencies, whereas figures VI-5 to VI-8 present similar results with respect to mode shape displacement, both are for the first four modes. In addition, Figs. VI-9 to VI-16 demonstrate convergency with increasing n

for modal seismic response parameters discussed in the next chapter.

Figures VI-1 to VI-16 present the results of the convergence study for flexural beams. The data indicate that the solution of the problem is convergent, and convergence increases with an increase of the number of terms n.

The maximum number of terms that could be considered in the case of flexure was limited to six. This occured due to the difficulty encountered in calculating the eigenvalues for the uniform beam (expressed in a form identical to that of Eq. (3.23c)) which were required for the generalized mass and stiffness matrices. These initial eigenvalues are the solutions of the frequency equation [6].

$$\text{Cosh}\ (\beta L)\ \ \text{Cos}\ (\beta L) + 1 = 0 \qquad (3.33)$$

The hyperbolic function in this equation is highly sensitive to changes in the eigenvalues thus making it difficult to obtain more than six roots with the required accuracy. The roots of the frequency equation were obtained with an accuracy up to thirteen decimal places by means of subroutine ZREALI [11] available at Concordia University Computing Centre. This routine calculates n real zeros of a real function F where the initial guesses are not known to be good.

Convergence for the analysis of the shear beams of Sec. 3.3 was similarly studied. No numerical difficulties arose and an arbitrarily large number of terms could be accommodated in

Eq. (2.25), limited only by the size of the dynamic matrix. Convergence for the modal properties of the first four modes of the non-uniform shear beam was obtained with n=5 or 6.

For the data presented in Chapter V, the number of terms employed in the calculations was kept constant at: (a) $n = 6$ for flexural, and (b) n=8 for shear beams.

CHAPTER IV

DERIVIATION OF SEISMIC RESPONSE PARAMETERS

This chapter presents the formulation of seismic response parameters, assuming that the structure's dynamic properties have been made available, according to the procedure of the preceding chapter, for example. Although the effect of structural taper τ_k is not explicitly involved, the seismic response parameters presented here are used to examine the stiffness taper behaviour discussed in Chapter V.

4.1 Base Shear and Overturning Moment

The rth mode shape of the non-uniform structure is given by Eq. (2.25) as

$$\bar{\phi}_r(x) = \sum_{i=1}^{n} q_i^{(r)} \phi_i(x) ,$$

To obtain seismic response analysis, it is convenient to introduce a factor which introduces the effect of the mode shape. This factor, the modal participation factor, for the rth mode, is defined by

$$\Gamma_r = \frac{\int_0^L m(x)\ \bar{\phi}_r(x)\ dx}{\int_0^L m(x)\ \bar{\phi}_r^2(x)\ dx} \qquad (4.1)$$

which, for uniform mass distribution becomes

$$\Gamma_r = \frac{\int_0^L \bar{\phi}_r(x)\ dx}{\int_0^L \bar{\phi}_r^2(x)\ dx} \qquad (4.2)$$

The numerator of Eq. (4.2) can be rewritten, using Eq. (2.25), as

$$\int_0^L \bar{\phi}_r(x)\ dx = \sum_{i=1}^{n} q_i^{(r)} \int_0^L \phi_i(x)\ dx \qquad (4.3)$$

Recalling Eq. (3.9), the mode shape of a uniform flexural beam for mode "i" was given as

$$\phi_i(x) = A_i \text{ Sin } (\beta_i x) + B_i \text{ Cos } (\beta_i x) + C_i \text{ Sinh } (\beta_i x) + D_i \text{ Cosh } (\beta_i x)$$

Thus, the R.H.S. of Eq. (4.3) can be evaluated, for the values of $q_i^{(r)}$ obtained from the eigenvalue problem of Eq. (3.21). The integration of displacement function $\phi_i(x)$ yields

$$\int_0^L \phi_i(x)\ dx = A_i \int_0^L \text{Sin } (\beta_i(x))\ dx + B_i \int_0^L \text{Cos } (\beta_i(x))\ dx + C_i \int_0^L \text{Sinh } (\beta_i(x))\ dx + D_i \int_0^L \text{Cosh } (\beta_i(x))\ dx \qquad (4.4)$$

The integrals of Eq. (4.4) are listed in Appendix V.

Similarly, the denominator of Eq. (4.2) can be written in the form

$$\int_0^L \bar{\phi}_r^2(x)\,dx = \sum_{i=1}^{n}\sum_{j=1}^{n} q_i^{(r)}\, q_j^{(r)} \int_0^L \phi_i(x)\,dx \int_0^L \phi_j(x)\,dx$$

$$= (q_1^{(r)})^2 \int_0^L \phi_1^2(x)\,dx + q_1^{(r)}\, q_2^{(r)} \int_0^L \phi_1(x)\,\phi_2(x)\,dx$$

$$+ (q_2^{(r)})^2 \int_0^L \phi_2^2(x)\,dx$$

$$+ \ldots\ldots + (q_n^{(r)})^2 \int_0^L \phi_n^2(x)\,dx \qquad (4.5)$$

The even terms in the previous expression are equal to zero because of the orthogonality condition for the uniform beam (6); thus Eq. (4.5) reduces to the form

$$\int_0^L \bar{\phi}_r^2(d)\,dx = (q_1^{(r)})^2 \int_0^L \phi_1^2(x)\,dx + (q_2^{(r)})^2 \int_0^L \phi_2^2(x)\,dx$$

$$+ \ldots + (q_n^{(r)})^2 \int_0^L \phi_n^2(x)\,dx = \sum (q_i^{(r)})^2 \int_0^L \phi_i^2(x)\,dx$$

(4.6)

Eq. (4.6) can be evaluated using the previously determined coefficients $q_i^{(r)}$ and the integration of the square of the mode shape functions of the uniform beam. The latter is given by the same expression as the generalized mass of the beam divided by unit mass m, listed in Appendix V.

Once the modal participation factor Γ has been evaluated for each mode, the modal absolute maximum acceleration for the rth mode is given by

$$|\ddot{u}(x)_{r_{max}}| = \Gamma_r \omega_r S_v^{(r)} \bar{\phi}_r(x) \tag{4.7}$$

in which $S_v^{(r)}$ is the spectral velocity at frequency ω_r.

The inertia force for mode "r" is the product of the mass and absolute acceleration

$$F_r(x) = m \Gamma_r \omega_r S_v^{(r)} \bar{\phi}_r(x) \tag{4.8}$$

The resulting maximum base shear for mode "r" is obtained by integration over the beam length

$$V_{r_{max}} = m \Gamma_r \omega_r S_v^{(r)} \int_0^L \bar{\phi}_r(x)\, dx \tag{4.9}$$

where the integral on the R.H.S. is listed in Appendix V.

Since the base shear is considered as one of the most important parameters in earthquake analysis, it is important to investigate the relation between this parameter and the flexural or shear stiffness tapers.

If velocity response spectrum $S_v^{(r)}$ is assumed to be constant in Eq. (4.9), the normalized modal base shear can be expressed as (See Appendix IV)

$$\frac{V_r L}{a\ m\ S_v^{(r)}} = \left(\frac{\omega_r L^2}{a}\right) C_v^{(r)} \qquad (4.10)$$

where

$$a = \sqrt{\frac{EI_o}{m}}$$

and $C_v^{(r)}$ is the rth modal base shear coefficient, defined by (See Appendix IV)

$$C_v^{(r)} = \frac{\left(\int_0^L \overline{\phi}_r(x)\ dx\right)^2}{\int_0^L \overline{\phi}_r^2(x)\ dx} \qquad (4.11)$$

It should be noted that $C_v^{(r)}$ represents also the modal unit effective mass [5]. From Eq. (4.11), one can determine the relation between the flexural (and shear) stiffness taper τ_k and the unit effective mass for different modes.

The overturning moment at the base of the structure is another important parameter which was investigated.

The overturning moment of mode "r" is the integration over the beam length of the product of the inertia force $F_r(x)$ at a level x and the distance x to the base of the beam. It can be expressed, using Eq. (4.3), as

$$M_{r_{max}} = m\ \Gamma_r\ \omega_r\ S_v^{(r)} \int_0^L x\ \overline{\phi}_r(x)\ dx \qquad (4.12)$$

The integration on the R.H.S. of Eq. (4.12) can be rewritten in the form

$$\int_0^L X\bar{\phi}_r(x)\, dx = \sum_{i=1}^{n} q_i^{(r)} \int_0^L X\phi_i(x)\, dx \qquad (4.13)$$

Again, the integration on the R.H.S. of Eq. (4.13) can be written in the expanded form

$$\int_0^L X\phi_i(x)\, dx = A_i \int_0^L x \text{ Sin } \beta_i(x) + B_i \int_0^L x \text{ Cos } \beta_i(x)$$
$$+ C_i \int_0^L x \text{ sinh } \beta_i(x) + D_i \int_0^L x \text{ Cosh } \beta_i(x) \qquad (4.14)$$

The integrals of Eq. (4.14) are listed in Appendix V.

The maximum overturning moment for mode "r" can be evaluated by using Eq. (4.13) together with the previously calculated value of the modal participation factor Γ_r.

The normalized modal base overturning moment assuming constant velocity response spectrum $S_v^{(r)}$ is (See Appendix IV)

$$\frac{M_{r_{max}}}{a\ m\ S_v^{(r)}} = \left(\frac{\omega_r L^2}{a}\right) C_M^{(r)} \qquad (4.15)$$

where $C_M^{(r)}$ is the rth modal base overturning moment coefficient, in the form (See Appendix IV)

$$C_M^{(r)} = \frac{\int_0^L \bar{\phi}_r(x)\, dx \int_0^L x\bar{\phi}_r(x)\, dx}{\int_0^L \bar{\phi}_r^2(x)\, dx} \qquad (4.16)$$

From Eq. (4.16), the relation between the stiffness taper τ_k and the effective modal moment $C_M^{(r)}$ can be investigated.

In order to determine maximum values of a specific response parameter, the maximum response of that parameter in each mode must be determined and the resulting modal maxima will then be combined using the "square root sum of squares" summation (SRSS) to obtain an estimate of the overall maximum for that parameter.

Using the SRSS approximation for the determination of the maximum value of response parameters, and including "n" contributing modes in the total response of the structure the maximum base shear and overturning moment are obtained, respectively, as

$$V_{max} = \sqrt{\sum_{i=1}^{n} V_{r_{max}}^2} \qquad (4.17)$$

$$M_{max} = \sqrt{\sum_{i=1}^{n} M_{r_{max}}^2} \qquad (4.18)$$

An alternate method to determine the maximum value of a response parameter is to add the absolute modal values, thus obtaining an upper bound. This criterion for the determination of the maximum value of response is termed the ABS method.

Using the ABS criterion and including n contributing modes in the total response of the structure, the maximum base shear and overturning moment are expressed as

$$|V|_{max} \leq \sum_{r=1}^{n} V_{r_{max}} \qquad (4.19)$$

$$|M|_{max} \leq \sum_{r=1}^{n} M_{r_{max}} \qquad (4.20)$$

In this investigation of the effect of stiffness taper on the response parameters of shear and flexural systems, the SRSS method will generally be used. However, SRSS and ABS assumptions will be compared when investigating the effect of stiffness taper on the base shear.

4.2 Moment Reduction Factor

The static seismic loading provisions of the 1975 National Building Code of Canada [9] include an overturning moment reduction factor. This factor was included in order to recognize that the overturning moment computed from the static load distribution is likely to be larger than the actual maximum dynamic moment.

The overturning moment reduction factor can be defined as "the ratio of dynamic base moment to static base moment when the dynamic base shear and the static base shear are taken to be equal". This definition can be expressed in terms of the maximum overturning moment and base shear in the form [4]

$$J = \frac{M}{VH} \Big/ \frac{M_o}{V_o H} \qquad (4.21)$$

in which J is the moment reduction factor computed for n modes in the dynamic response, V_o and M_o are the base shear and overturning moment computed from the static loading, and H is the height of the structure. The static non-dimensional moment to shear ratio can be substituted by a factor which depends on the form of the structure. Using notation "a_o" for this ratio allows the moment reduction factor to be expressed in the form

$$J = \frac{1}{a_o} \left(\frac{M}{VH} \right) \qquad (4.22)$$

where

$$a_o = \frac{M_o}{V_o H} \qquad (4.23)$$

The 1975 National Building Code of Canada discussed in more detail the choice of factor a_o. It specifies that the factor a_o equals 0.667 in case of the normal triangular static loading. In case of slender buildings, the code requires an additional concentrated force F_t at the top of the structure, as shown in Fig. 3. The maximum value of this top force if 15% of the base shear, and the corresponding value of a_o is 0.715.

CHAPTER V

RESULTS AND DISCUSSION.

In this Chapter, modal frequencies and shapes, obtained from the dynamic analysis described in Chapter III for non-uniform beams of both the shear and flexural types, are presented as functions of stiffness taper τ_k varied between 1 and 24. In addition, the seismic response parameters, discussed in Chapter IV, are similarly investigated for both types of beams, and the importance of the effect of stiffness taper is evaluated from the data.

5.1 Effect of Taper on Modal Frequencies

Figure 4 presents the effect of flexural stiffness taper on beam modal frequencies. The curves indicate that increasing τ_k leads to a continuous decrease in the normalized beam frequencies. For the fundamental mode, the decrease in frequency due to increasing τ_k from 1 to 5 represents 78% of the total decrease that would result from increasing τ_k up to 24. The behaviour of the higher modes is seen to be similar. Thus, structures with small flexural stiffness taper are more sensitive to variation of τ_k than those having large taper.

The effect of shear stiffness taper on beam modal frequencies is presented in Fig. 5. It can be seen that the behaviour of the tapered stiffness shear beam for increasing τ_k is similar to that of the flexural beam.

5.2 Effect of Taper on Mode Shapes

Figures 6 and 7 show the first and second mode shapes for tapered flexural and shear beams, respectively. Both beams indicate larger fundamental mode displacements at the top than occur in the corresponding uniform beams. If the top displacements are normalized to the value of the top displacement for the uniform beam, the modal displacements of tapered stiffness beams along the height of the beam will be less than those of uniform beams.

In order to examine the validity of this conclusion, the effect of taper on mode shapes has been verified using both the Myklestad-Prohl and the Stodola methods [1]. The results obtained from both methods conform with the pointed conclusion.

5.3 Effect of Taper on Distribution of Modal Strains

Figures 8 and 9 examine modal strains as given by $\bar{\phi}'_r$ and $\bar{\phi}''_r$, respectively, for beams with tapered stiffness in flexure for the first two modes. The figures confirm the conclusion by Pekau [5] that "the effect of increasing τ_k is to shift the region of maximum strain towards the upper portions of the structure". The "whiplash" phenomenon is evident in the first and second modes presented here.

Fig. 10 shows the effect of shear stiffness taper on the first derivative of mode shapes for the first two modes. The "whiplash" effect is evident in both modes.

Figs. 11 and 12 show the shear force distribution* for tapered flexural and tapered shear beams, respectively, for the first two modes.

The shear distribution presented in Fig. 11 shows a slight decrease with increasing values of stiffness taper for both modes.

In Fig. 12, increasing values of stiffness taper leads to a slight increase in the shear force distribution for the first mode. As for the second mode, the figure shows an increase in the lower portions accompanied by a similar decrease in the upper portions of the structure with increasing value of stiffness taper. Moreover, the stresses are shifted towards the upper portions of the structure.

5.4 Effect of Taper on Base Shear

The effect of flexural stiffness taper on beam modal base shear coefficients $C_v^{(r)}$ is shown if Fig. 13 for the first four modes. Increasing τ_k leads to a decrease in the modal shear coefficient for the first two modes and a corresponding increase in the higher modes.

---

*. Shear force is given by

$$V_r(x) = K(x)\,\bar{\phi}_r(x) \qquad \text{for shear beams}$$

$$V_r(x) = EI_o\left[-\bar{\phi}_r'(x)\,\frac{(\tau_k-1)}{\tau_k L\, EI_o} + \frac{EI(x)}{EI_o}\,\bar{\phi}_r''(x)\right]$$

for flexural beams

Fig. 14 shows the effect of flexural stiffness taper on the total base shear obtained from the first four modes, calculated by the SRSS, using Eq. (4.11). Increasing τ_k results in a significant decrease in the total base shear. The decrease in the total base shear for $\tau_k = 24$ is approximately 24% of the corresponding value for $\tau_k = 1$.

Fig. 15 shows the effect of shear stiffness taper on the modal base shear coefficient $C_v^{(r)}$ for tapered stiffness shear beams. Increasing value of τ_k leads to a decrease in the beam modal base shear coefficient for the first mode and a corresponding increase for the higher modes.

Fig. 16 shows the effect of shear stiffness taper on the total base shear obtained from the first four modes, calculated by the SRSS using Eq. (4.11). It can be noticed that the shear beam behaves in a manner similar to the flexural beam; i.e., increasing τ_k from 1 to 24 results in decreasing the base shear by 26% approximately.

Table I lists the values of the $C_v^{(r)}$, the modal base shear coefficients (or the unit effective modal masses), for tapered shear, flexural and also hybrid beams. The latter was defined as a beam whose behaviour is given by the average of the coefficients for tapered flexural and tapered shear beams.

Fig. 17 compares the variation of the total base shear with τ_k for shear and flexural beams using ABS and SRSS combination rules for modal contributions. It can be seen that

increasing τ_k decreases the total base shear, using both rules of combination, for both shear as well as flexural beams.

5.5 Effect of Taper on Overturning Moment

Fig. 18 shows the effect of flexural stiffness taper on beam modal overturning moment coefficient $C_M^{(r)}$ for the first four modes. Increasing stiffness taper τ_k results in a decrease in the modal overturning moment coefficient for the fundamental mode and a corresponding increase in the higher modes.

Fig. 19 shows the effect of flexural stiffness taper on the total base overturning moment obtained from Eq. (4.16) using the first four modes and the SRSS method. Increasing τ_k results in a significant decrease in the total base overturning moment. The decrease in the total overturning moment at $\tau_k = 24$ is approximately 13% of the value of $\tau_k = 1$.

Fig. 20 shows the effect of shear stiffness taper on beam modal overturning moment coefficient $C_M^{(r)}$ for the first four modes. Increasing τ_k leads to a decrease in the beam modal overturning moment coefficient for the first mode and corresponding increases in the higher modes.

Fig. 21 shows the effect of shear stiffness taper τ_k on the total overturning moment obtained from Eq. (4.16) for the first four modes and the SRSS method. Increasing τ_k results in a significant decrease in the total overturning moment. The decrease for $\tau_k = 24$ is approximately 26% of the value at $\tau_k = 1$.

5.6 Base Shear and Overturning Moment for Tapered Hybrid Beams

The results obtained by Pekau [5] as well as those of this study for the base shear and overturning moment of tapered stiffness shear beams can be combined with the corresponding data for tapered stiffness flexural beams to estimate the behaviour of tapered hybrid beams.

It is well known that a cantilever structure is a combination of a pure shear and a pure flexural beam. The ratio of the base shear stiffness k_o to the base flexural stiffness EI_o determines its location between the two limiting types of behaviour for a particular taper τ_k. If, for example, the ratio [4]

$$\alpha H = \sqrt{\frac{k_o H^2}{EI_o}} \qquad (5.1)$$

for the hybrid beam approaches zero, the base shear or the overturning moment can be determined from the curves of a pure shear beam. On the other hand, if the same ratio approaches infinity, the required parameter can be obtained from the curves of a pure flexural beam. For any value of the ratio, other than zero and infinity, the required parameter can be approximated by interpolation between shear and flexural behaviour.

5.7 Effect of Taper on Moment Reduction Factor

Figure 22 shows the effect of flexural stiffness taper on the non-dimensional base moment reduction factor J obtained

from Eq. (4.22) for both normal and slender structures. Increasing τ_k leads to an increase in the moment reduction factor for both types of structures. Morevoer, the maximum effect of variation in τ_k occurs for structures with small values of stiffness taper but for those already having large values of taper further increase in τ_k has little significance.

Similarly, Fig. 23 compares the effect of shear stiffness taper on the non-dimensional base moment reduction factor J for both normal and slender structures. The behaviour is similar to that of flexural taper except that the variation in J with shear taper is practically insignificant compared to that of the flexural taper (14% for flexural taper vs. 0.54% for shear taper over a change in the stiffness taper from 1 to 24).

Fig. 24 gives the moment reduction factor J for tapered hybrid beams as the average of the factors for tapered shear stiffness and tapered flexural stiffness beams.

CHAPTER VI

CONCLUSIONS

This study presents an investigation of the dynamic properties of tower-like structures which have been idealized as cantilever beams with uniform mass and linearly tapered stiffness distributions. The results of this study are applicable to tall structures having uniform mass and non-uniform stiffness distributions (e.g., as is common for high-rise buildings). The frequencies, mode shapes and seismic response parameters for such structures known to be similar to those of the idealized beam models treated in this study.

The analysis which has been performed in this study of the behaviour of tapered stiffness beams shows that structural taper in both flexure and shear has a significant effect on both the dynamic properties as well as seismic response parameters.

Data has been presented in graphical form, representing the results of this study. These provide a first estimate of expected seismic behaviour of tall structures where the effect of slenderness may be examined in terms of taper in structural stiffness.

In particular, the 1975 National Building Code of Canada [9] gives the value of the moment reduction factor for uniform stiffness structures. The results presented here have shown that moment reduction factor J for tapered stiffness structures is larger than that for corresponding uniform stiffness struc-

tures. The increase in some cases may be as much as 14% ($\tau_k = 24$). This means that the value given in the NBC Code is not conservative for structures with tapered stiffness since it underestimates the value of the dynamic base moment.

In order to analyze the effects of earthquake forces on tall or unusual buildings the NBC Code recommends the use of dynamic analysis. The dynamic analysis may be simplified by using the results obtained in this study to treat tall and slender structures.

A suggested future study is an investigation of a more refined hybrid shear-flexural system to model actual structural behaviour where both column axial deformation as well as frame action are important.

FIGURES AND TABLE

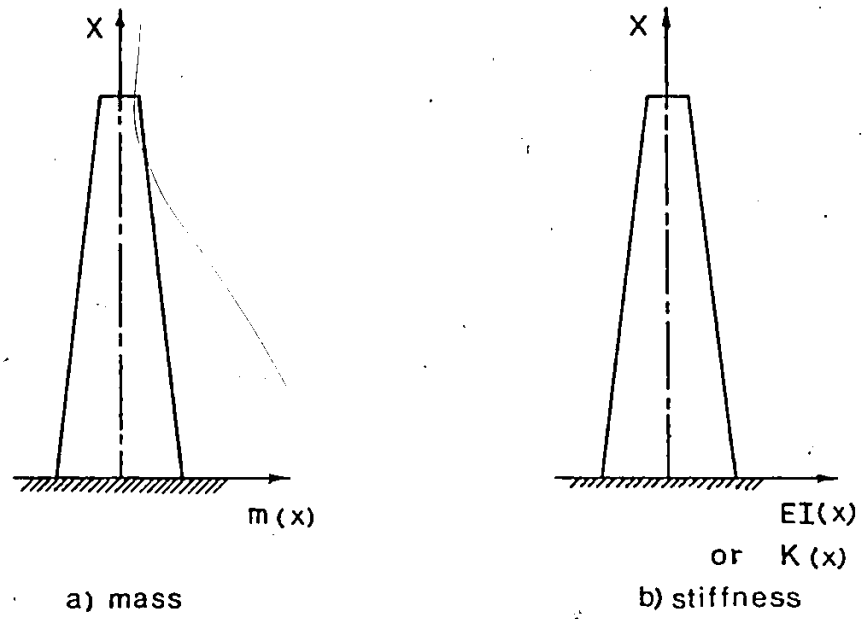

FIG. 1 DISTRIBUTED MASS AND STIFFNESS

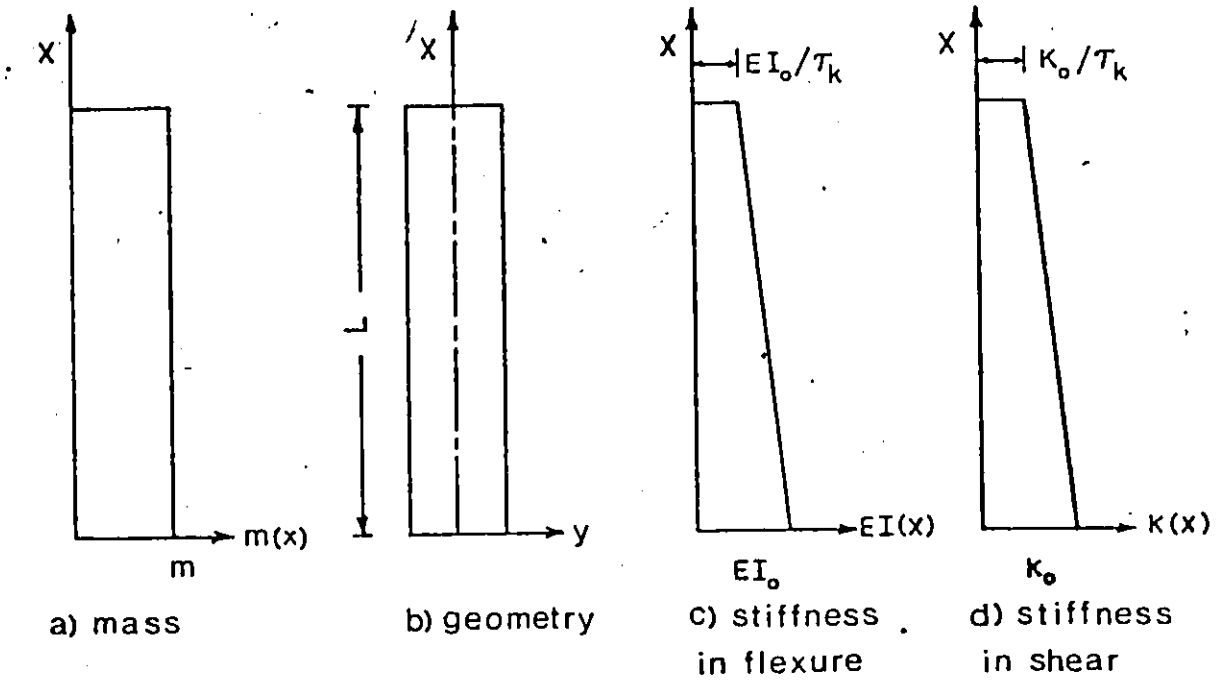

FIG. 2 PROPERTIES OF VARIABLE STIFFNESS CANTILEVER BEAM

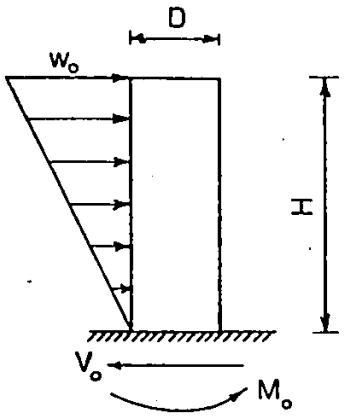

$$V_o = \frac{w_o H}{2}$$

$$M_o = \frac{w_o H^2}{3}$$

$$a_o = \frac{M}{V_o H} = \frac{2}{3}$$

a) NORMAL STRUCTURES (H/D≤3)

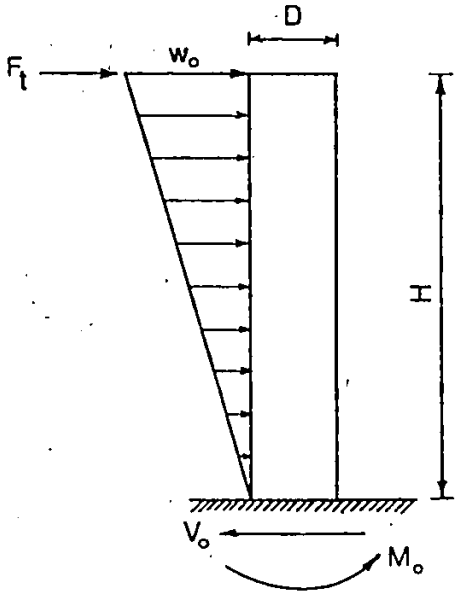

$$V_o = \frac{w_o H}{2} + F_t$$

$$M_o = \frac{w_o H^2}{3} + F_t H$$

For max value $F_t = 0.15\ V_o$;

$$a_o = 0.715$$

b) SLENDER STRUCTURES (H/D>3)

FIG. 3 STATIC SEISMIC LOADING [REF. 4]

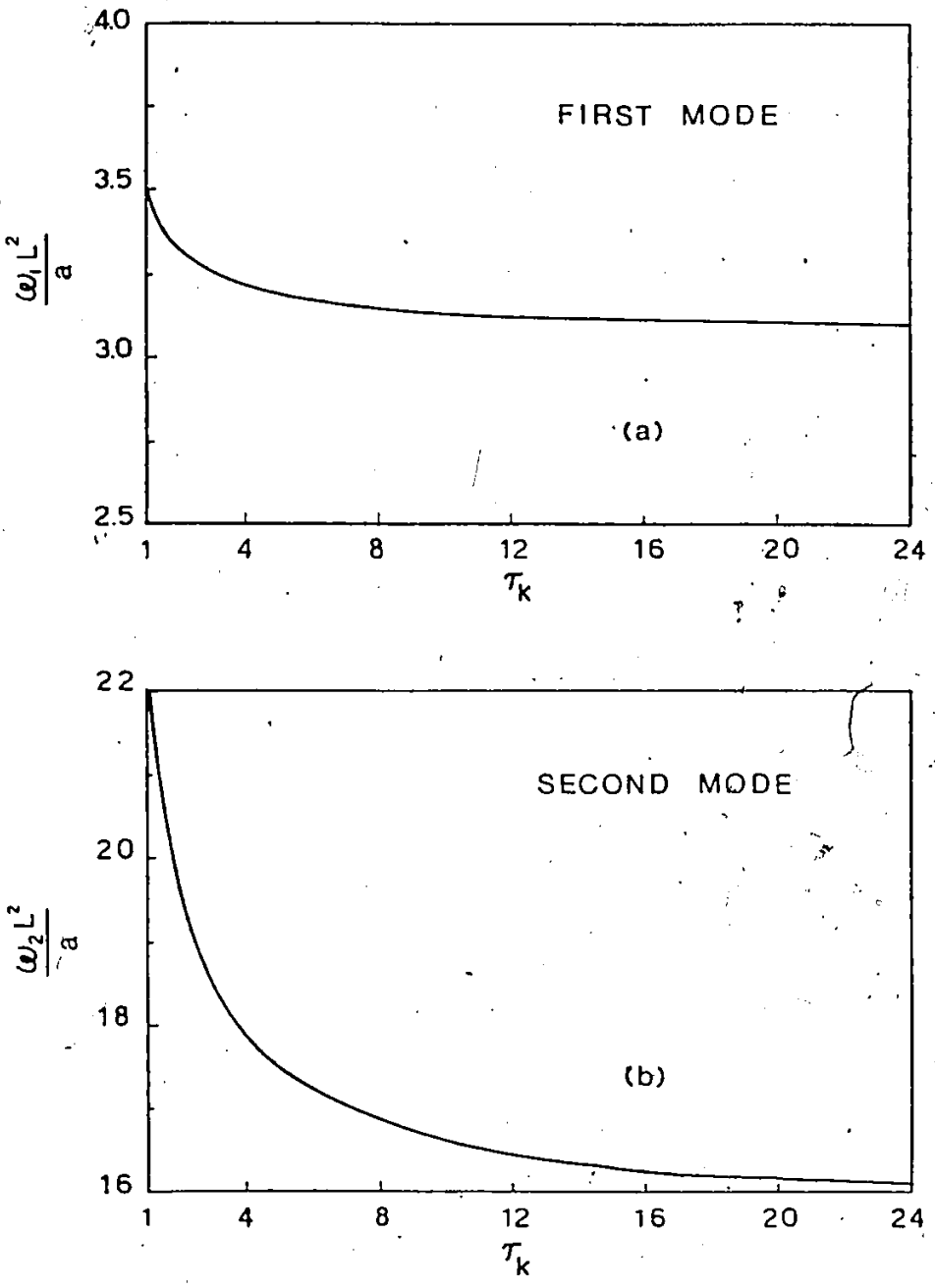

FIG. 4 FLEXURAL STIFFNESS TAPER AND MODAL FREQUENCIES

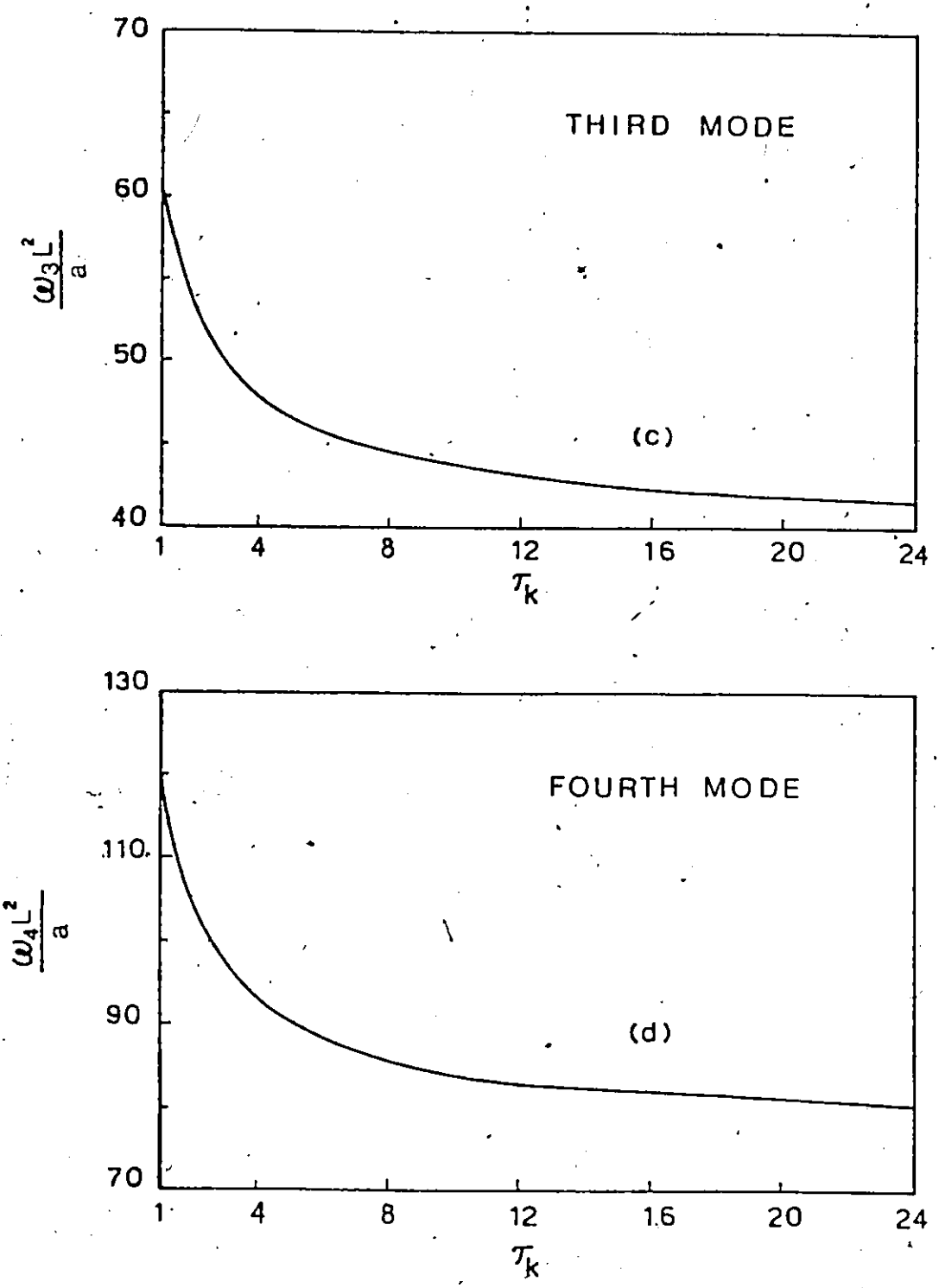

FIG. 4 (Cont'd) FLEXURAL STIFFNESS TAPER AND MODAL FREQUENCIES

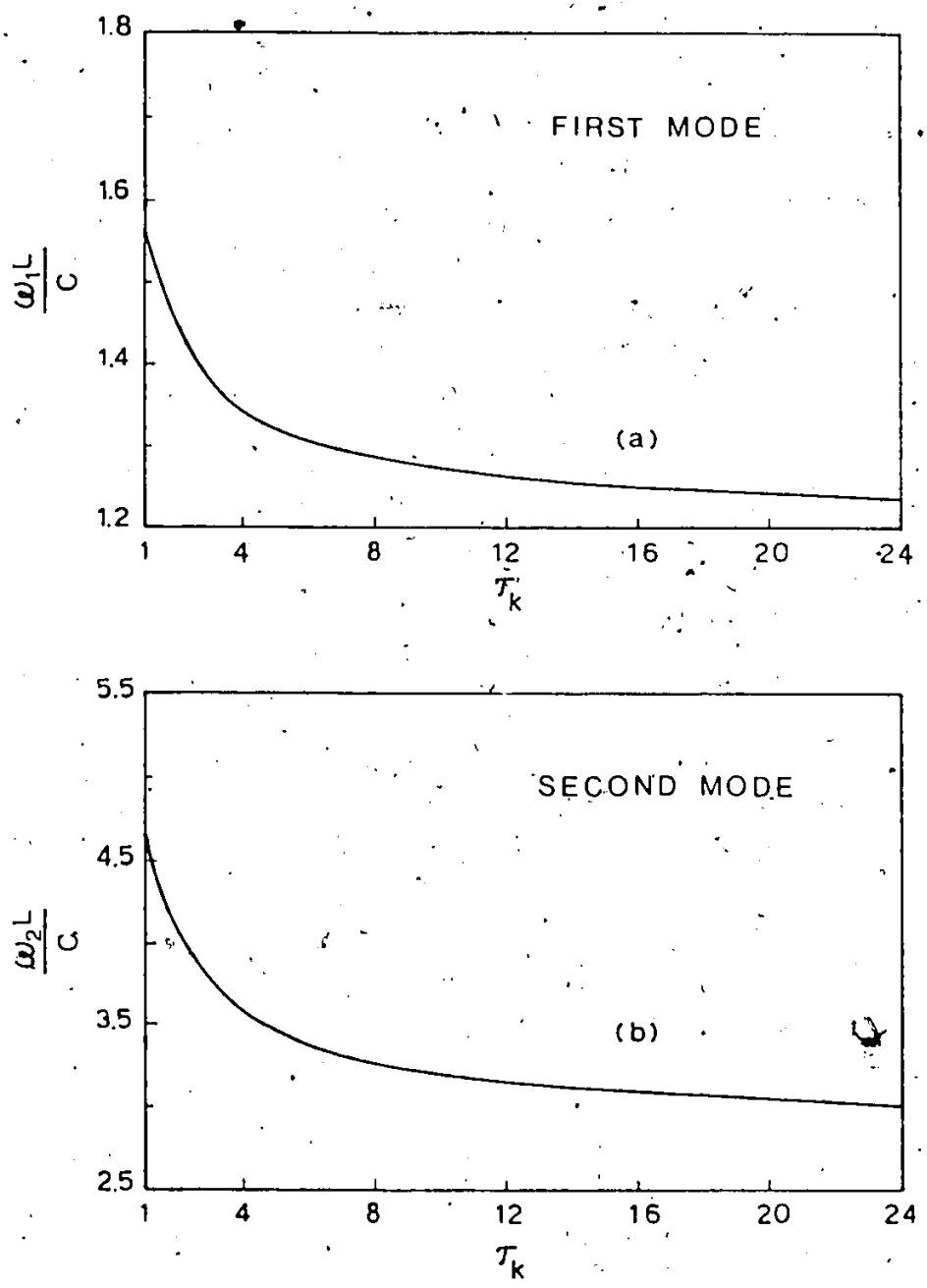

FIG. 5 SHEAR STIFFNESS TAPER AND MODAL FREQUENCIES

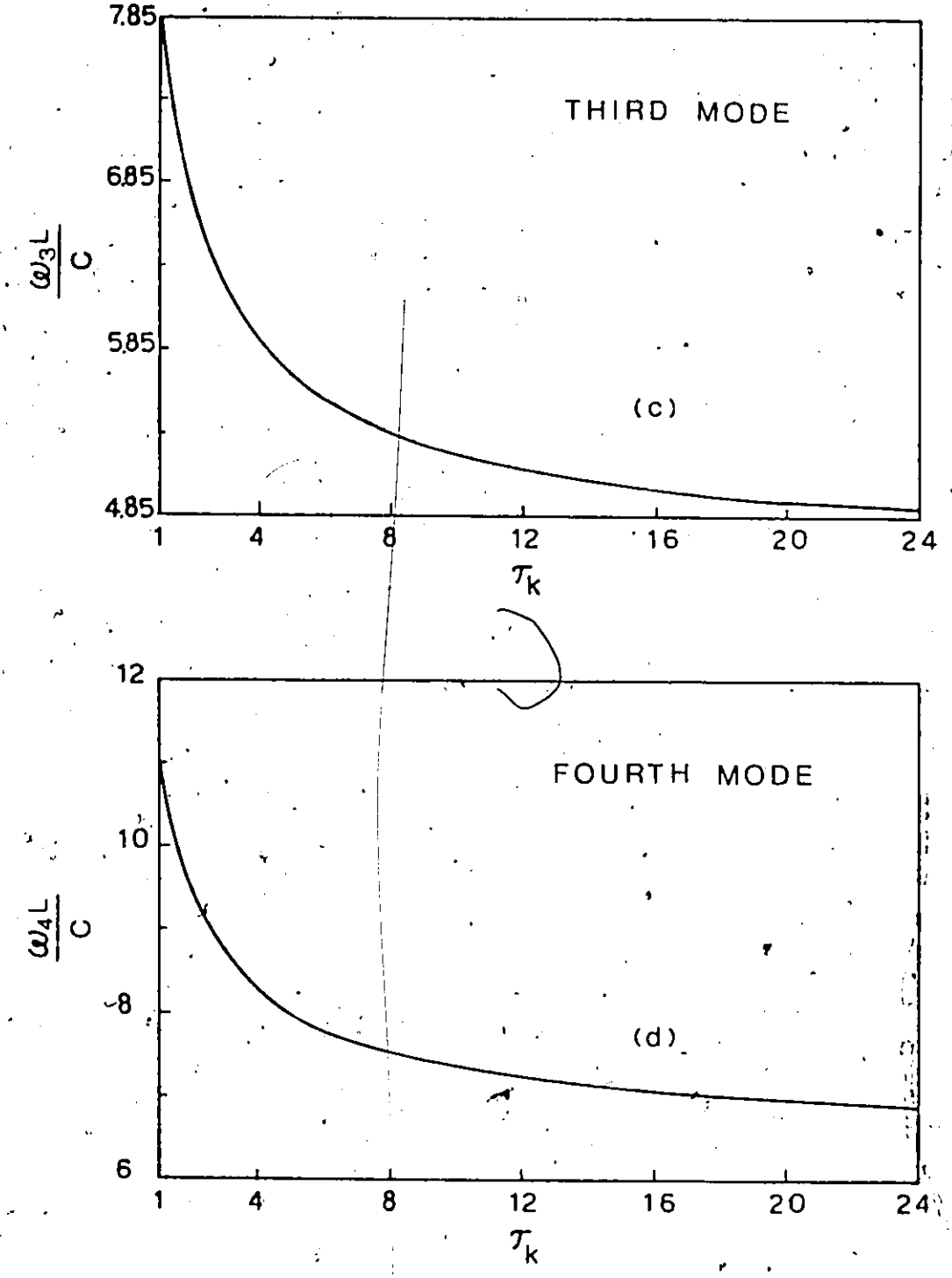

FIG. 5 (Cont'd) SHEAR STIFFNESS TAPER AND MODAL FREQUENCIES

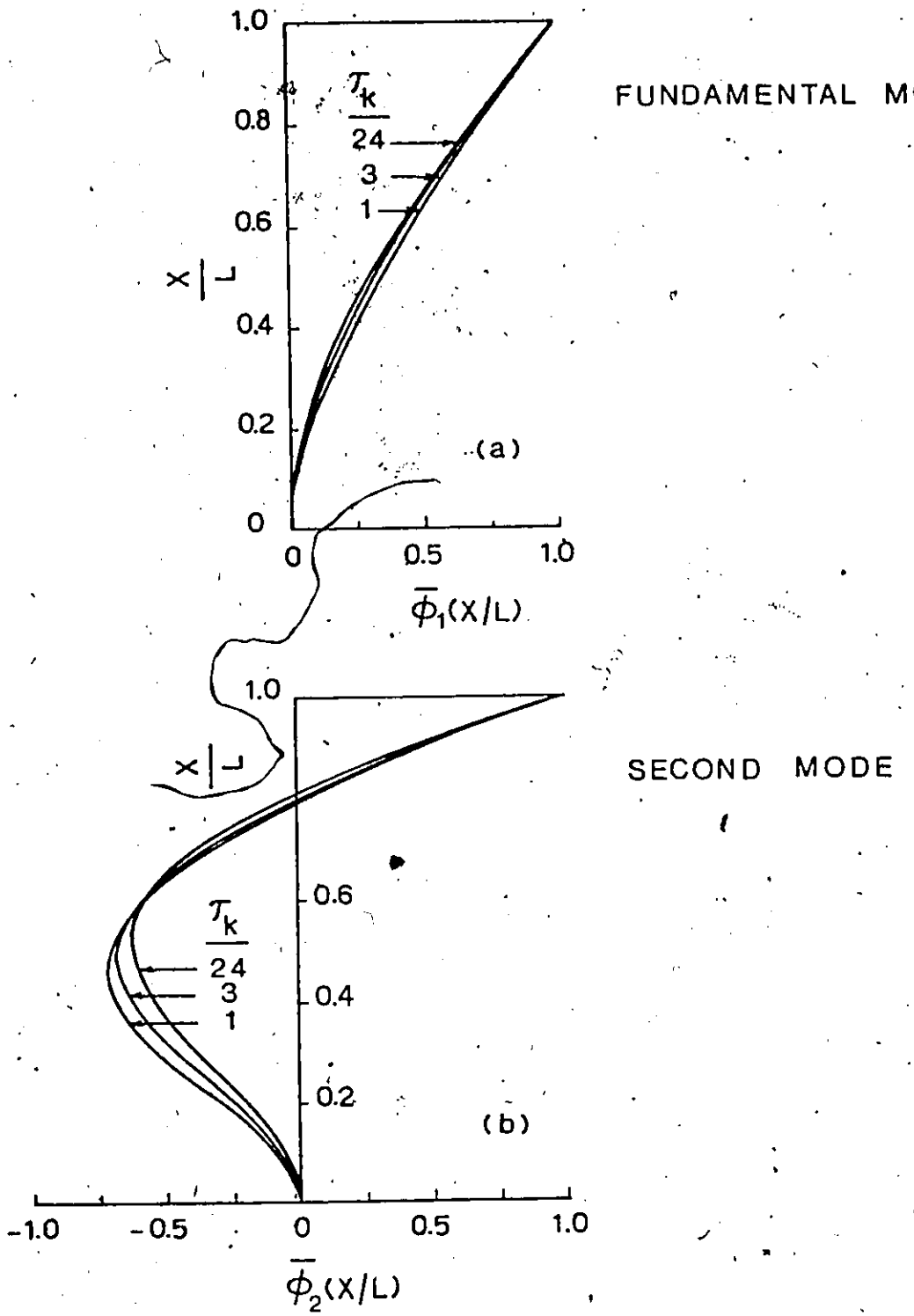

FIG. 6 FLEXURAL STIFFNESS TAPER AND MODE SHAPES

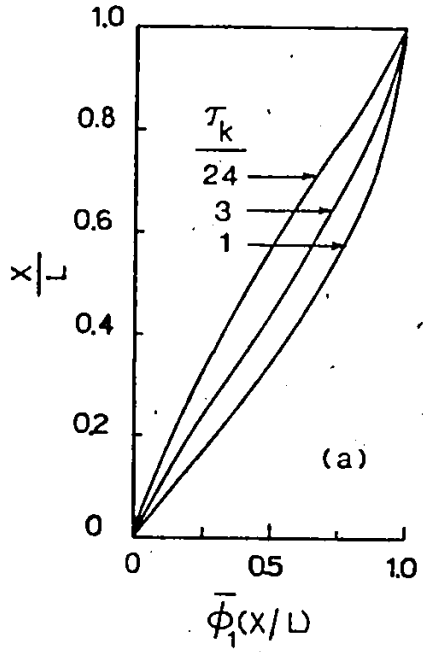

FUNDAMENTAL MODE

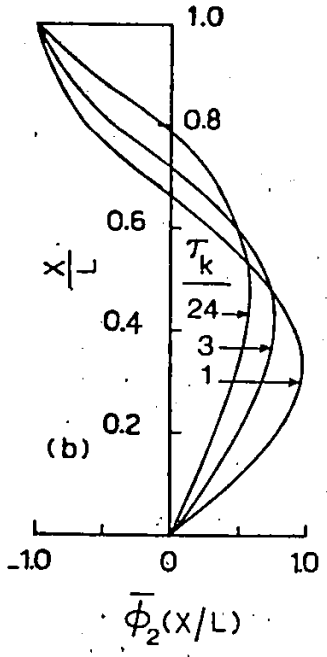

SECOND MODE

FIG. 7 SHEAR STIFFNESS TAPER AND MODE SHAPES

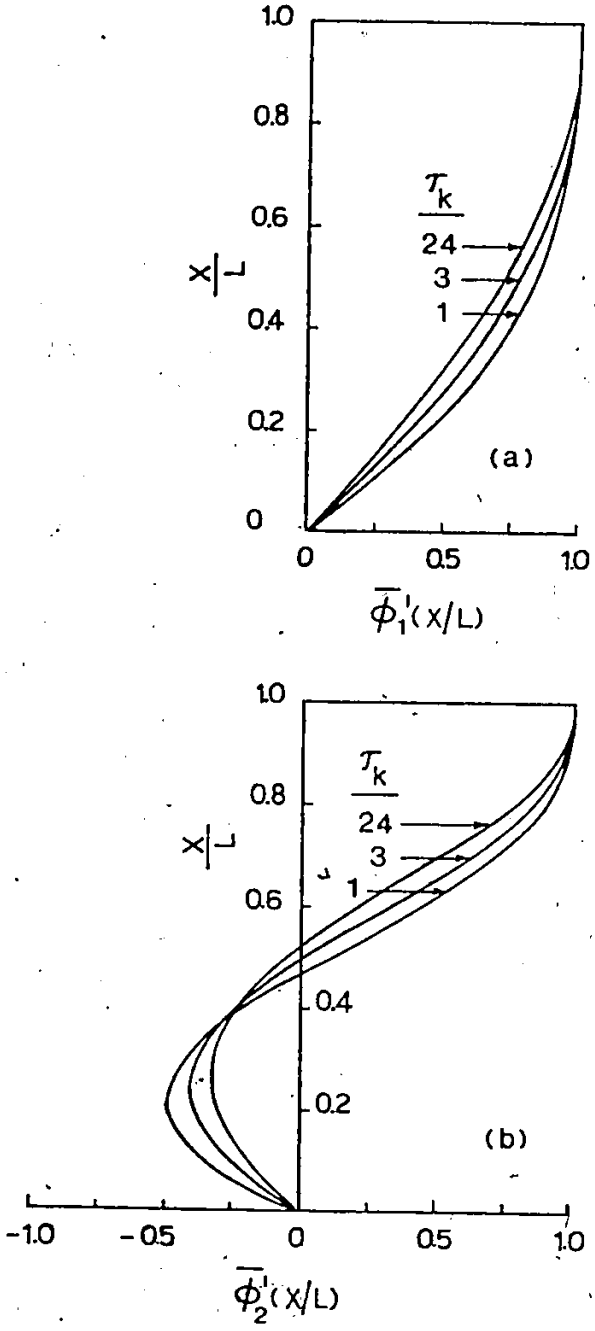

FIG. 8 FLEXURAL STIFFNESS TAPER AND FIRST DERIVATIVE OF MODE SHAPES

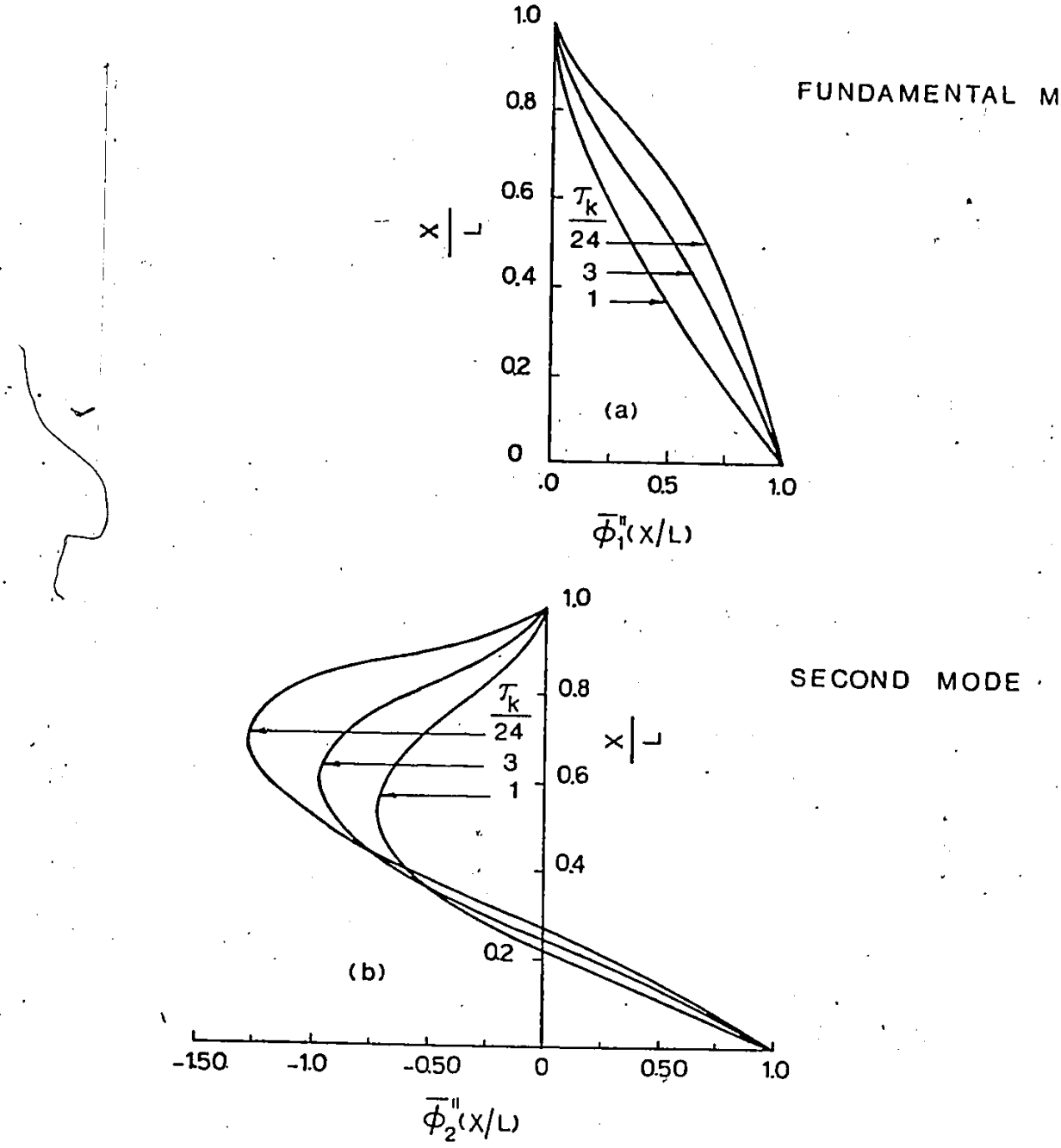

FIG. 9 FLEXURAL STIFFNESS TAPER AND SECOND DERIVATIVE OF MODE SHAPES

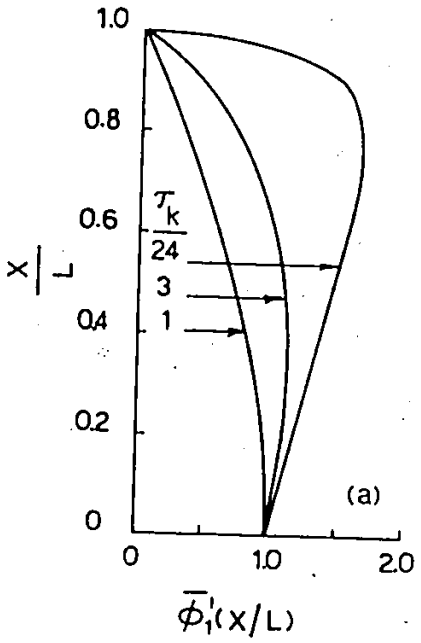

FUNDAMENTAL MODE

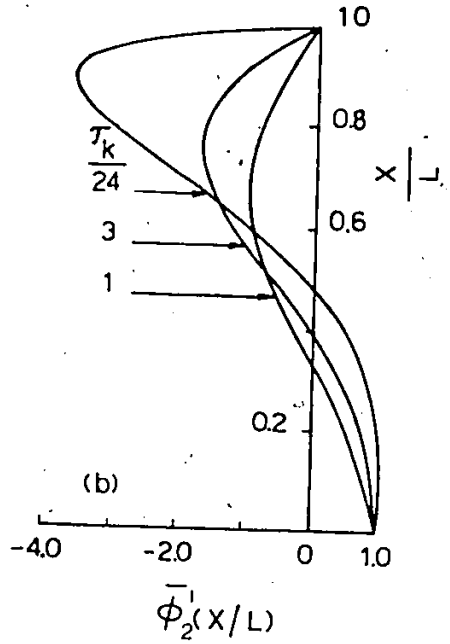

SECOND MODE

FIG. 10 SHEAR STIFFNESS TAPER AND FIRST DERIVATIVE OF MODE SHAPES

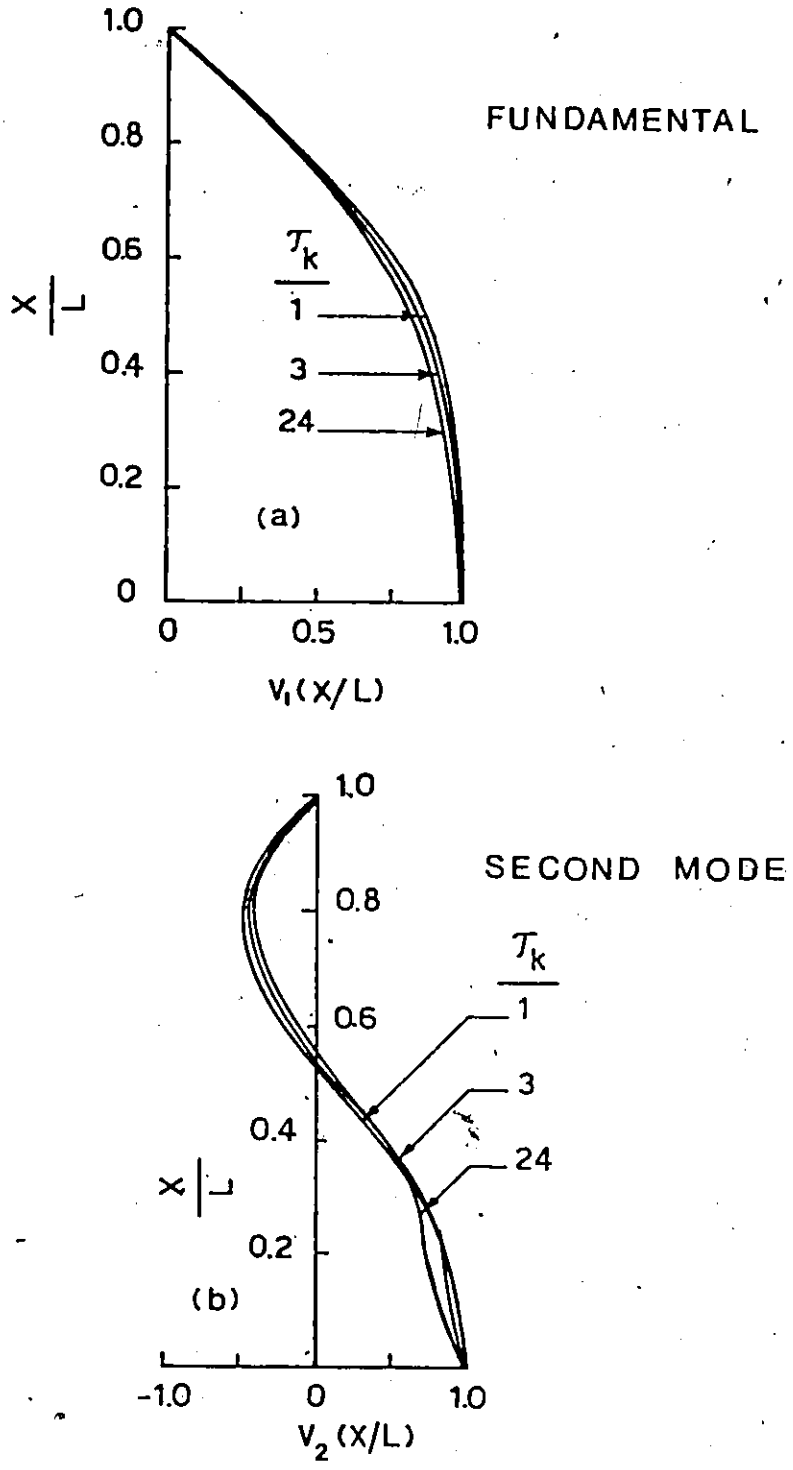

FIG. 11 FLEXURAL STIFFNESS TAPER AND BEAM SHEAR

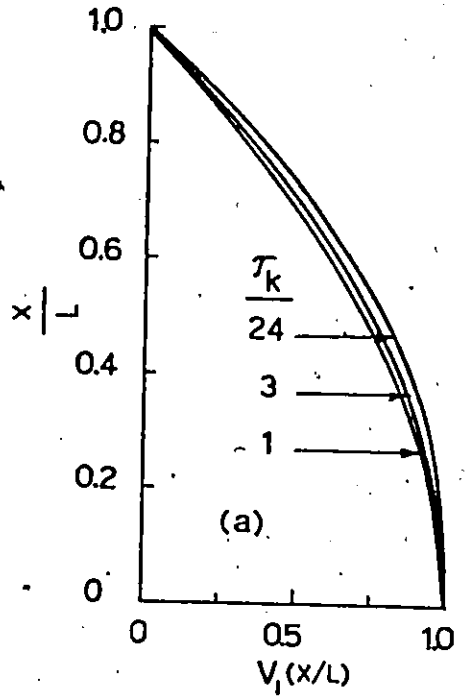

FUNDAMENTAL MODE

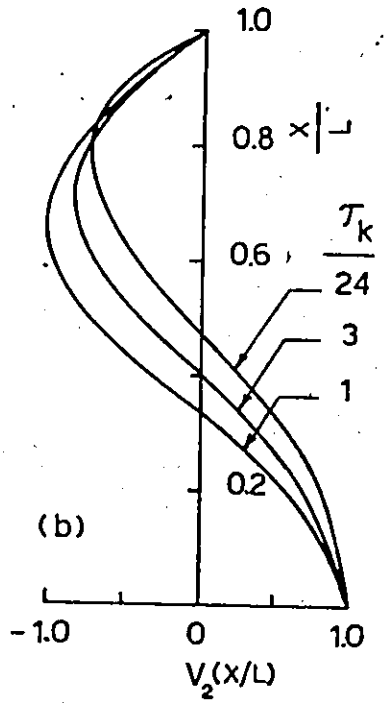

SECOND MODE

FIG. 12 SHEAR STIFFNESS TAPER AND BEAM SHEAR

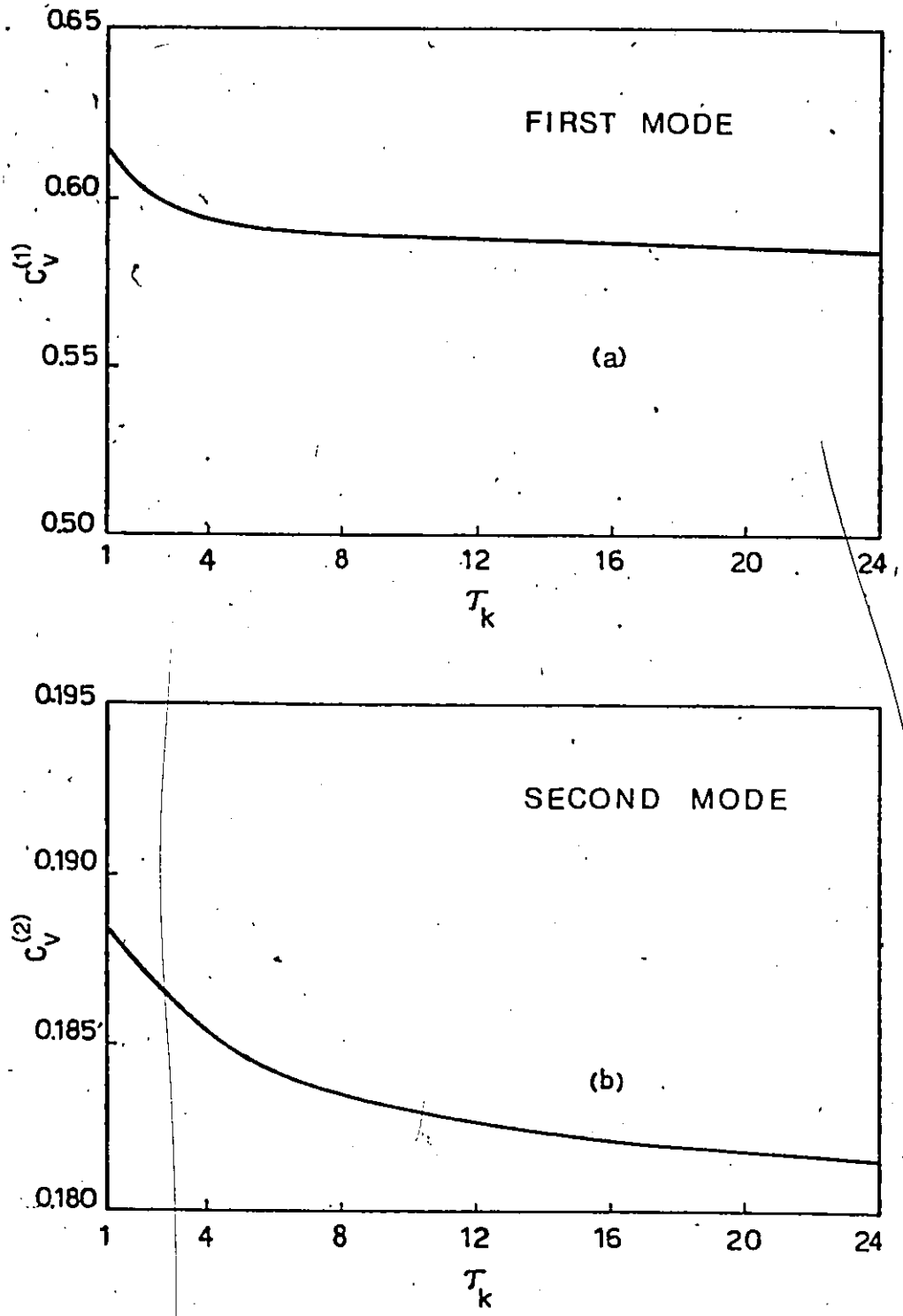

FIG. 13 FLEXURAL STIFFNESS TAPER AND MODAL SHEAR COEFFICIENTS

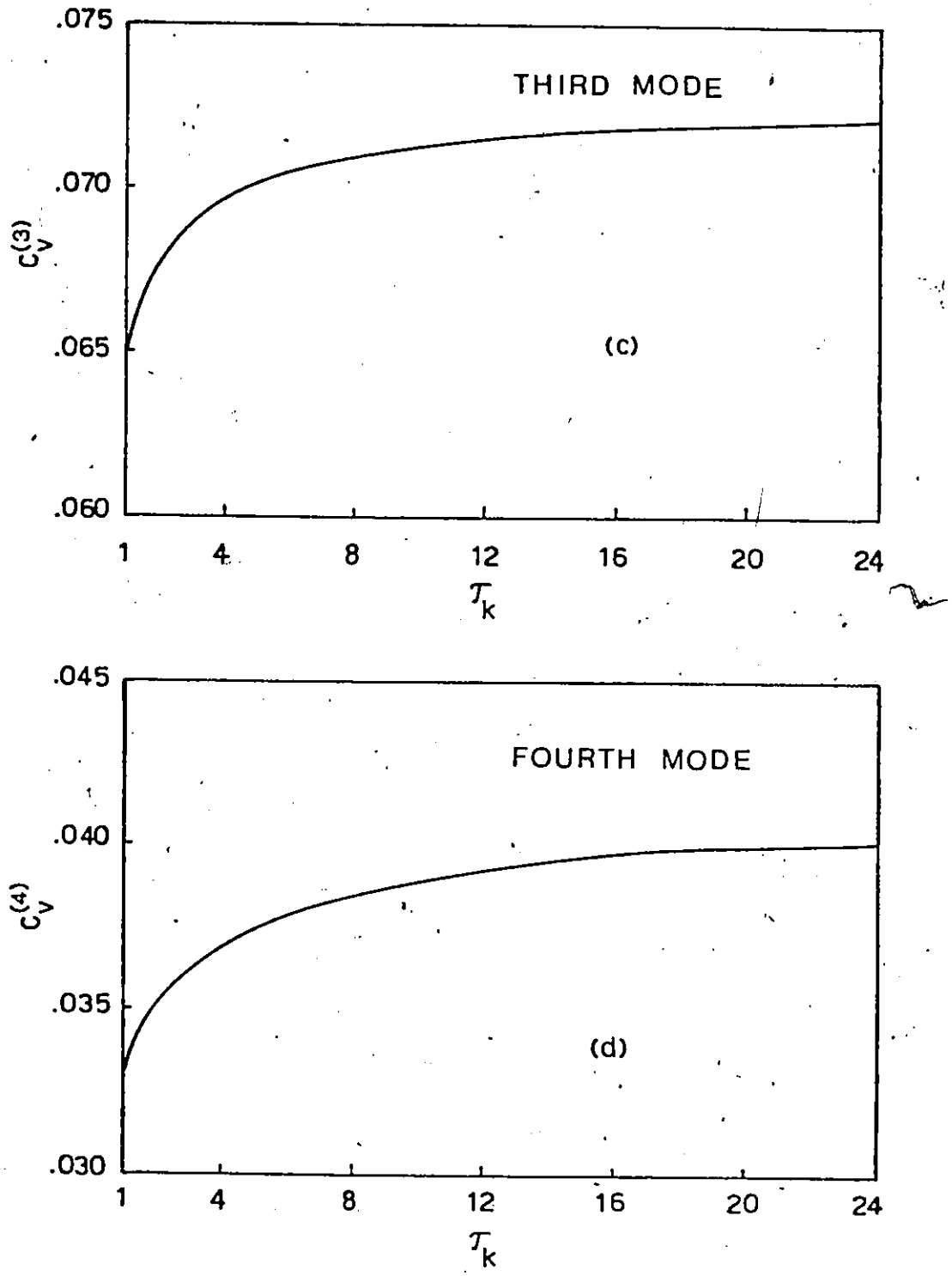

FIG. 13 (Cont'd) FLEXURAL STIFFNESS TAPER AND MODAL SHEAR COEFFICIENTS

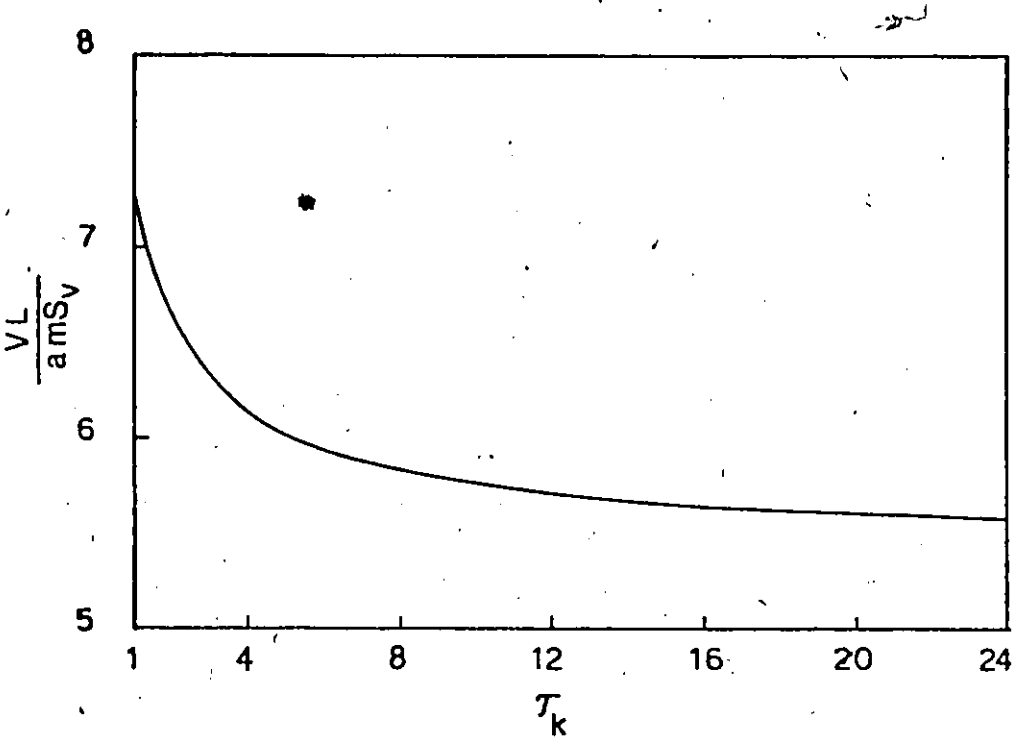

FIG. 14 FLEXURAL STIFFNESS TAPER AND TOTAL BASE SHEAR (SRSS)

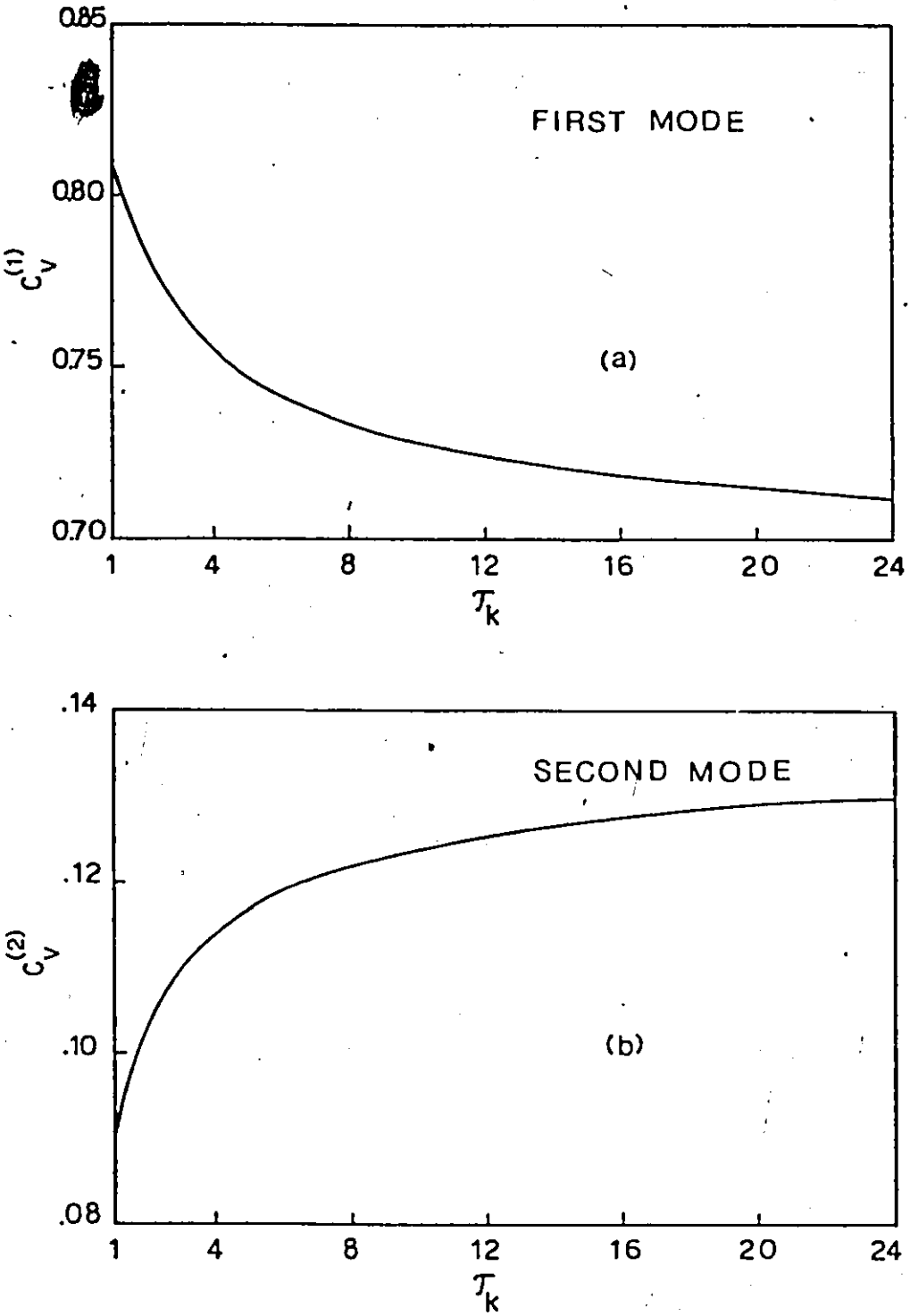

FIG. 15 SHEAR STIFFNESS TAPER AND MODAL SHEAR COEFFICIENTS

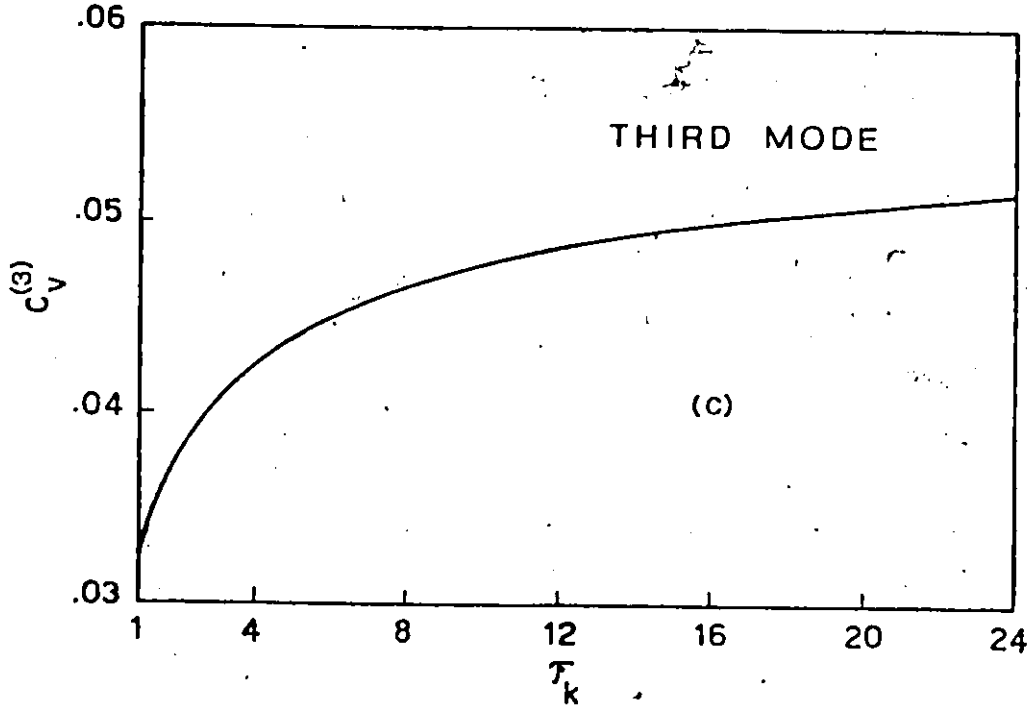

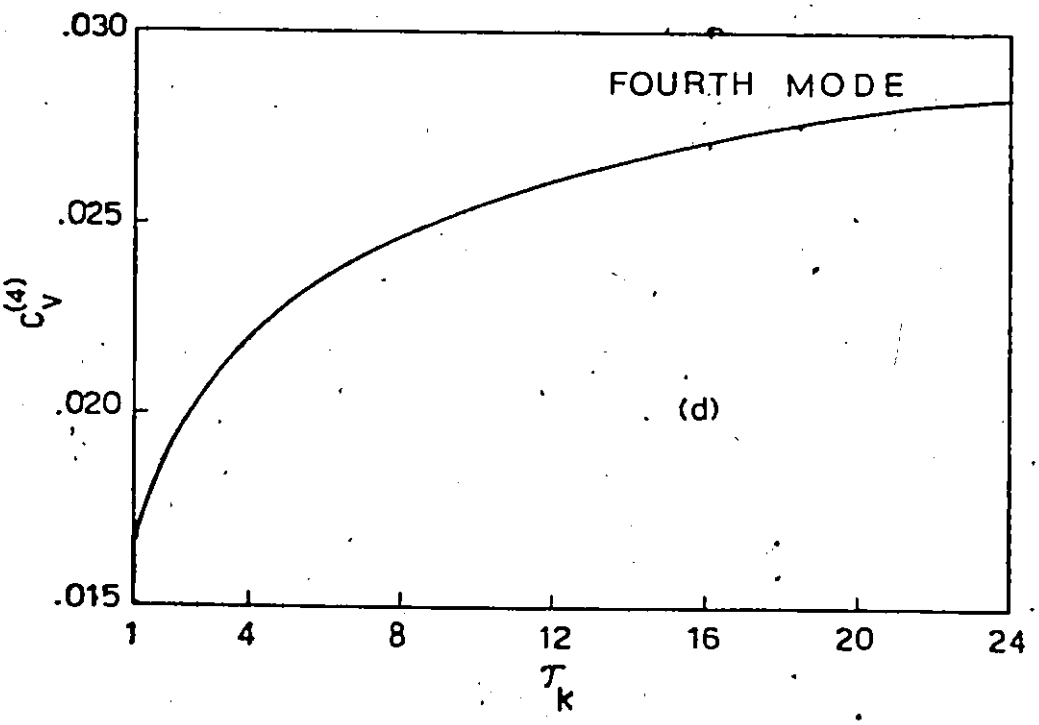

FIG. 15 (Cont'd) SHEAR STIFFNESS TAPER AND MODAL SHEAR COEFFICIENTS

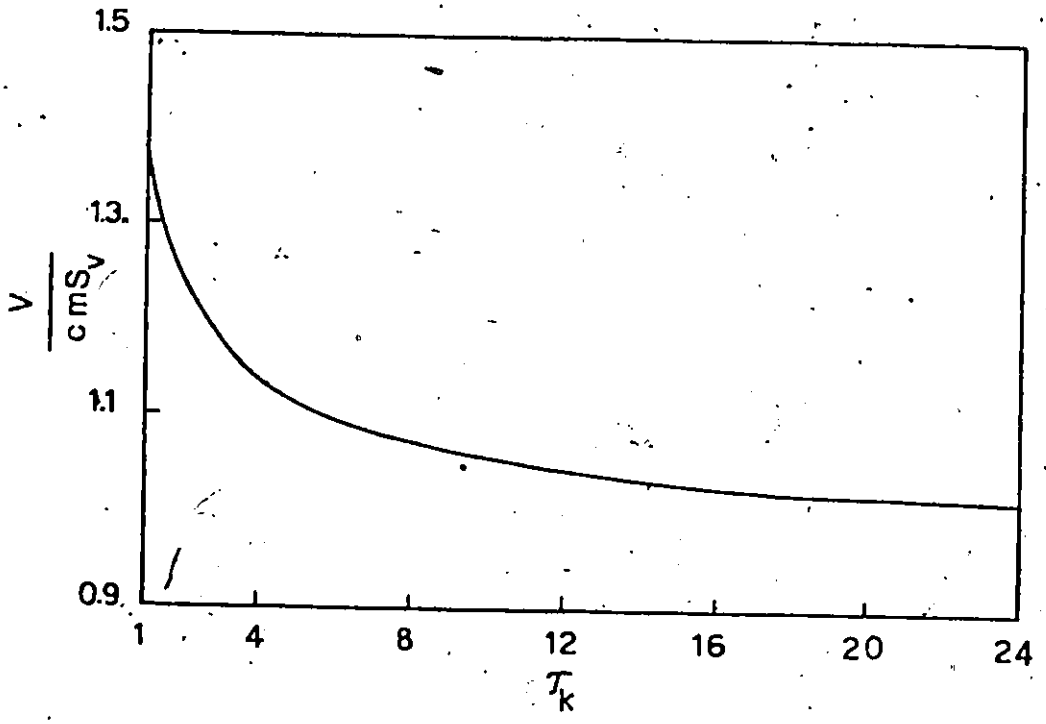

FIG. 16 SHEAR STIFFNESS TAPER AND TOTAL BASE SHEAR (SRSS)

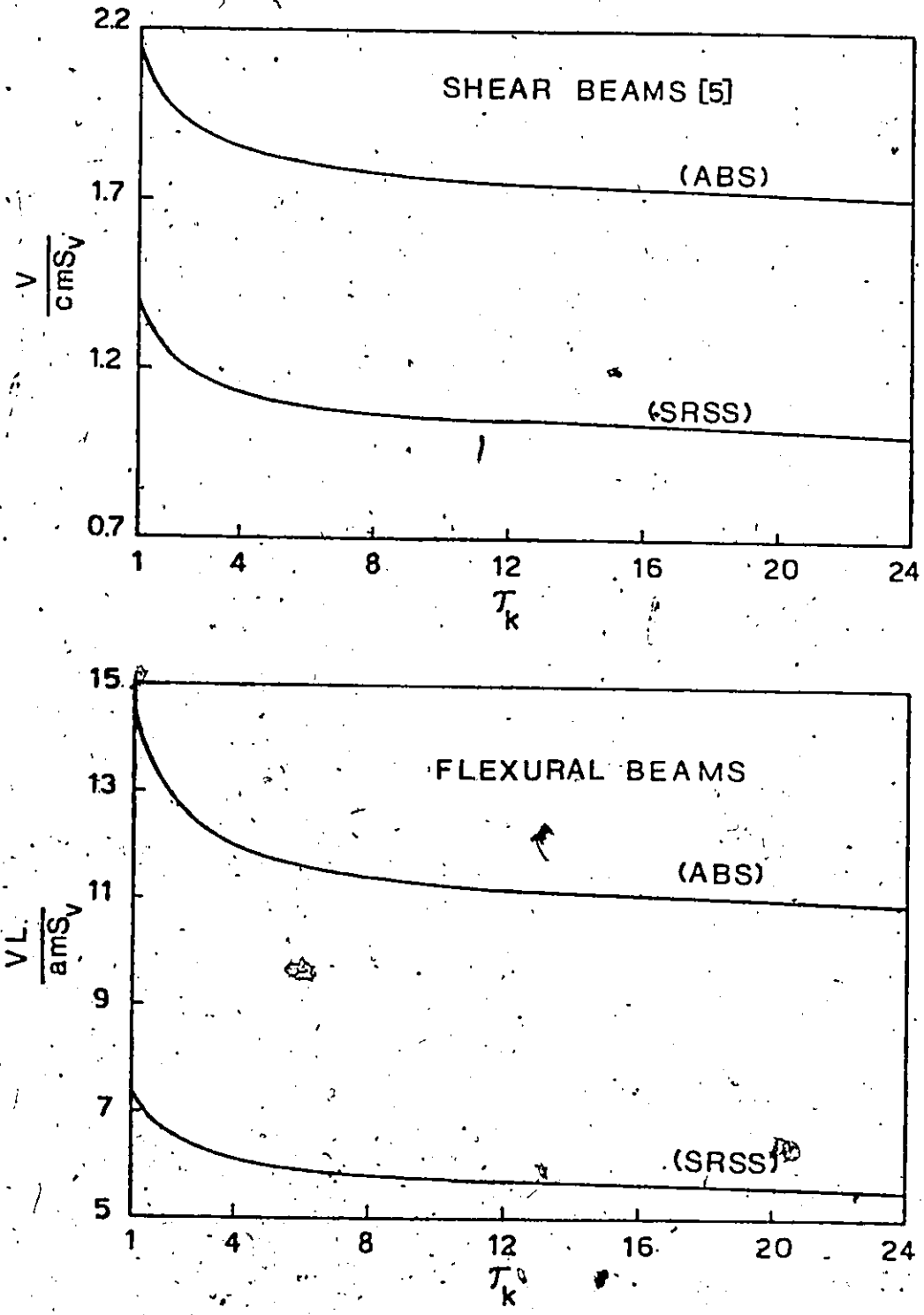

FIG. 17 EFFECT OF TAPER ON TOTAL BASE SHEAR

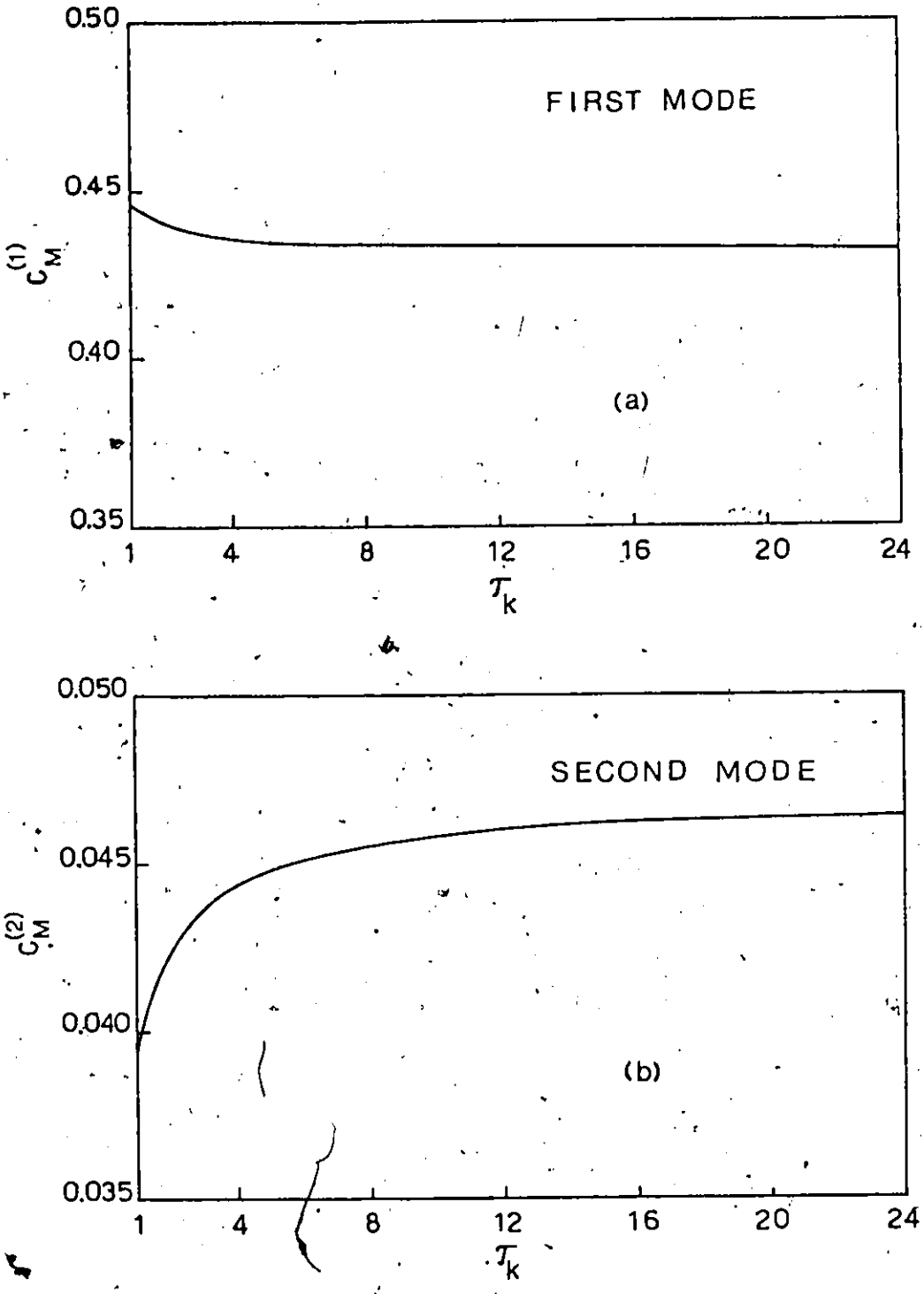

FIG. 18 FLEXURAL STIFFNESS TAPER AND MODAL OVERTURNING MOMENT COEFFICIENTS

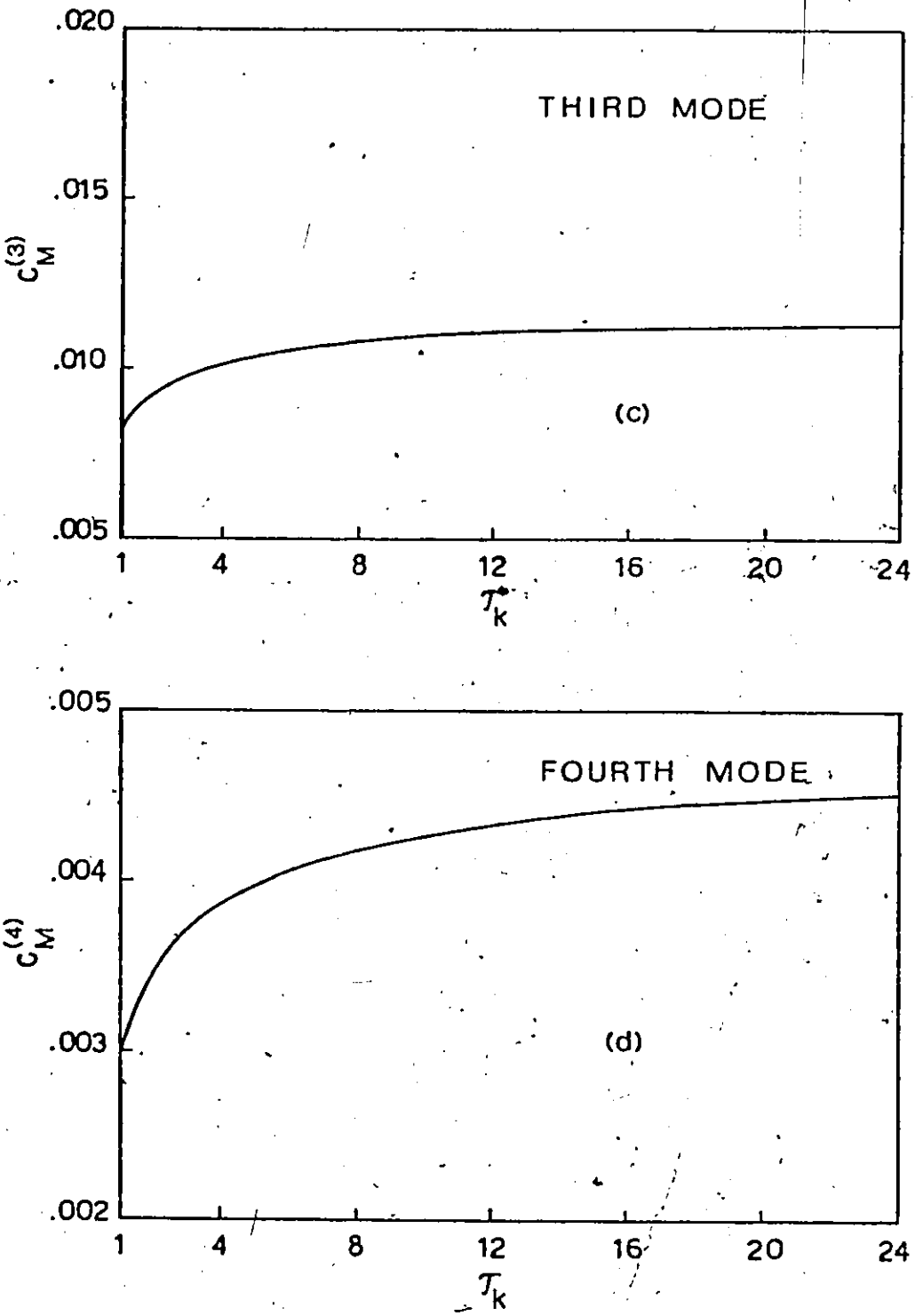

FIG. 18 (Cont'd) FLEXURAL STIFFNESS TAPER AND MODAL OVERTURNING MOMENT COEFFICIENTS

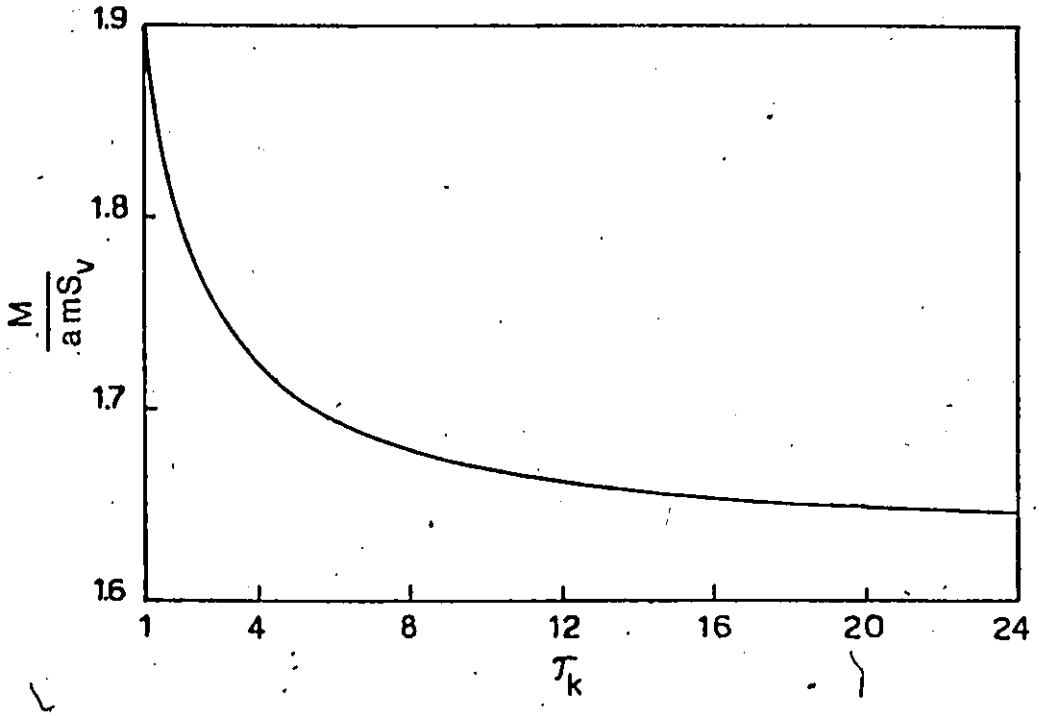

FIG. 19 FLEXURAL STIFFNESS TAPER AND TOTAL OVERTURNING MOMENT (SRSS)

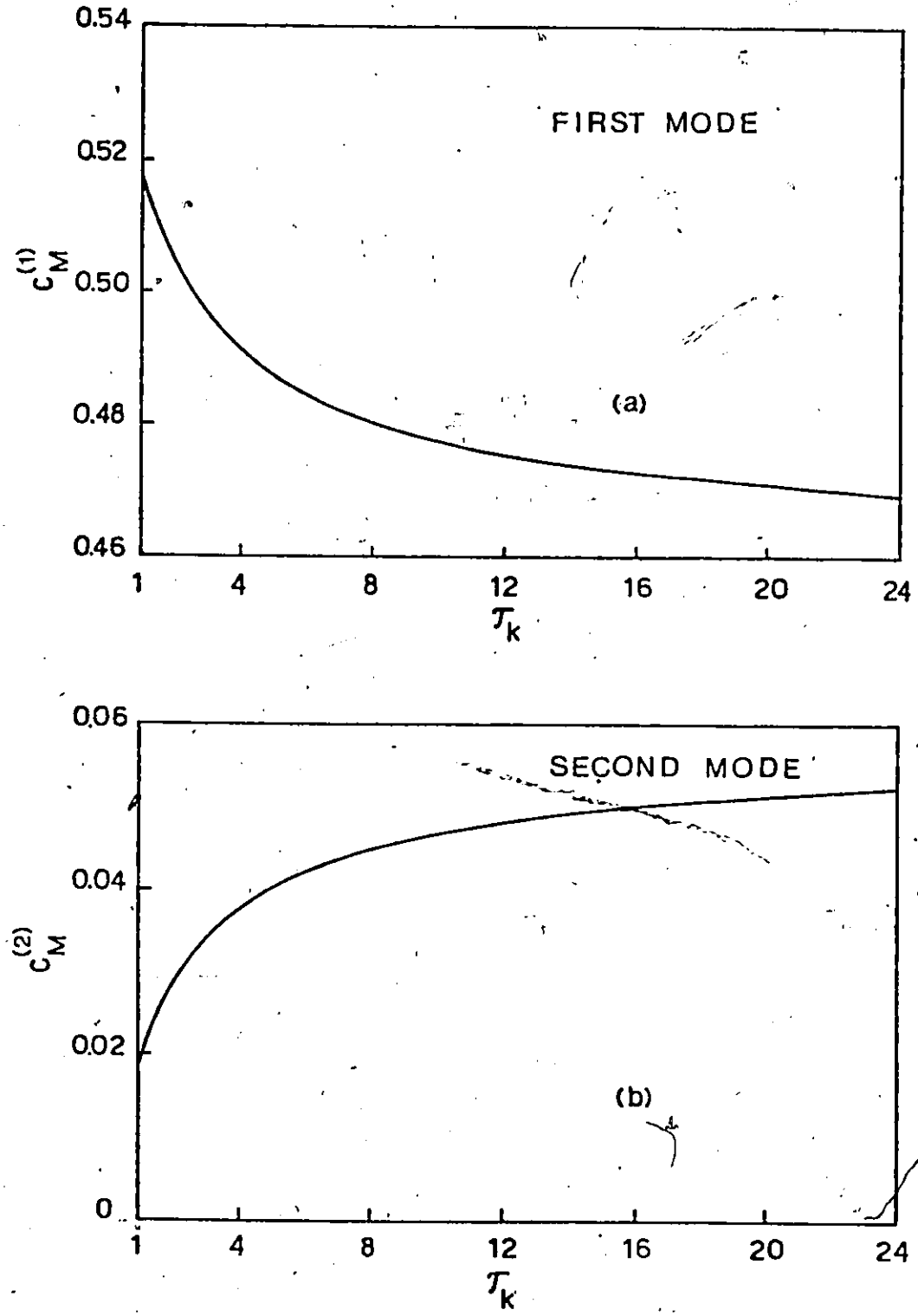

FIG. 20 SHEAR STIFFNESS TAPER AND MODAL OVERTURNING MOMENT COEFFICIENTS

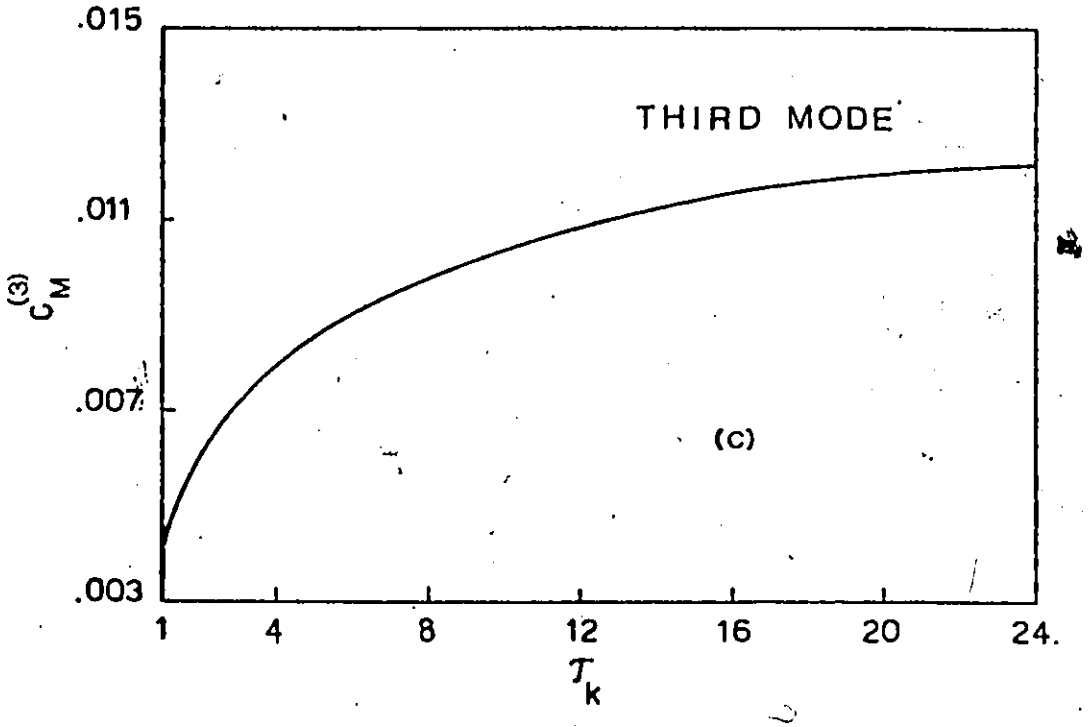

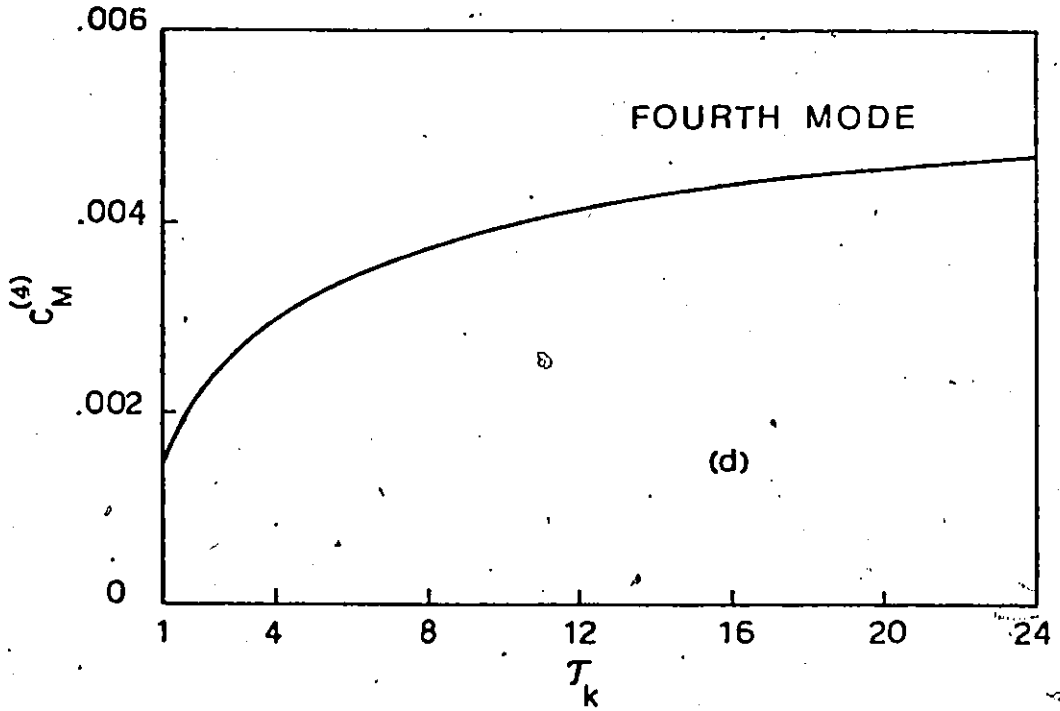

FIG. 20 (Cont'd) SHEAR STIFFNESS TAPER AND MODAL OVERTURNING MOMENT COEFFICIENTS

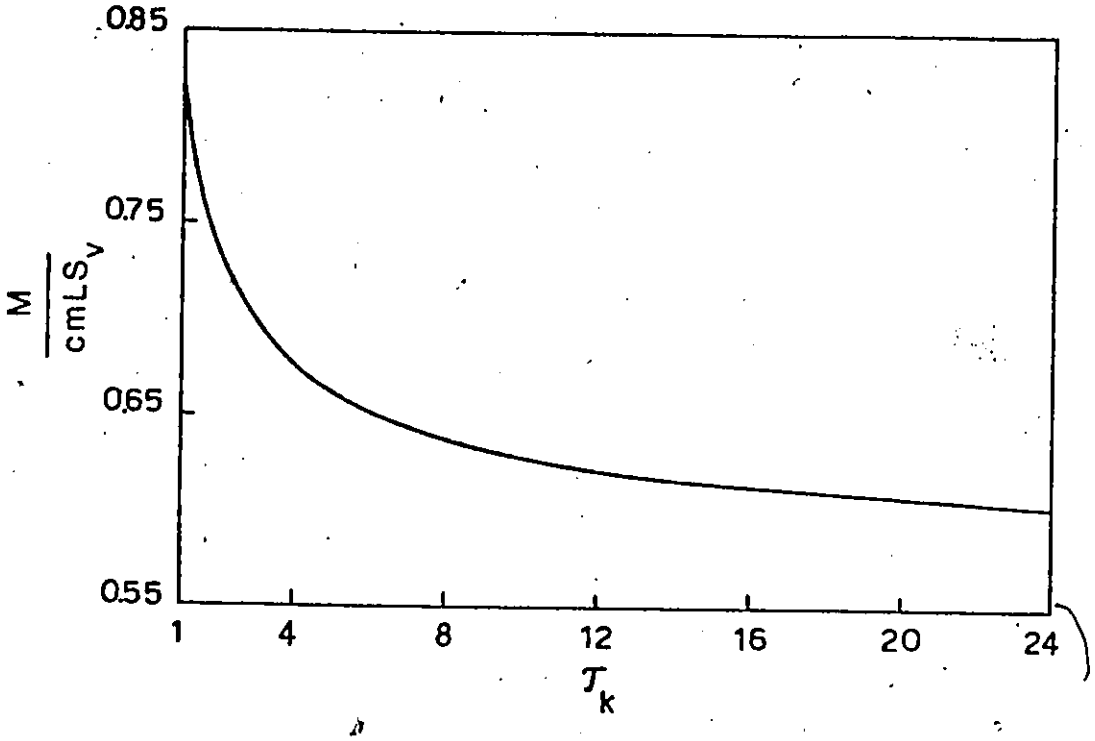

FIG. 21 SHEAR STIFFNESS TAPER AND TOTAL BASE OVERTURNING MOMENT (SRSS)

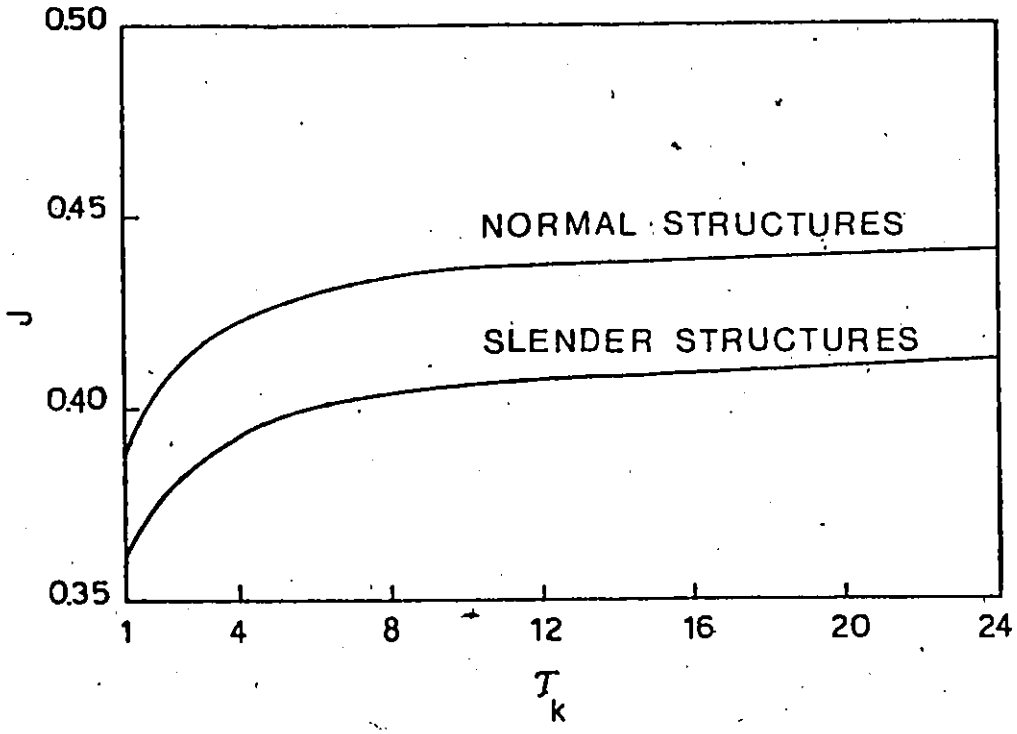

FIG. 22 FLEXURAL STIFFNESS TAPER AND MOMENT REDUCTION FACTOR

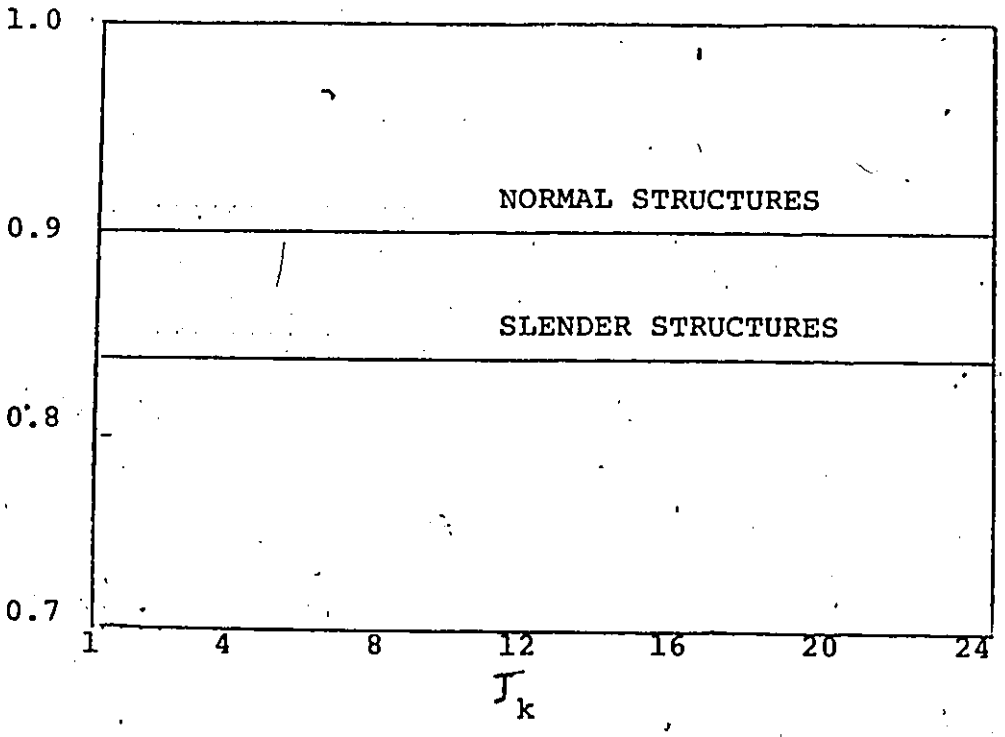

Fig 23 . SHEAR STIFFNESS TAPER AND MOMENT REDUCTION FACTOR

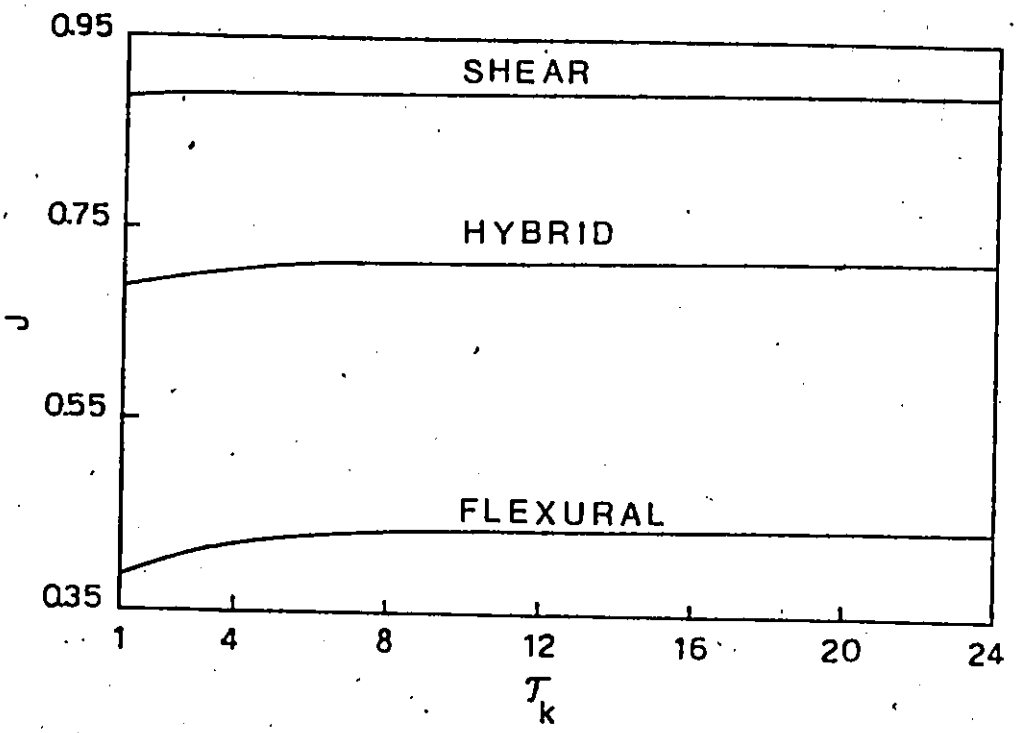

FIG. 24 MOMENT REDUCTION FACTOR FOR TAPERED HYBRID BEAMS

TABLE I - SUMMARY OF MODAL SHEAR COEFFICIENTS

Type of Beam	τ_k	$C_v^{(1)}$	$C_v^{(2)}$	$C_v^{(3)}$	$C_v^{(4)}$	$\sum_{r=1}^{4} C_v^{(r)}$
SHEAR	1.0	0.811	0.090	0.032	0.016	0.949
	3.0	0.765	0.110	0.040	0.020	0.935
	6.0	0.765	0.119	0.044	0.023	0.928
	9.0	0.730	0.123	0.046	0.024	0.923
FLEXURAL	1.0	0.613	0.188	0.065	0.033	0.899
	3.0	0.597	0.186	0.069	0.036	0.888
	6.0	0.591	0.184	0.071	0.038	0.884
	9.0	0.588	0.183	0.072	0.039	0.882
HYBRID	1.0	0.712	0.139	0.049	0.025	0.925
	3.0	0.681	0.148	0.055	0.028	0.912
	6.0	0.667	0.152	0.058	0.031	0.908
	9.0	0.659	0.153	0.059	0.032	0.903

REFERENCES

[1] Housner, G.W., and Keightely, W.O., "Vibrations of linearly Tapered Cantilever Beams", A.S.C.E. Transactions, Vol. 128, 1963, Part I.

[2] Salvadori, M.G., and Heer, E., "Periods of Framed Buildings for Earthquake Analysis", proceedings of the ASCE., Vol. 86, No. ST12, December, 1960.

[3] Humar, J.L., and Wright, E.Q., "Shear and Overturning Moment for Earthquake-Resistant Building Design", Canadian Journal of Civil Engineers, Vol. 2, 1975.

[4] Heidebrecht, A.C., "Dynamic Evaluation of Overturning Moment Reduction Factor Used in Static Seismic Loading", Canadian Journal of Civil Engineers, Vol. 2, 1975.

[5] Pekau, O.A., "Seismic Behaviour of Structures with Taper", Proceedings of the Fifth European Conference on Earthquakes, Istanbul, Turkey, 1975.

[6] Hurty, W.C., and Rubenstein, M.F., "Dynamics of Structures", Prentice-Hall Inc., 1964.

[7] Sir George Williams University - Digital Computer Centre, "Scientific Subroutine Specifications".

[8] Warburton, G.B., "The Dynamical Behaviour of Structures", Pergamon Press Ltd., 1964.

[9] National Building Code of Canada, 1975.

[10] Michie, J.N., "Differential and Integral Calculus", D. Van Nostrand Company Inc., 1947.

[11] ImsLib - International Mathematical and Statistical Libraries Inc. Fifth Edition, Huston, Texas.

[12] Pekau, O.A., "Earthquake Engineering", Lecture Notes for CE N700, Cancordia University, 1976.

APPENDIX I

VIBRATIONS OF UNIFORM SLENDER CANTILEVER BEAMS

1. Flexural Beams

The equation of equilibrium of a uniform cantilever beam [6], for free vibrations and neglecting the effect of shear deformations and rotary inertia is

$$\frac{\partial^2}{\partial x^2}\left[EI\,\frac{\partial^2 y}{\partial x^2}\right] + M\,\frac{\partial^2 y}{\partial t^2} = 0 \qquad (I.1)$$

With m constant, separation of variables gives the solution in terms of variables t and x; respectively as

$$g(t) = A \sin(\omega t) + B \cos(\omega t) \qquad (I.2)$$

in which A and B are arbitrary constants.

The second part of the solution, in terms of x, is in the form

$$\phi^{IV}(x) - \beta^4 \phi(x) = 0 \qquad (I.3)$$

The eigenvalue problem of Eq. (I.3) for boundary conditions of a cantilever beam has the frequency equation

$$\cosh(\beta L)\cos(\beta L) + 1 = 0 \qquad (I.4)$$

The corresponding natural frequencies are expressed in the form

$$\omega = (\beta L)^2 \sqrt{\frac{EI}{mL^4}} \qquad (I.5)$$

The following equation defines the mode shapes normalized to unit top displacement

$$\phi(x/L) = \frac{1}{2} \frac{[\cosh(\beta L) + \cos(\beta L)][\sinh(\beta L)(x/L) - \sin(\beta L)(x/L)]}{\sinh(\beta L)\cos(\beta L) - \cosh(\beta L)\sin(\beta L)}$$

$$- \frac{1}{2} \frac{[\sinh(\beta L) + \sin(\beta L)][\cosh(\beta L)(x/L) - \cos(\beta L)\, x/L)]}{\sinh(\beta L)\cos(\beta L) - \cosh(\beta L)\sin(\beta L)} \qquad (I.6)$$

2. Shear Beams

From Ref. [5], the equation defining the mode shapes is given in the form

$$\phi_i(x/L) = \sin(2i-1)\frac{\pi x}{2L} \qquad (I.7)$$

where i is the mode number.

APPENDIX II

GOVERNING EQUATIONS FOR TAPERED STIFFNESS BEAMS

1. Flexural Beams

The equation of equilibrium of a non-uniform cantilever beam, for free vibrations and neglecting the effect of shear deformations and rotary inertia is

$$\frac{\partial^2}{\partial x^2}\left[EI(x)\frac{\partial^2 y}{\partial x^2}\right] + m\frac{\partial^2 y}{\partial t^2} = 0 \qquad \text{(II.1)}$$

The solution of this equation is a function of x and t in the form

$$y(x,t) = \phi(x)g(t) \qquad \text{(II.2)}$$

The partial differentiation with respect to each of x and t leads to the equations

$$\frac{\partial^4 y(x,t)}{\partial x^4} = \phi^{IV}(x)g(t) \qquad \text{(II.3)}$$

$$\frac{\partial^2 y(x,t)}{\partial t^2} = \phi(x)\ddot{g}(t) \qquad \text{(II.4)}$$

The flexural stiffness of the beam EI(x) is a linear function of x. This function can be expressed in the form

$$EI(x) = EI_o\left[1 - \frac{(\tau_k - 1)}{\tau_k L}\right]x \qquad \text{(II.5a)}$$

where

$$EI_o = EI(o) = \text{flexural stiffness at the base} \quad \text{(II.5b)}$$

$$\tau_k = \frac{EI(o)}{EI(L)} = \text{ratio of base to top flexural stiffness} \quad \text{(II.5c)}$$

Substituting Eq. (5) into Eq. (1) leads, after rearranging terms, to

$$\frac{\phi^{IV}(x)}{\phi(x)} - 2\left(\frac{\tau_k - 1}{\tau_k L - \tau_k x + x}\right) \frac{\phi'''(x)}{\phi(x)} + \frac{m}{EI(x)} \frac{\ddot{g}(t)}{g(t)} = 0 \quad \text{(II.6)}$$

The corresponding eigenvalue problem consists of the following governing equation

$$\phi^{IV}(x) - 2\,(Ax + B)\phi'''(x) + C\,\phi(x) = 0 \quad \text{(II.7)}$$

for which a closed form solution is not available.

2. Shear Beams

From Ref. [5], the differential equation for tapered stiffness shear beam is

$$\frac{d^2\bar{\phi}}{d\nu^2} + \frac{1}{\nu}\frac{d\bar{\phi}}{d\nu} + \lambda^2\bar{\phi} = 0 \quad \text{(II.8)}$$

(where the bars denote transformed variables) with the transformation

$$\nu^2 = 4\left[1 - \frac{(\tau_k - 1)}{\tau_k L} x\right], \quad \nu > 0 \quad \text{(II.9)}$$

and

$$= \left(\frac{\omega L}{c}\right) \frac{\tau_k}{(\tau_k - 1)}$$

$$c = \sqrt{k_o/M}$$

The boundary conditions, in the transformed form, are (II.10)

$$\frac{d\bar{\phi}}{d\nu} = 0 \quad , \quad \nu = 2/\sqrt{\tau_k}$$

$$\bar{\phi} = 0 \quad , \quad \nu = 2 \qquad \text{(II.11)}$$

The non-dimensional frequency of the rth mode is

$$\frac{\omega_r L}{c} = \frac{(\tau_k - 1)}{\tau_k} \lambda_r \qquad \text{(II.12)}$$

The corresponding eigenfunction is

$$\bar{\phi}_r(\nu) = J_o(\lambda_r \nu) - \frac{J_o(2\lambda_r)}{Y_o(2\lambda_r)} Y_o(\lambda_r \nu) \qquad \text{(II.13)}$$

APPENDIX III

ORTHOGONALITY CONDITIONS FOR NON-UNIFORM BEAMS

1. Flexural Beams

The orthogonality conditions for flexural beams having constant mass and non-uniform stiffness distributions can be summarized as [8]

$$\int_0^L \bar{\phi}_r \, \bar{\phi}_s \, dx = 0 \qquad \text{(III.1)}$$

$$\int_0^L EI(x) \, \frac{d^2\bar{\phi}_r}{dx^2} \, \frac{d^2\bar{\phi}_s}{dx^2} \, dx = 0 \qquad \text{(III.2)}$$

$$\int_0^L \bar{\phi}_s \, \frac{d^2}{dx^2} \left[EI(x) \, \frac{d^2\bar{\phi}_r}{dx^2} \right] dx = 0 \qquad \text{(III.3)}$$

Eqs. (III.1), (III.2) and (III.3) are true for $r \neq s$ for uniform and non-uniform beams for any combination of free, simply supported anc clamped ends. For end conditions containing elastic constraints, Eqs. (III.1,3) are valid but not Eq. (III.2). For the special case of $r = s$, the orthogonality condition is given as [8]

$$m \, \omega_r^2 \int_0^L \bar{\phi}_r^2 \, dx = \int_0^L \bar{\phi}_r \, \frac{d^2}{dx^2} \left[EI(x) \, \frac{d^2\bar{\phi}_r}{dx^2} \right] dx \qquad \text{(III.4)}$$

2. Shear Beams

The orthogonality condition for non-uniform shear beams is given in Ref [5] as

$$\int_0^L k\ (x) \left[\frac{d\overline{\phi}_r}{dx}\ (x)\right]^2 dx = m\ \omega_r^2 \int_0^L \left[\overline{\phi}_r(x)\right]^2 dx \qquad \text{(III.5)}$$

APPENDIX IV

DERIVATION OF MODAL BASE SHEAR AND MODAL BASE OVERTURNING MOMENT EXPRESSIONS

1. Modal Base Shear

The base shear of the beam can be expressed in terms of the spectral velocity in the form

$$V_{r_{max}} = m\Gamma_r \omega_r S_v^{(r)} \int_0^L \overline{\phi}_r(x)\, dx \qquad (4\text{-}9)$$

$$V_{r_{max}} = m \frac{\int_0^L \overline{\phi}_r(x)\, dx}{\int_0^L \overline{\phi}_r^2(x)\, dx} \omega_r S_v^{(r)} \int_0^L \overline{\phi}(x)\, dx$$

$$\doteq m \frac{L \int_0^1 \overline{\phi}_r(x)\, dx}{L \int_0^1 \overline{\phi}_r^2(x)\, dx} \omega_r S_v^{(r)} L \int_0^1 \overline{\phi}_r(x)\, dx$$

$$= m\omega_r S_v^{(r)} L\, c_v^{(r)}$$

where

$$c_v^{(r)} = \frac{\left(\int_0^L \overline{\phi}_r(x)\, dx\right)^2}{\int_0^L \overline{\phi}_r^2(x)\, dx}$$

The normalized base shear can be expressed as

$$\frac{V_{r_{max}} \cdot L}{a\ m\ S_v} = \left(\frac{\omega_r L^2}{a}\right) \cdot c_v^{(r)} \qquad (4\text{-}10)$$

2. Modal Base Overturning Moment

The overturning moment at the base of the beam can be expressed in terms of the spectral velocity in the form

$$M_{r_{max}} = m\ \Gamma_r\ \omega_r\ S_v^{(r)} \int_0^L x\ \bar{\phi}_r(x)\ dx \qquad (4\text{-}12)$$

Using Eq. (4.2) for Γ_r in the preceding equation yields

$$M_{r_{max}} = m \frac{\int_0^L \bar{\phi}_r(x)\ dx}{\int_0^L \bar{\phi}_r^2(x)\ dx}\ \omega_r\ S_v^{(r)} \int_0^L x\bar{\phi}_r(x)\ dx$$

$$= m \frac{L\int_0^L \bar{\phi}_r(x)\ dx}{\int_0^L \bar{\phi}_r^2(x)\ dx}\ \omega_r\ S_v^{(r)} \cdot L^2 \int_0^L x\ \bar{\phi}_r(x)\ dx$$

$$= m\ \omega_r\ S_v^{(r)}\ L^2\ c_M^{(r)}$$

where

$$c_M^{(r)} = \frac{\int_0^1 \bar{\phi}_r(x)\ dx \int_0^1 x\bar{\phi}_r(x)\ dx}{\int_0^1 \bar{\phi}_r^2(x)\ dx}$$

The normalized base overturning moment can be expressed as

$$\frac{M_{r_{max}}}{a\ m\ S_v^{(r)}} = \left(\frac{\omega_r L^2}{a}\right) \cdot c_M^{(r)} \qquad (4\text{-}15)$$

APPENDIX V

EVALUATION OF INTEGRALS

1. Generalized Mass and Stiffness

(1) $\int_0^L \sin(\beta_i x)\sin(\beta_j x) = \int_0^L \sin\left(\beta L_i \frac{x}{L}\right)\sin\left(\beta L_j \frac{x}{L}\right) dx$

using the transformation $Z = \frac{x}{L}$

leads to $dx = L\,dZ$

$$\int_0^L \sin\left(\beta L_i \frac{x}{L}\right)\sin\left(\beta L_j \frac{x}{L}\right) dx = L\int_0^1 \sin(\beta L_i . Z)\sin(\beta L_j . Z)\,dZ$$

$$= L\left(\frac{\sin(\beta L_i - \beta L_j)}{2(\beta L_i - \beta L_j)} - \frac{\sin(\beta L_i + \beta L_j)}{2(\beta L_i + \beta L_j)}\right).$$

If $\beta L_i = \beta L_j$, the previous expression takes the form

$$\int_0^1 \sin^2(\beta L_i . Z)\,dZ = \left(\frac{1}{2} - \frac{1}{4\beta L_i}\sin(2\beta L_i)\right).$$

(2) $$\int_0^1 \cos(\beta L_i . Z)\sin(\beta L_j . Z)\,dZ = -1\left(\frac{\cos(\beta L_i + \beta L_j)}{2(\beta L_i + \beta L_j)} + \frac{\cos(\beta L_j - \beta L_i)}{2(\beta L_j - \beta L_i)} - \frac{1}{2(\beta L_i + \beta L_j)} - \frac{1}{2(\beta L_j - \beta L_i)}\right).$$

If $\beta L_i = \beta L_j$,

$$\int_0^1 \cos(\beta L_i . Z)\sin(\beta L_i . Z)\,dZ = \frac{1}{2(\beta L_i)}\sin^2(\beta L_i)$$

(3) $$\int_0^1 \sinh(\beta L_i . Z)\sin(\beta L_j . Z)\,dZ = \frac{1}{\beta L_i^2 + \beta L_j^2}\left(\beta L_i \sin(\beta L_j)\cosh(\beta L_i) - \beta L_j \cos(\beta L_j)\sinh(\beta L_i)\right)$$

If $\beta L_i = \beta L_j$,

$$\int_0^1 \sinh(\beta L_i . Z)\sin(\beta L_i . Z)\,dZ = \frac{1}{2\beta L_i}\left(\sin(\beta L_i)\cosh(\beta L_i) - \cos(\beta L_i)\sinh(\beta L_i)\right).$$

$$(4)\ \int_0^1 \cosh(\beta L_i . z)\ \sin(\beta L_j . z)\, dz = \frac{1}{\beta L_i^2 + \beta L_j^2} \left(\beta L_i \sin(\beta L_j) \sinh(\beta L_i) - \beta L_j \cos(\beta L_j) \cosh(\beta L_i) + \beta L_j \right)$$

If $\beta L_i = \beta L_j$,

$$\int_0^1 \cosh(\beta L_i . z)\ \sin(\beta L_i . z)\, dz = \frac{1}{2\beta L_i} \left(\sin(\beta L_i) \sinh(\beta L_i) - \cos(\beta L_i) \cosh(\beta L_i) + 1 \right).$$

$$(5)\ \int_0^1 \sin(\beta L_i . z)\ \cos(\beta L_j . z)\, dz = -1 \left(\frac{\cos(\beta L_i + \beta L_j)}{2(\beta L_i + \beta L_j)} + \frac{\cos(\beta L_i - \beta L_j)}{2(\beta L_i - \beta L_j)} - \frac{1}{2(\beta L_i + \beta L_j)} - \frac{1}{2(\beta L_i - \beta L_j)} \right).$$

If $\beta L_i = \beta L_j$,

$$\int_0^1 \sin(\beta L_i . z)\ \cos(\beta L_i . z)\, dz = \frac{1}{2\beta L_i} \sin^2 \beta L_i .$$

$$(6)\ \int_0^1 \cos(\beta L_i . z)\ \cos(\beta L_j . z)\, dz = \frac{\sin(\beta L_i - \beta L_j)}{2(\beta L_i - \beta L_j)} + \frac{\sin(\beta L_i + \beta L_j)}{2(\beta L_i + \beta L_j)} .$$

If $\beta L_i = \beta L_j$,

$$\int_0^1 \cos^2(\beta L_i . z)\, dz = \frac{\sin(2\beta L_i)}{4\beta L_i} + \frac{1}{2} .$$

$$(7)\ \int_0^1 \sinh(\beta L_i . z)\ \cos(\beta L_j . z)\, dz = \frac{1}{\beta L_i^2 + \beta L_j^2} \left(\beta L_j \sin(\beta L_j) \sinh(\beta L_i) + \beta L_i \cos(\beta L_j) \cosh(\beta L_i) - \beta L_i \right).$$

If $\beta L_i = \beta L_j$,

$$\int_0^1 \sinh(\beta L_i . z)\ \cos(\beta L_i . z)\, dz = \frac{1}{2\beta L_i} \left(\sin(\beta L_i) \sinh(\beta L_i) + \cos(\beta L_i) \cosh(\beta L_i) - 1 \right).$$

$$(8)\ \int_0^1 \cosh(\beta L_i . z)\ \cos(\beta L_j . z)\, dz = \frac{1}{\beta L_i^2 + \beta L_j^2} \left(\beta L_j \sin(\beta L_j) \cosh(\beta L_i) + \beta L_i \cos(\beta L_j) \sinh(\beta L_i) \right).$$

If $\beta L_i = \beta L_j$

$$\int_0^1 \cosh(\beta L_i . z)\ \cos(\beta L_i . z)\, dz = \frac{1}{2\beta L_i} \left(\sin(\beta L_i) \cosh(\beta L_i) + \cos(\beta L_i) \sinh(\beta L_i) \right).$$

$$(9)\quad \int_0^1 \sin(\beta L_i . z)\,\sinh(\beta L_j . z)\,dz = \frac{1}{\beta L_i^2 + \beta L_j^2}\left(\beta L_j \sin(\beta L_i)\cosh(\beta L_j) - \beta L_i \cos(\beta L_i)\sinh(\beta L_j)\right).$$

If $\beta L_i = \beta L_j$,

$$\int_0^1 \sin(\beta L_i . z)\,\sinh(\beta L_i . z)\,dz = \frac{1}{2\beta L_i}\left(\sin(\beta L_i)\cosh(\beta L_i) - \cos(\beta L_i)\sinh(\beta L_i)\right).$$

$$(10)\quad \int_0^1 \cos(\beta L_i . z)\,\sinh(\beta L_j . z)\,dz = \frac{1}{\beta L_i^2 + \beta L_j^2}\left(\beta L_i \sin(\beta L_i)\sinh(\beta L_j) + \beta L_j \cos(\beta L_i)\cosh(\beta L_j) - \beta L_j\right).$$

If $\beta L_i = \beta L_j$,

$$\int_0^1 \cos(\beta L_i . z)\,\sinh(\beta L_i . z)\,dz = \frac{1}{2\beta L_i}\left(\sin(\beta L_i)\sinh(\beta L_i) + \cos(\beta L_i)\cosh(\beta L_i) - 1\right).$$

$$(11)\quad \int_0^1 \sinh(\beta L_i . z)\,\sinh(\beta L_j . z)\,dz = \frac{\sinh(\beta L_i + \beta L_j)}{2(\beta L_i + \beta L_j)} - \frac{\sinh(\beta L_i - \beta L_j)}{2(\beta L_i - \beta L_j)}.$$

If $\beta L_i = \beta L_j$,

$$\int_0^1 \sinh^2(\beta L_i . z)\,dz = \frac{\sinh(2\beta L_i)}{4\beta L_i} - \frac{1}{2}.$$

$$(12)\quad \int_0^1 \cosh(\beta L_i . z)\,\sinh(\beta L_j . z)\,dz = \frac{\cosh(\beta L_i + \beta L_j)}{2(\beta L_i + \beta L_j)} + \frac{\cosh(\beta L_i - \beta L_j)}{2(\beta L_i - \beta L_j)} - \frac{1}{2(\beta L_i + \beta L_j)} - \frac{1}{2(\beta L_i - \beta L_j)}.$$

If $\beta L_i = \beta L_j$,

$$\int_0^1 \cosh(\beta L_i . z)\,\sinh(\beta L_i . z)\,dz = \frac{\cosh(2\beta L_i)}{4\beta L_i} - \frac{1}{4\beta L_i}.$$

$$(13)\quad \int_0^1 \sin(\beta L_i . z)\,\cosh(\beta L_j . z)\,dz = \frac{1}{\beta L_i^2 + \beta L_j^2}\left(\beta L_j \sin(\beta L_i)\sinh(\beta L_j) - \beta L_i \cos(\beta L_i)\cosh(\beta L_j) + \beta L_j\right).$$

If $\beta L_i = \beta L_j$

$$\int_0^1 \sin(\beta L_i . z)\,\cosh(\beta L_i . z)\,dz = \frac{1}{2\beta L_i}\left(\sin(\beta L_i)\sinh(\beta L_i) - \cos(\beta L_i)\cosh(\beta L_i) + 1\right).$$

$$(14)\quad \int_0^1 \cos(\beta L_i . z)\cosh(\beta L_j . z)\,dz = \frac{1}{\beta L_i^2 + \beta L_j^2}\left(\beta L_i \sin(\beta L_i)\cosh(\beta L_j) + \beta L_j \cos(\beta L_i)\sinh(\beta L_j)\right).$$

If $\beta L_i = \beta L_j$,

$$\int_0^1 \cos(\beta L_i . z)\cosh(\beta L_i . z)\,dz = \frac{1}{2\beta L_i}\left(\sin(\beta L_i)\cosh(\beta L_i) + \cos(\beta L_i)\sinh(\beta L_i)\right).$$

$$(15)\quad \int_0^1 \sinh(\beta L_i . z)\cosh(\beta L_j . z)\,dz = \frac{\cosh(\beta L_i + \beta L_j)}{2(\beta L_i + \beta L_j)} + \frac{\cosh(\beta L_i - \beta L_j)}{2(\beta L_i - \beta L_j)} - \frac{1}{2(\beta L_i + \beta L_j)} - \frac{1}{2(\beta L_i - \beta L_j)}.$$

If $\beta L_i = \beta L_j$,

$$\int_0^1 \sinh(\beta L_i . z)\cosh(\beta L_i . z)\,dz = \frac{\cosh(2\beta L_i)}{4\beta L_i} - \frac{1}{4\beta L_i}.$$

$$(16)\quad \int_0^1 \cosh(\beta L_i . z)\cosh(\beta L_j . z)\,dz = \frac{\sinh(\beta L_i + \beta L_j)}{2(\beta L_i + \beta L_j)} + \frac{\sinh(\beta L_i - \beta L_j)}{2(\beta L_i - \beta L_j)}$$

If $\beta L_i = \beta L_j$,

$$\int_0^1 \cosh^2(\beta L_i . z)\,dz = \frac{\sinh(2\beta L_i)}{4\beta L_i} + \frac{1}{2}.$$

$$(17)\quad \int_0^1 z \sin(\beta L_i . z)\sin(\beta L_j . z)\,dz = \frac{\sin(\beta L_i - \beta L_j)}{2(\beta L_i - \beta L_j)} - \frac{\sin(\beta L_i + \beta L_j)}{2(\beta L_i + \beta L_j)} + \frac{\cos(\beta L_i - \beta L_j)}{2(\beta L_i - \beta L_j)^2} - \frac{\cos(\beta L_i + \beta L_j)}{2(\beta L_i + \beta L_j)^2} - \frac{1}{2(\beta L_i - \beta L_j)^2} + \frac{1}{2(\beta L_i + \beta L_j)^2}.$$

If $\beta L_i = \beta L_j$,

$$\int_0^1 z \sin^2(\beta L_i . z)\,dz = -\frac{\sin(2\beta L_i)}{4\beta L_i} - \frac{\cos(2\beta L_i)}{8\beta L_i^2} + \frac{1}{4} + \frac{1}{8\beta L_i^2}.$$

$$(18)\quad \int_0^1 z\cos(\beta L_i z)\sin(\beta L_j z)\,dz = -\frac{\cos(\beta L_j-\beta L_i)}{2(\beta L_j-\beta L_i)} + \frac{\cos(\beta L_i+\beta L_j)}{2(\beta L_i+\beta L_j)} + \frac{\sin(\beta L_j-\beta L_i)}{2(\beta L_j-\beta L_i)^2} + \frac{\sin(\beta L_i+\beta L_j)}{2(\beta L_i+\beta L_j)^2}.$$

If $\beta L_i = \beta L_j$

$$\int_0^1 z\cdot\cos(\beta L_i z)\sin(\beta L_i z)\,dz = \frac{\sin(2\beta L_i)}{8\beta L_i^2} - \frac{\cos(2\beta L_i)}{4\beta L_i}.$$

$$(19)\quad \int_0^1 z\sinh(\beta L_i z)\sin(\beta L_j z)\,dz = \frac{1}{\beta L_i^2+\beta L_j^2}\left(\beta L_i\sin(\beta L_j)\cosh(\beta L_i) - \beta L_j\cos(\beta L_j)\sinh(\beta L_i)\right) - \frac{\beta L_i}{(\beta L_i^2+\beta L_j^2)^2}\left(\beta L_i\sin(\beta L_j)\sinh(\beta L_i) - \beta L_j\cos(\beta L_j)\cosh(\beta L_i)+\beta L_j\right) + \frac{\beta L_j}{(\beta L_i^2+\beta L_j^2)^2}\left(\beta L_j\sin(\beta L_j)\sinh(\beta L_i) + \beta L_i\cos(\beta L_j)\cosh(\beta L_i)-\beta L_i\right).$$

If $\beta L_i = \beta L_j$

$$\int_0^1 z\sinh(\beta L_i z)\sin(\beta L_i z)\,dz = \frac{1}{2\beta L_i}\left(\sin(\beta L_i)\cosh(\beta L_i) - \cos(\beta L_i)\sinh(\beta L_i)\right) + \frac{1}{2\beta L_i^2}\cos(\beta L_i)\cosh(\beta L_i) - \frac{1}{2\beta L_i^2}.$$

$$(20)\quad \int_0^1 z\cosh(\beta L_i z)\sin(\beta L_j z)\,dz = \frac{1}{\beta L_i^2+\beta L_j^2}\left(\beta L_i\sin(\beta L_j)\sinh(\beta L_i) - \beta L_j\cos(\beta L_j)\cosh(\beta L_i)+\beta L_j\right) - \frac{\beta L_i}{(\beta L_i^2+\beta L_j^2)^2}\left(\beta L_i\sin(\beta L_j)\cosh(\beta L_i) - \beta L_j\cos(\beta L_j)\sinh(\beta L_i)\right) + \frac{\beta L_j}{(\beta L_i^2+\beta L_j^2)^2}\left(\beta L_j\sin(\beta L_j)\cosh(\beta L_i) + \beta L_i\cos(\beta L_j)\sinh(\beta L_i)\right).$$

If $\beta L_i = \beta L_j$

$$\int_0^1 z\cosh(\beta L_i z)\sin(\beta L_i z)\,dz = \frac{1}{2\beta L_i}\left(\sin(\beta L_i)\sinh(\beta L_i) - \cos(\beta L_i)\cosh(\beta L_i)\right) + \frac{1}{2\beta L_i^2}\cos(\beta L_i)\sinh(\beta L_i).$$

$$(21)\ \int_0^1 z \sin(\beta L_i . z) \cos(\beta L_j . z)\, dz = \frac{\cos(\beta L_i - \beta L_j)}{2(\beta L_i - \beta L_j)} + \frac{\cos(\beta L_i + \beta L_j)}{2(\beta L_i + \beta L_j)} + \frac{\sin(\beta L_i - \beta L_j)}{2(\beta L_i - \beta L_j)^2} + \frac{\sin(\beta L_i + \beta L_j)}{2(\beta L_i + \beta L_j)^2}$$

If $\beta L_i = \beta L_j$, See expression 18

$$(22)\ \int_0^1 z \cos(\beta L_i . z) \cos(\beta L_j . z)\, dz = \frac{\sin(\beta L_i - \beta L_j)}{2(\beta L_i - \beta L_j)} + \frac{\sin(\beta L_i + \beta L_j)}{2(\beta L_i + \beta L_j)} + \frac{\cos(\beta L_i - \beta L_j)}{2(\beta L_i - \beta L_j)^2} + \frac{\cos(\beta L_i + \beta L_j)}{2(\beta L_i + \beta L_j)^2} - \frac{1}{2(\beta L_i - \beta L_j)^2} - \frac{1}{2(\beta L_i + \beta L_j)^2}$$

If $\beta L_i = \beta L_j$,

$$\int_0^1 z \cos^2(\beta L_i . z)\, dz = \frac{\sin(2\beta L_i)}{4\beta L_i} + \frac{\cos(2\beta L_i)}{8\beta L_i^2} + \frac{1}{4} - \frac{1}{8\beta L_i^2}$$

$$(23)\ \int_0^1 z \sinh(\beta L_i . z) \cos(\beta L_j z)\, dz = \frac{1}{\beta L_i^2 + \beta L_j^2}\left(\beta L_j \sin(\beta L_j) \sinh(\beta L_i) + \beta L_i \cos(\beta L_j) \cosh(\beta L_i) - \beta L_i\right) - \frac{\beta L_j}{(\beta L_i^2 + \beta L_j^2)^2}\left(\beta L_i \sin(\beta L_j) \cosh(\beta L_i) - \beta L_j \cos(\beta L_j) \sinh(\beta L_i)\right) - \frac{\beta L_i}{(\beta L_i^2 + \beta L_j^2)^2}\left(\beta L_j \sin(\beta L_j) \sinh(\beta L_i) + \beta L_i \cos(\beta L_j) \cosh(\beta L_i)\right)$$

If $\beta L_i = \beta L_j$,

$$\int_0^1 z \sinh(\beta L_i . z) \cos(\beta L_i z)\, dz = \frac{1}{2\beta L_i}\left(\sin(\beta L_i) \sinh(\beta L_i) + \cos(\beta L_i) \cosh(\beta L_i)\right) - \frac{1}{2\beta L_i^2}\left(\sin(\beta L_i) \cosh(\beta L_i)\right)$$

$$(24)\ \int_0^1 z\cosh(\beta L_i z)\cos(\beta L_j z)\,dz = \frac{1}{\beta L_i^2+\beta L_j^2}\left(\beta L_j \sin(\beta L_j)\cosh(\beta L_i) + \beta L_i \cos(\beta L_j)\sinh(\beta L_i)\right)$$
$$- \frac{\beta L_j}{(\beta L_i^2+\beta L_j^2)^2}\left(\beta L_i \sin(\beta L_j)\sinh(\beta L_i) - \beta L_j \cos(\beta L_j)\cosh(\beta L_i) + \beta L_j\right)$$
$$- \frac{\beta L_i}{(\beta L_i^2+\beta L_j^2)^2}\left(\beta L_j \sin(\beta L_j)\sinh(\beta L_i) + \beta L_i \cos(\beta L_j)\cosh(\beta L_i) - \beta L_i\right).$$

If $\beta L_i = \beta L_j$,

$$\int_0^1 z\cosh(\beta L_i z)\cos(\beta L_i z)\,dz = \frac{1}{2\beta L_i}\left(\sin(\beta L_i)\cosh(\beta L_i) + \cos(\beta L_i)\sinh(\beta L_i)\right)$$
$$- \frac{1}{2\beta L_i^2}\left(\sin(\beta L_i)\sinh(\beta L_i)\right).$$

$$(25)\ \int_0^1 z\sin(\beta L_i z)\sinh(\beta L_j z)\,dz = \frac{1}{\beta L_i^2+\beta L_j^2}\left(\beta L_j \sin(\beta L_i)\cosh(\beta L_j) - \beta L_i \cos(\beta L_i)\sinh(\beta L_j)\right)$$
$$- \frac{\beta L_j}{(\beta L_i^2+\beta L_j^2)^2}\left(\beta L_j \sin(\beta L_i)\sinh(\beta L_j) - \beta L_i \cos(\beta L_i)\cosh(\beta L_j) + \beta L_i\right)$$
$$+ \frac{\beta L_i}{(\beta L_i^2+\beta L_j^2)^2}\left(\beta L_i \sin(\beta L_i)\sinh(\beta L_j) + \beta L_j \cos(\beta L_i)\cosh(\beta L_j) - \beta L_j\right).$$

If $\beta L_i = \beta L_j$, See expression 19 .

$$(26)\ \int_0^1 z\cos(\beta L_i z)\sinh(\beta L_j z)\,dz = \frac{1}{\beta L_i^2+\beta L_j^2}\left(\beta L_i \sin(\beta L_i)\sinh(\beta L_j) + \beta L_j \cos(\beta L_i)\cosh(\beta L_j) - \beta L_j\right)$$
$$- \frac{\beta L_i}{(\beta L_i^2+\beta L_j^2)^2}\left(\beta L_j \sin(\beta L_i)\cosh(\beta L_j) - \beta L_i \cos(\beta L_i)\sinh(\beta L_j)\right)$$
$$- \frac{\beta L_j}{(\beta L_i^2+\beta L_j^2)^2}\left(\beta L_i \sin(\beta L_i)\cosh(\beta L_j) + \beta L_j \cos(\beta L_i)\sinh(\beta L_j)\right).$$

If $\beta L_i = \beta L_j$, See expression 23 .

$$(27)\quad \int_0^1 z \sinh(\beta L_i z) \sinh(\beta L_j z)\, dz = -\frac{\sinh(\beta L_i - \beta L_j)}{2(\beta L_i - \beta L_j)} + \frac{\sinh(\beta L_i + \beta L_j)}{2(\beta L_i + \beta L_j)} - \frac{\cosh(\beta L_i + \beta L_j)}{2(\beta L_i + \beta L_j)^2} + \frac{\cosh(\beta L_i - \beta L_j)}{2(\beta L_i - \beta L_j)^2} + \frac{1}{2(\beta L_i + \beta L_j)^2} - \frac{1}{2(\beta L_i - \beta L_j)^2}$$

If $\beta L_i = \beta L_j$,

$$\int_0^1 z \sinh^2(\beta L_i z)\, dz = \frac{\sinh(2\beta L_i)}{4\beta L_i} - \frac{\cosh(2\beta L_i)}{8\beta L_i^2} - \frac{1}{4} - \frac{1}{8\beta L_i^2}$$

$$(28)\quad \int_0^1 z \cosh(\beta L_i z) \sinh(\beta L_j z)\, dz = \frac{\cosh(\beta L_i + \beta L_j)}{2(\beta L_i + \beta L_j)} + \frac{\cosh(\beta L_j - \beta L_i)}{2(\beta L_j - \beta L_i)} - \frac{\sinh(\beta L_i + \beta L_j)}{2(\beta L_i + \beta L_j)^2} - \frac{\sinh(\beta L_j - \beta L_i)}{2(\beta L_j - \beta L_i)^2}$$

If $\beta L_i = \beta L_j$,

$$\int_0^1 z \cosh(\beta L_i z) \sinh(\beta L_i z)\, dz = \frac{\cosh(2\beta L_i)}{4\beta L_i} - \frac{\sinh(2\beta L_i)}{8\beta L_i^2}$$

$$(29)\quad \int_0^1 z \sin(\beta L_i z) \cosh(\beta L_j z)\, dz = \frac{1}{\beta L_i^2 + \beta L_j^2}\left(\beta L_j \sin(\beta L_i)\sinh(\beta L_j) - \beta L_i \cos(\beta L_i)\cosh(\beta L_j) + \beta L_i\right) - \frac{\beta L_j}{(\beta L_i^2 + \beta L_j^2)^2}\left(\beta L_j \sin(\beta L_i)\cosh(\beta L_j) - \beta L_i \cos(\beta L_i)\sinh(\beta L_j)\right) + \frac{\beta L_i}{(\beta L_i^2 + \beta L_j^2)^2}\left(\beta L_i \sin(\beta L_i)\cosh(\beta L_j) + \beta L_j \cos(\beta L_i)\sinh(\beta L_j)\right)$$

If $\beta L_i = \beta L_j$, see expression 20 .

$$(30)\quad \int_0^1 z \cos(\beta L_i z) \cosh(\beta L_j z)\, dz = \frac{1}{\beta L_i^2 + \beta L_j^2}\left(\beta L_i \sin(\beta L_i)\cosh(\beta L_j) + \beta L_j \cos(\beta L_i)\sinh(\beta L_j)\right) - \frac{\beta L_i}{(\beta L_i^2 + \beta L_j^2)^2}\left(\beta L_j \sin(\beta L_i)\sinh(\beta L_j) - \beta L_i \cos(\beta L_i)\cosh(\beta L_j) + \beta L_i\right)$$

(30)_Cont'd

$$- \frac{\beta L_j}{(\beta L_i^2 + \beta L_j^2)^2} \left(\beta L_i \sin(\beta L_i) \sinh(\beta L_j) + \beta L_j \cos(\beta L_i) \cosh(\beta L_j) - \beta L_j \right)$$

If $\beta L_i = \beta L_j$, See expression 24 .

(31) $$\int^1 z \sinh(\beta L_i z) \cosh(\beta L_j z)\, dz = \frac{\cosh(\beta L_i + \beta L_j)}{2(\beta L_i + \beta L_j)} + \frac{\cosh(\beta L_i - \beta L_j)}{2(\beta L_i - \beta L_j)} - \frac{\sinh(\beta L_i + \beta L_j)}{2(\beta L_i + \beta L_j)^2} - \frac{\sinh(\beta L_i - \beta L_j)}{2(\beta L_i - \beta L_j)^2}$$

If $\beta L_i = \beta L_j$, See expression 28 .

(32) $$\int^1 z \cosh(\beta L_i z) \cosh(\beta L_j z)\, dz = \frac{\sinh(\beta L_i + \beta L_j)}{2(\beta L_i + \beta L_j)} + \frac{\sinh(\beta L_i - \beta L_j)}{2(\beta L_i - \beta L_j)} - \frac{\cosh(\beta L_i + \beta L_j)}{2(\beta L_i + \beta L_j)^2} - \frac{\cosh(\beta L_i - \beta L_j)}{2(\beta L_i - \beta L_j)^2} + \frac{1}{2(\beta L_i + \beta L_j)^2} + \frac{1}{2(\beta L_i - \beta L_j)^2}$$

If $\beta L_i = \beta L_j$,

$$\int^1 z \cosh^2(\beta L_i z)\, dz = \frac{\sinh(2\beta L_i)}{4\beta L_i} - \frac{\cosh(2\beta L_i)}{8\beta L_i^2} + \frac{1}{4} + \frac{1}{8\beta L_i^2}$$

2. Expressions for Modal Analysis

(1) $\int_0^1 \sin(\beta L_i z)\, dz = \frac{1-\cos(\beta L_i)}{\beta L_i}$

(2) $\int_0^1 \cos(\beta L_i z)\, dz = \frac{\sin(\beta L_i)}{\beta L_i}$

(3) $\int_0^1 \sinh(\beta L_i z)\, dz = \frac{\cosh(\beta L_i)-1}{\beta L_i}$

(4) $\int_0^1 \cosh(\beta L_i z)\, dz = \frac{\sinh(\beta L_i)}{\beta L_i}$

(5) $\int_0^1 z \sin(\beta L_i z)\, dz = \frac{\sin(\beta L_i)}{\beta L_i^2} - \frac{\cos(\beta L_i)}{\beta L_i}$

(6) $\int_0^1 z \cos(\beta L_i z)\, dz = \frac{\cos(\beta L_i)}{\beta L_i^2} + \frac{\sin(\beta L_i)}{\beta L_i} - \frac{1}{\beta L_i^2}$

(7) $\int_0^1 z \sinh(\beta L_i z)\, dz = \frac{\cosh(\beta L_i)}{\beta L_i} - \frac{\sinh(\beta L_i)}{\beta L_i^2}$

(8) $\int_0^1 z \cosh(\beta L_i z)\, dz = \frac{\sinh(\beta L_i)}{\beta L_i} - \frac{\cosh(\beta L_i)}{\beta L_i^2} + \frac{1}{\beta L_i^2}$

APPENDIX VI

RESULTS OF TESTS FOR CONVERGENCE

The following figures show the results obtained when the number of terms, n, used to compute dynamic properties and seismic response parameters was varied over the range $2 \leq n \leq 6$ for the case of flexural beams. For the shear beams convergence was less of a problem; hence, the data for this case is not presented here.

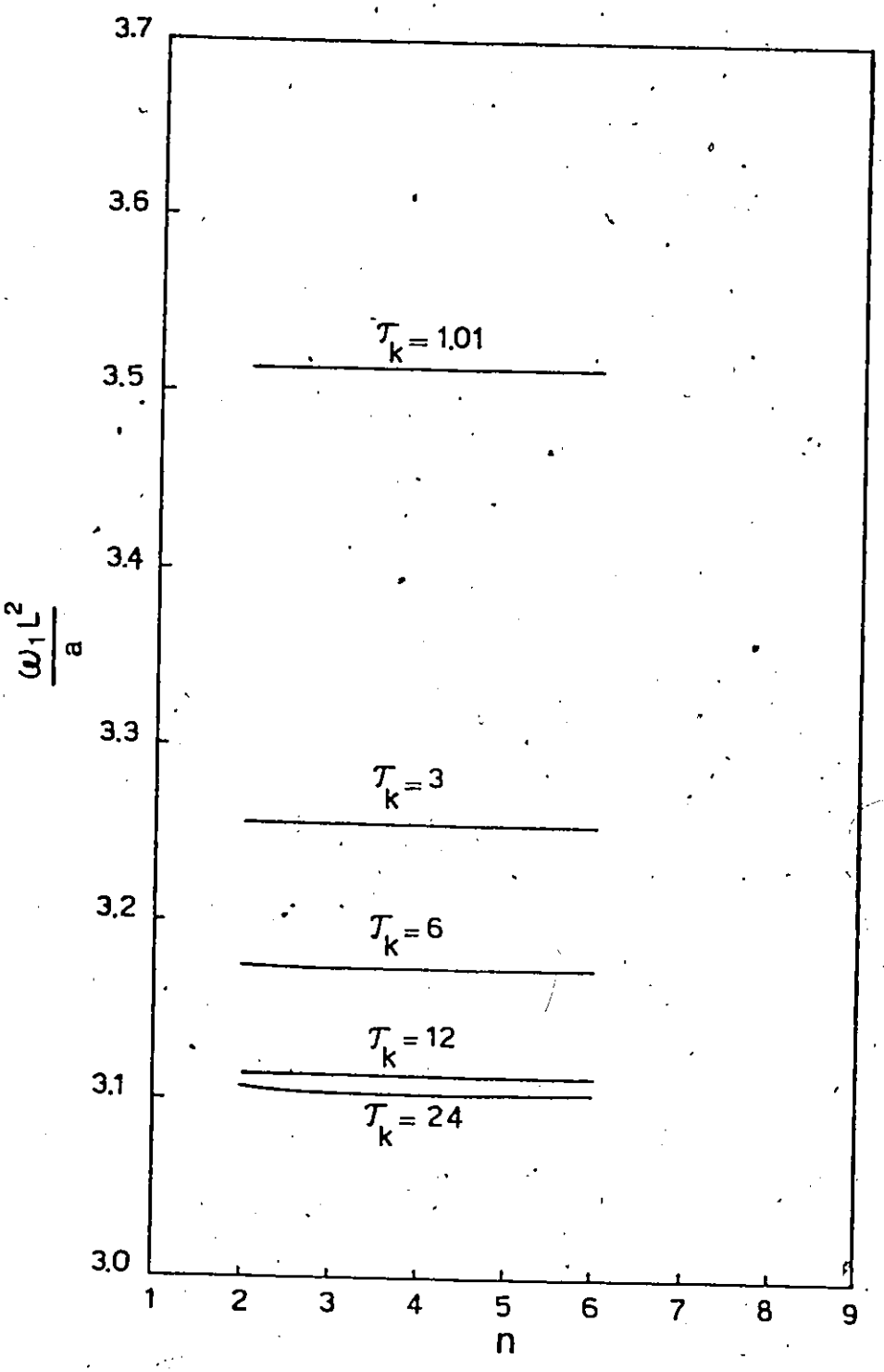

FIG. V1-1 RATE OF CONVERGENCE OF FUNDAMENTAL MODE FREQUENCY

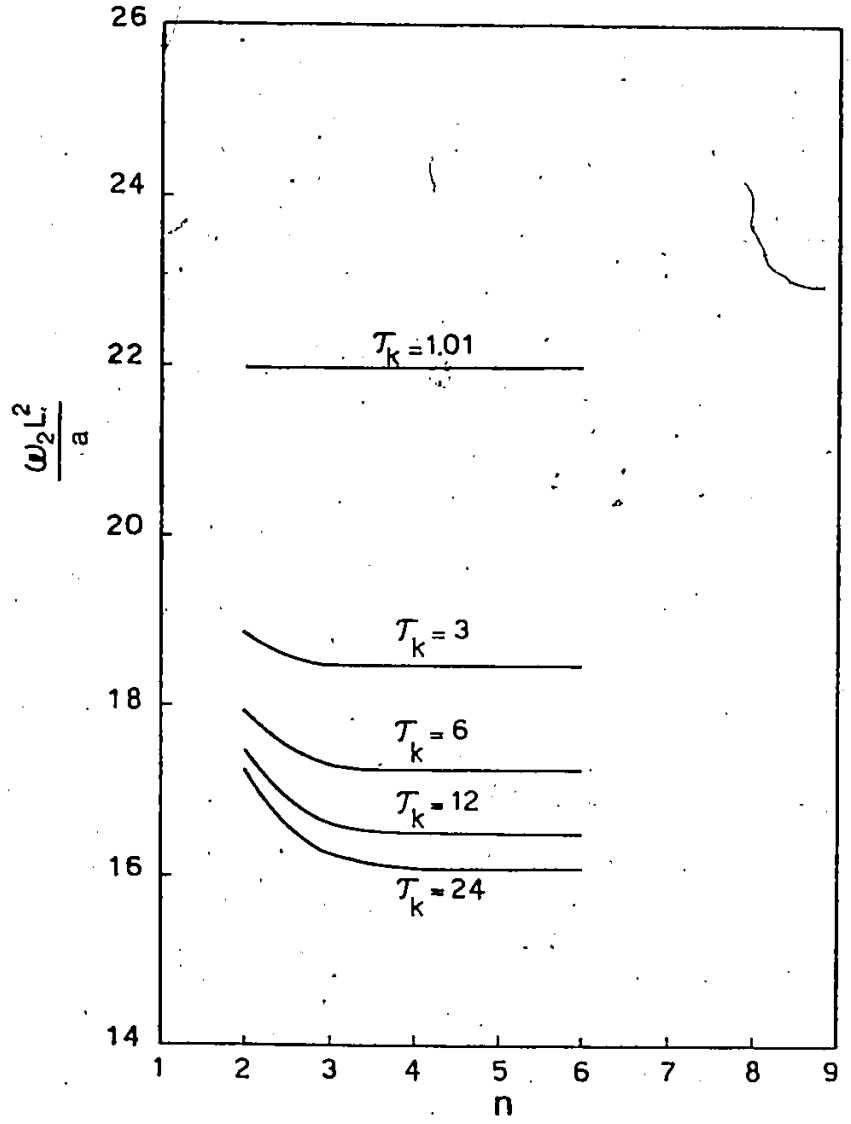

FIG. V1-2 RATE OF CONVERGENCE OF SECOND MODAL FREQUENCY

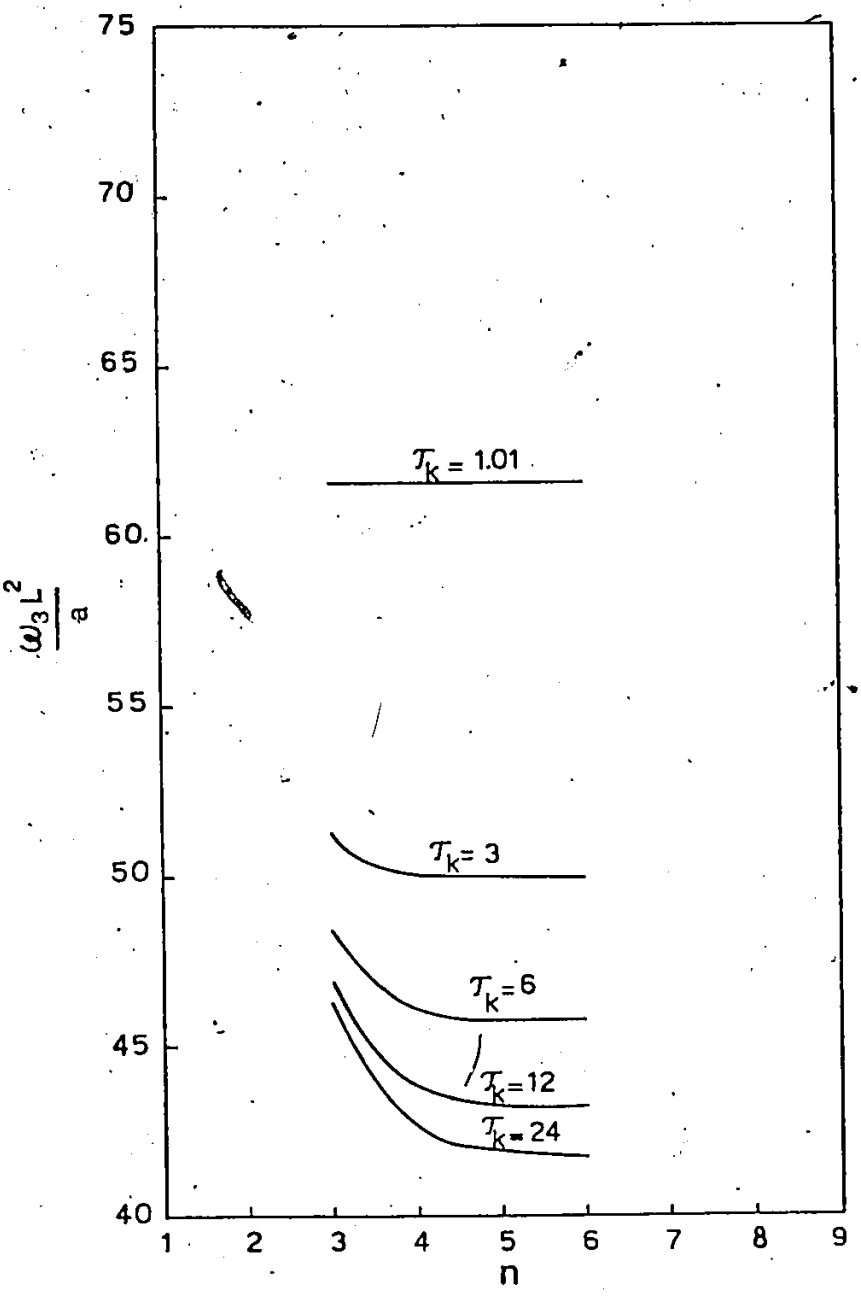

FIG. V1-3 RATE OF CONVERGENCE OF THIRD MODAL FREQUENCY

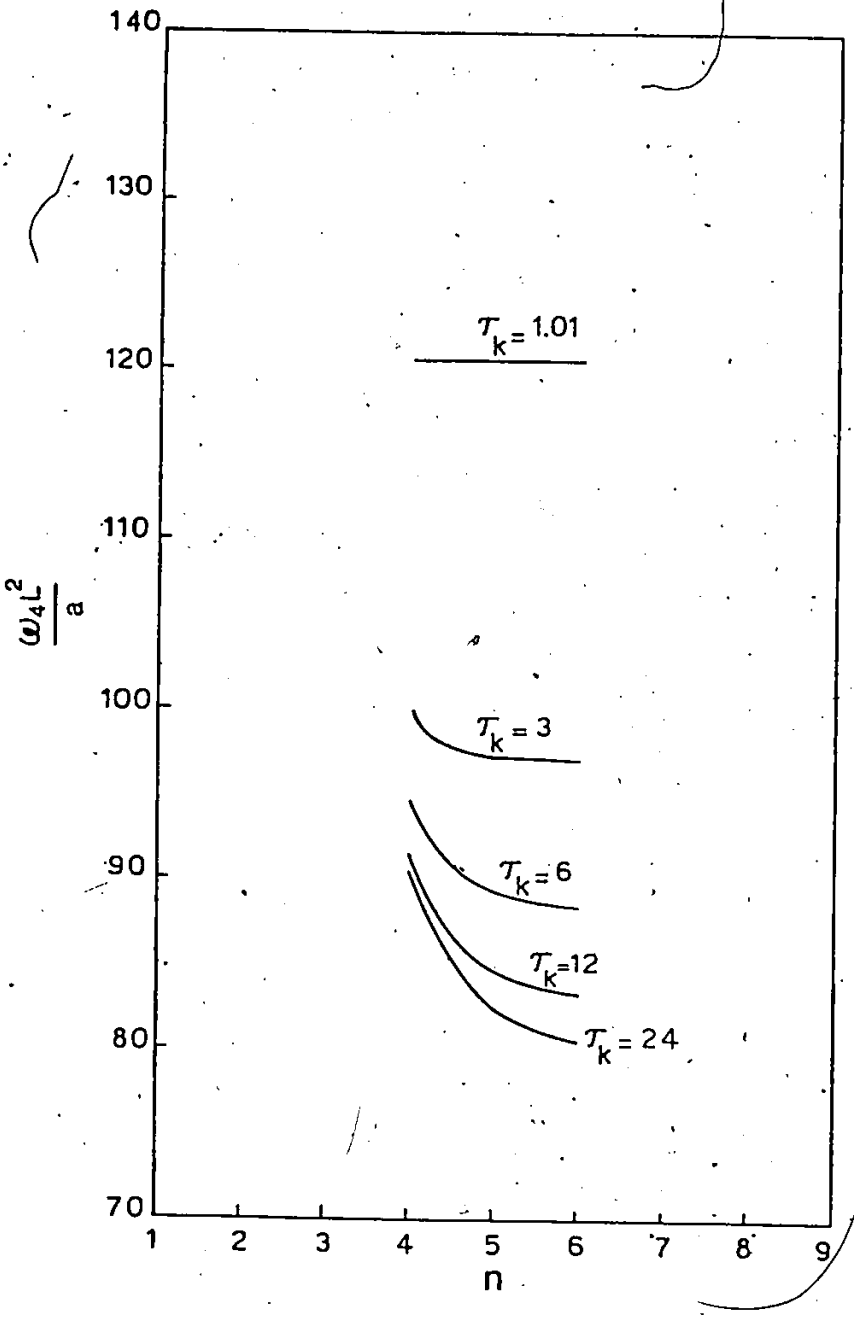

FIG. V1-4 RATE OF CONVERGENCE OF FOURTH MODAL FREQUENCY

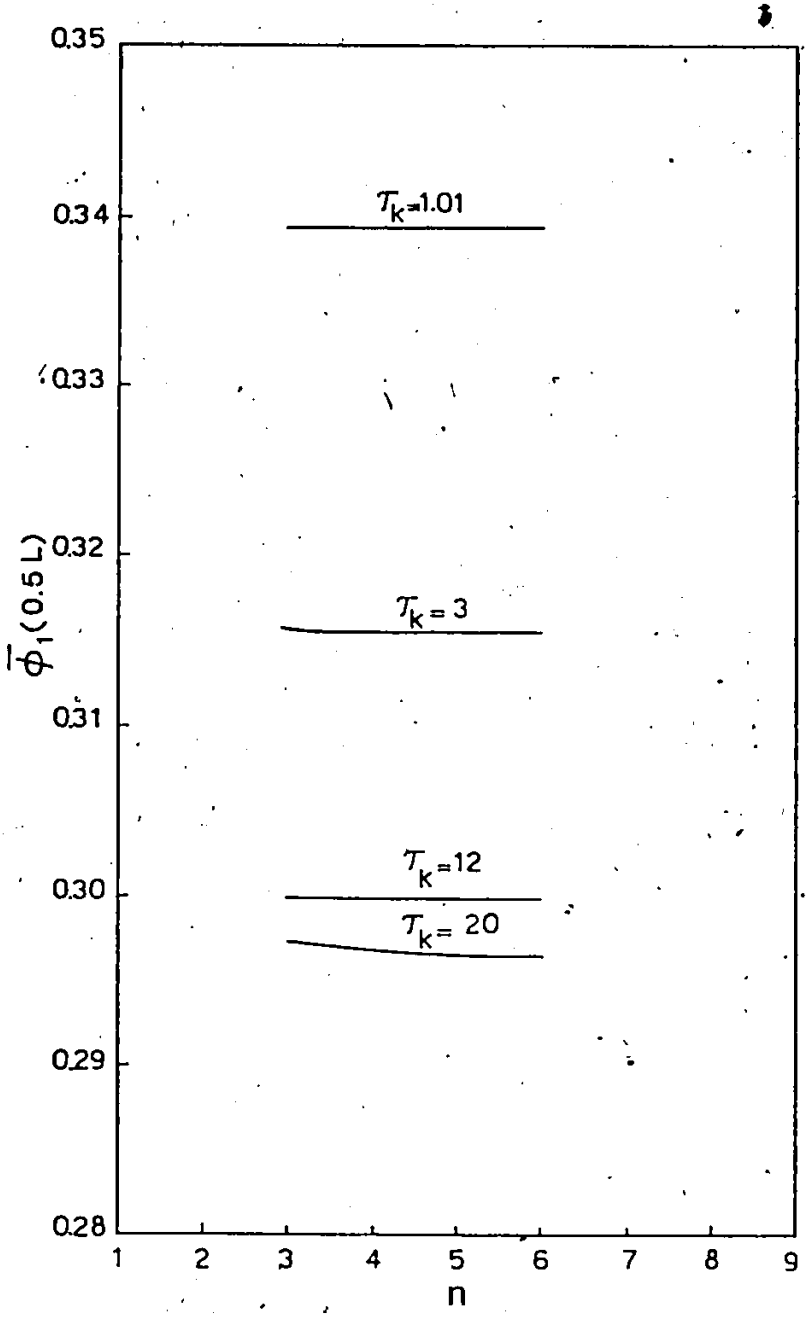

FIG. V1-5 RATE OF CONVERGENCE OF FUNDAMENTAL MODE SHAPE

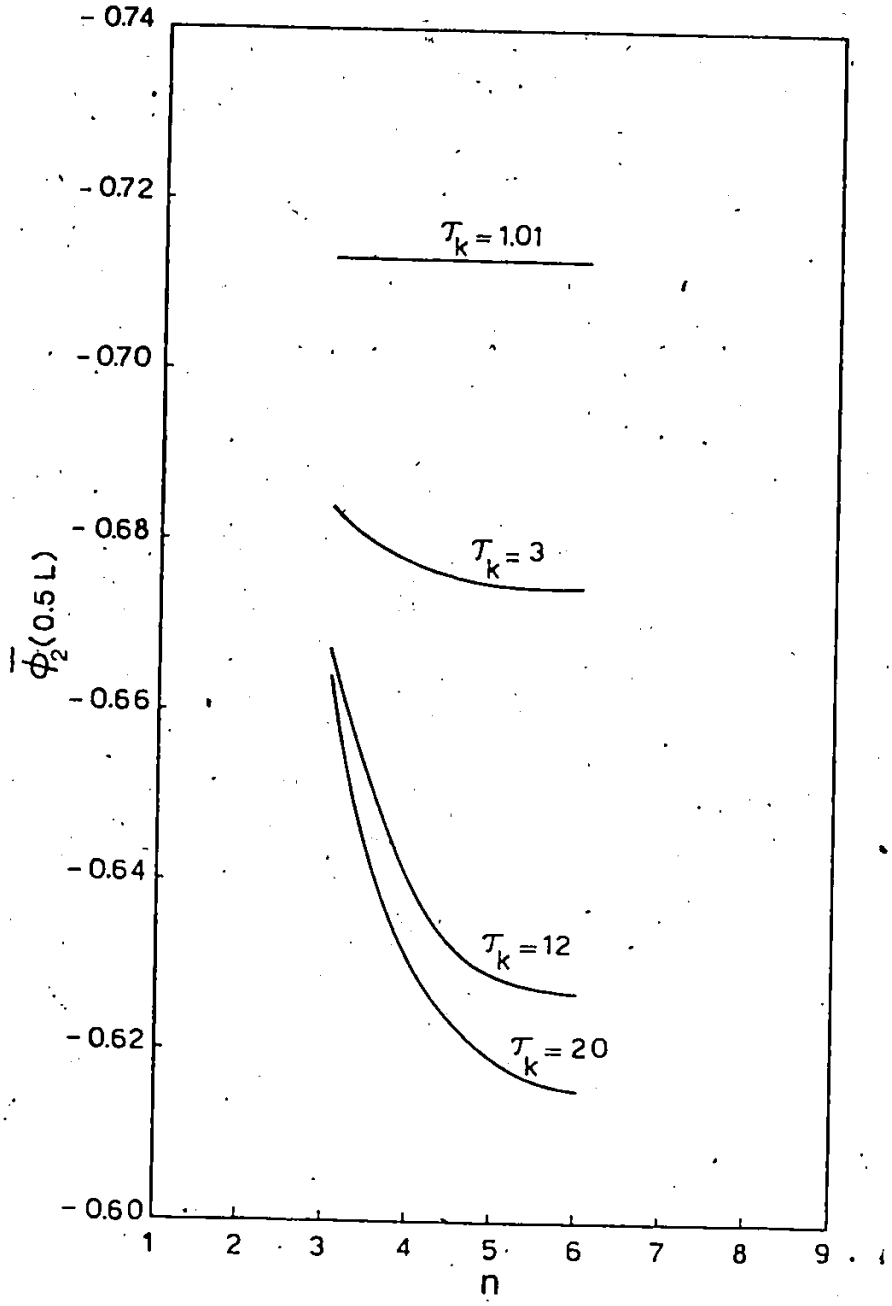

FIG. V1-6 RATE OF CONVERGENCE OF SECOND MODE SHAPE

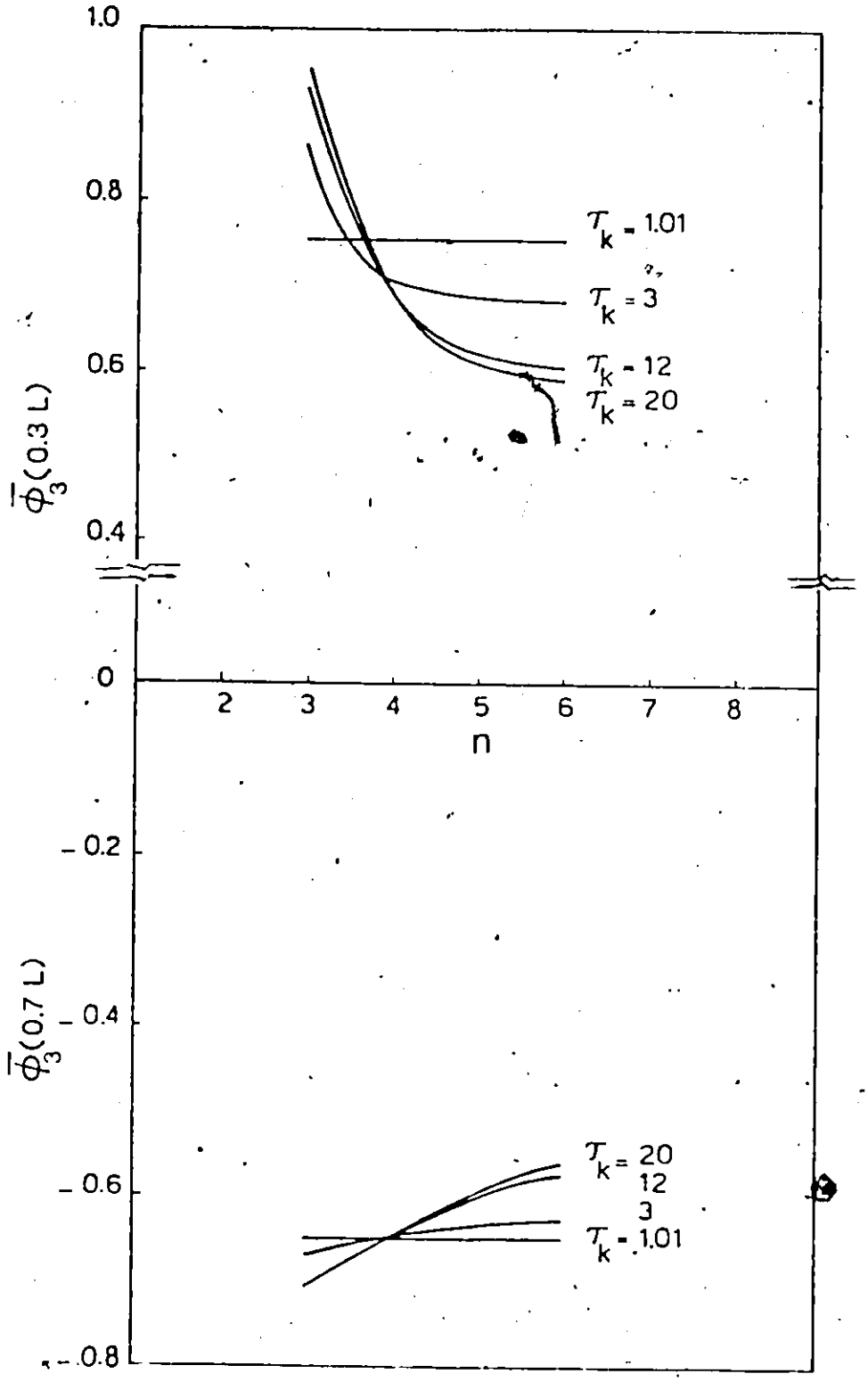

FIG. V1-7 RATE OF CONVERGENCE OF THIRD MODE SHAPE

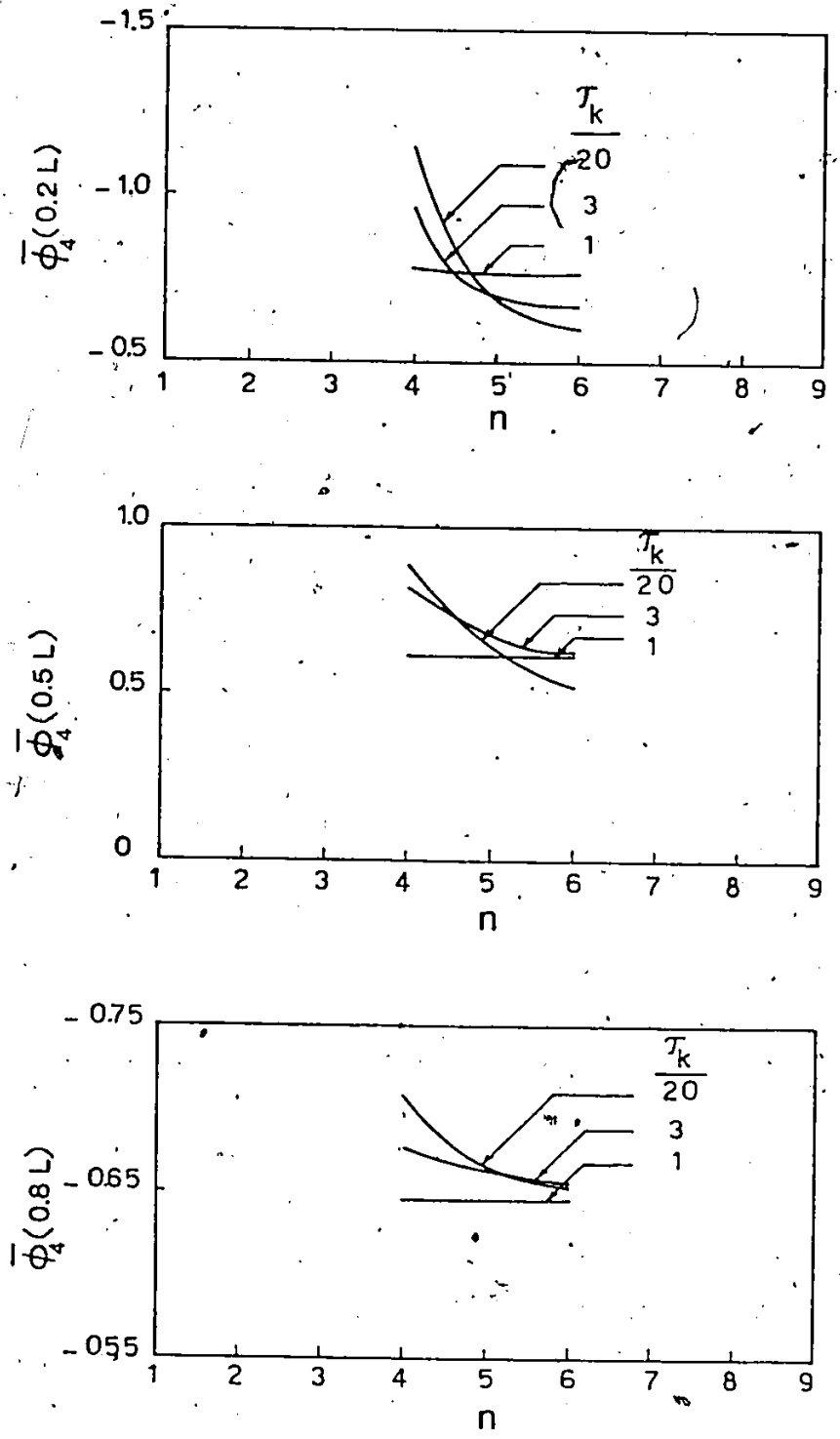

FIG. V1-8. RATE OF CONVERGENCE OF FOURTH MODE SHAPE

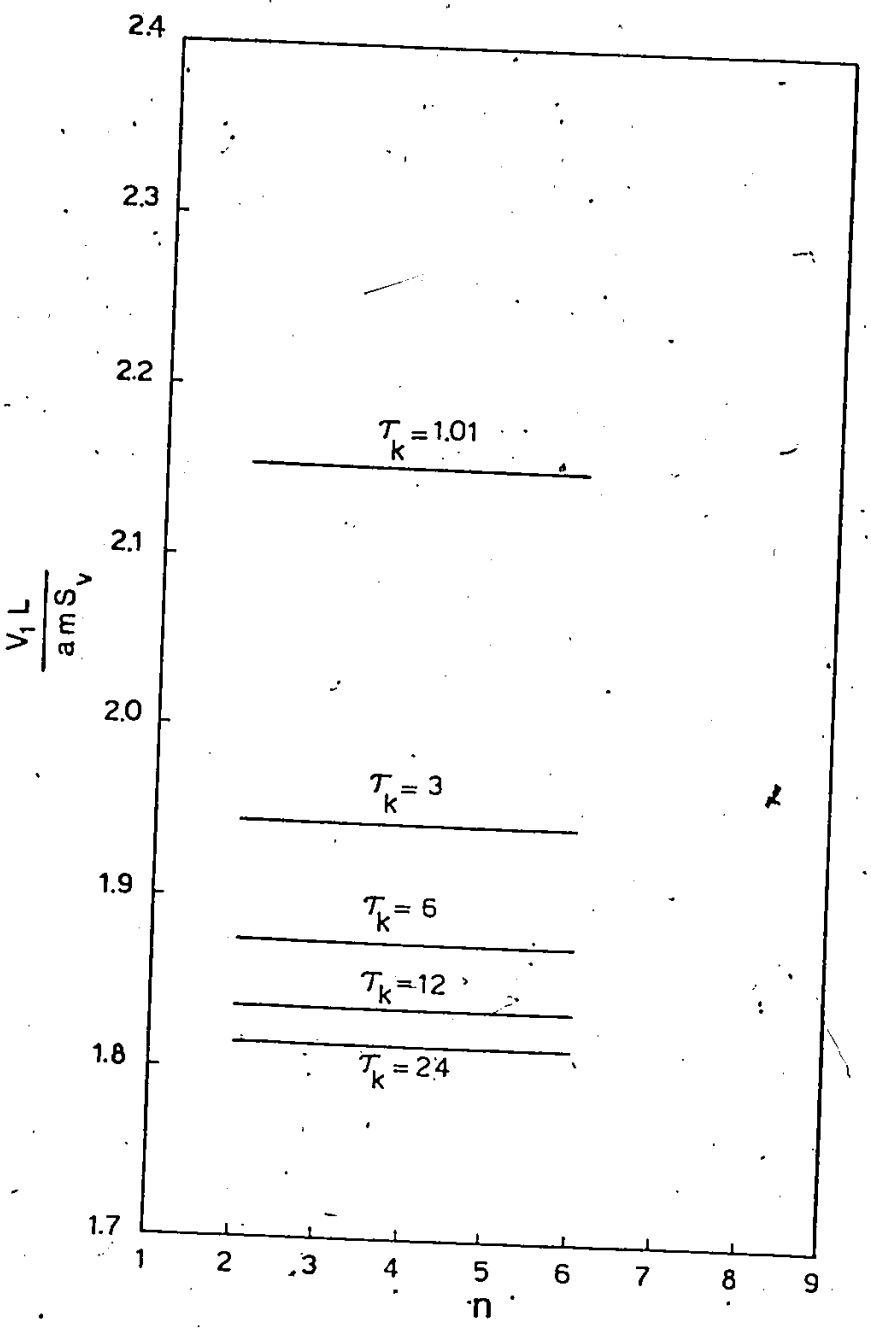

FIG. V1-9 RATE OF CONVERGENCE OF FIRST MODAL BASE SHEAR

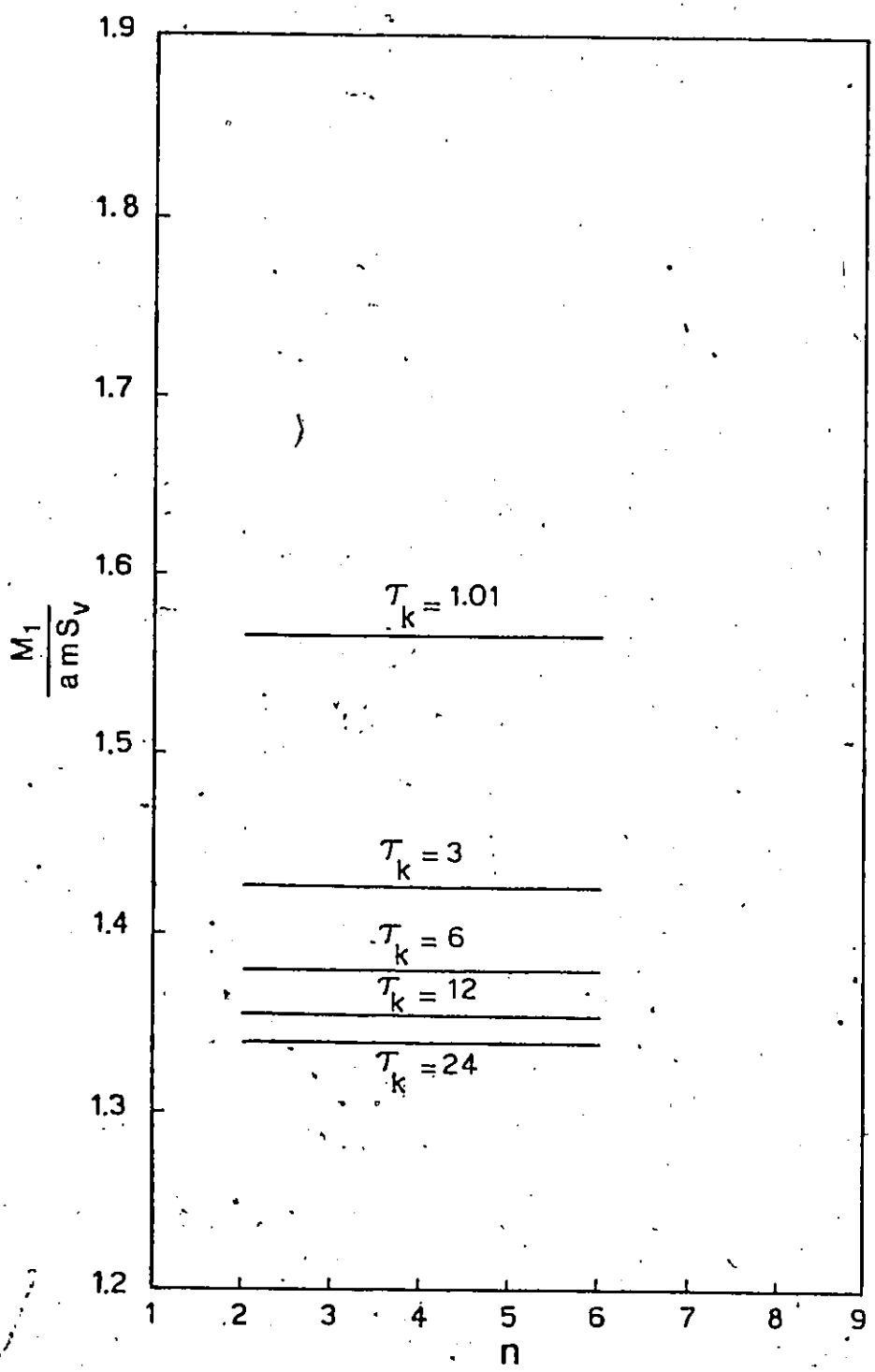

FIG. V1-10 RATE OF CONVERGENCE OF FIRST MODAL OVERTURNING MOMENT

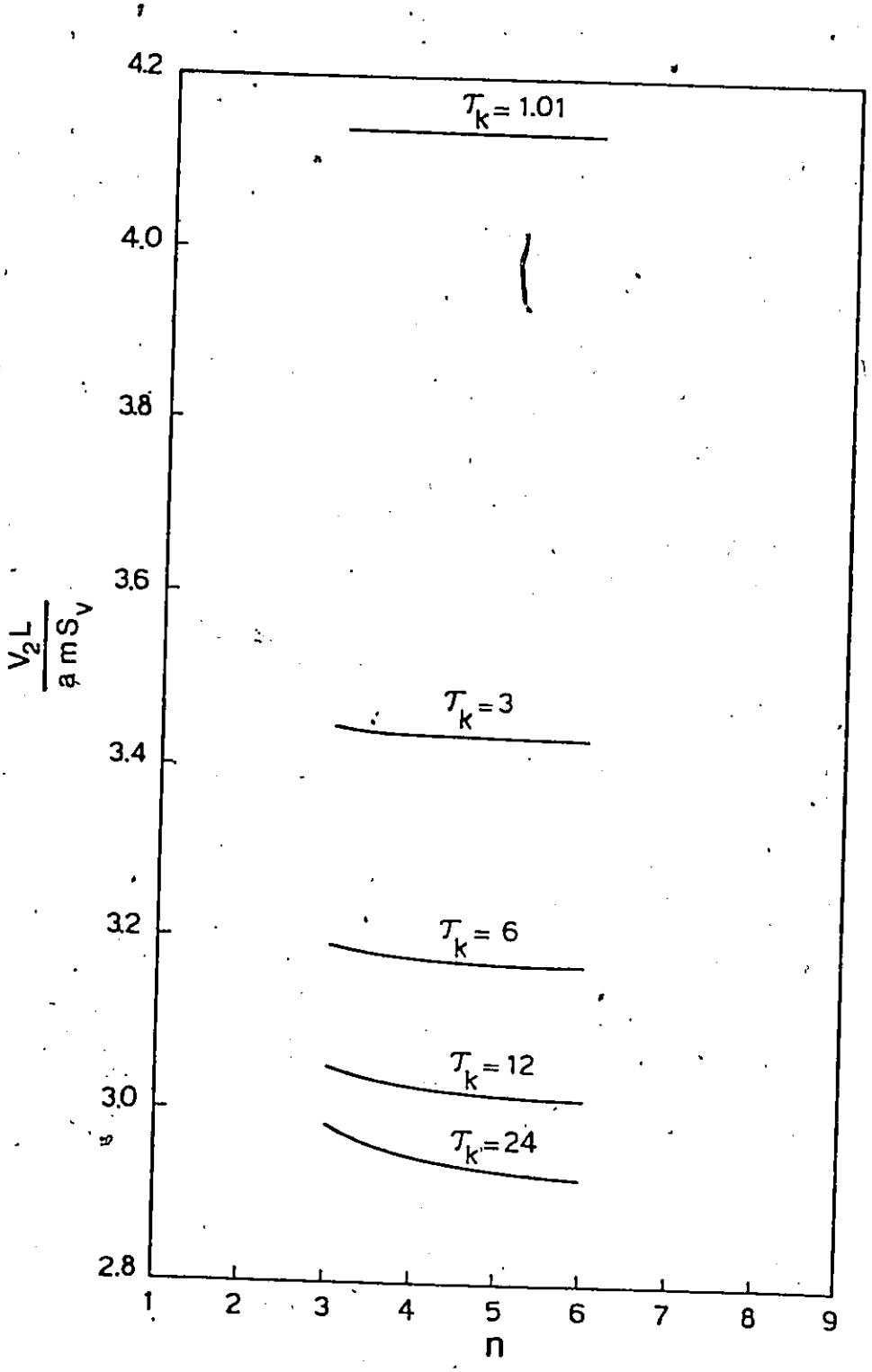

FIG. V1-11 RATE OF CONVERGENCE OF SECOND MODAL BASE SHEAR

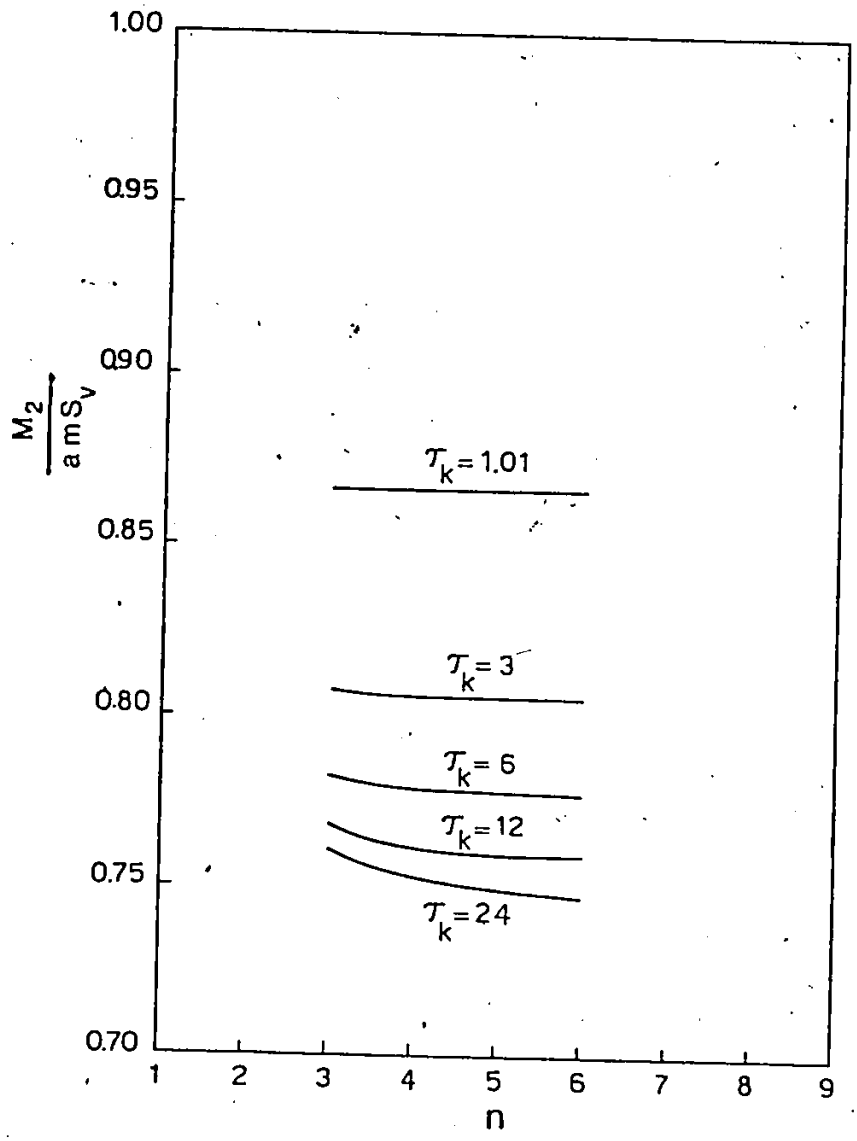

FIG. V1-12 RATE OF CONVERGENCE OF SECOND MODAL OVERTURNING MOMENT

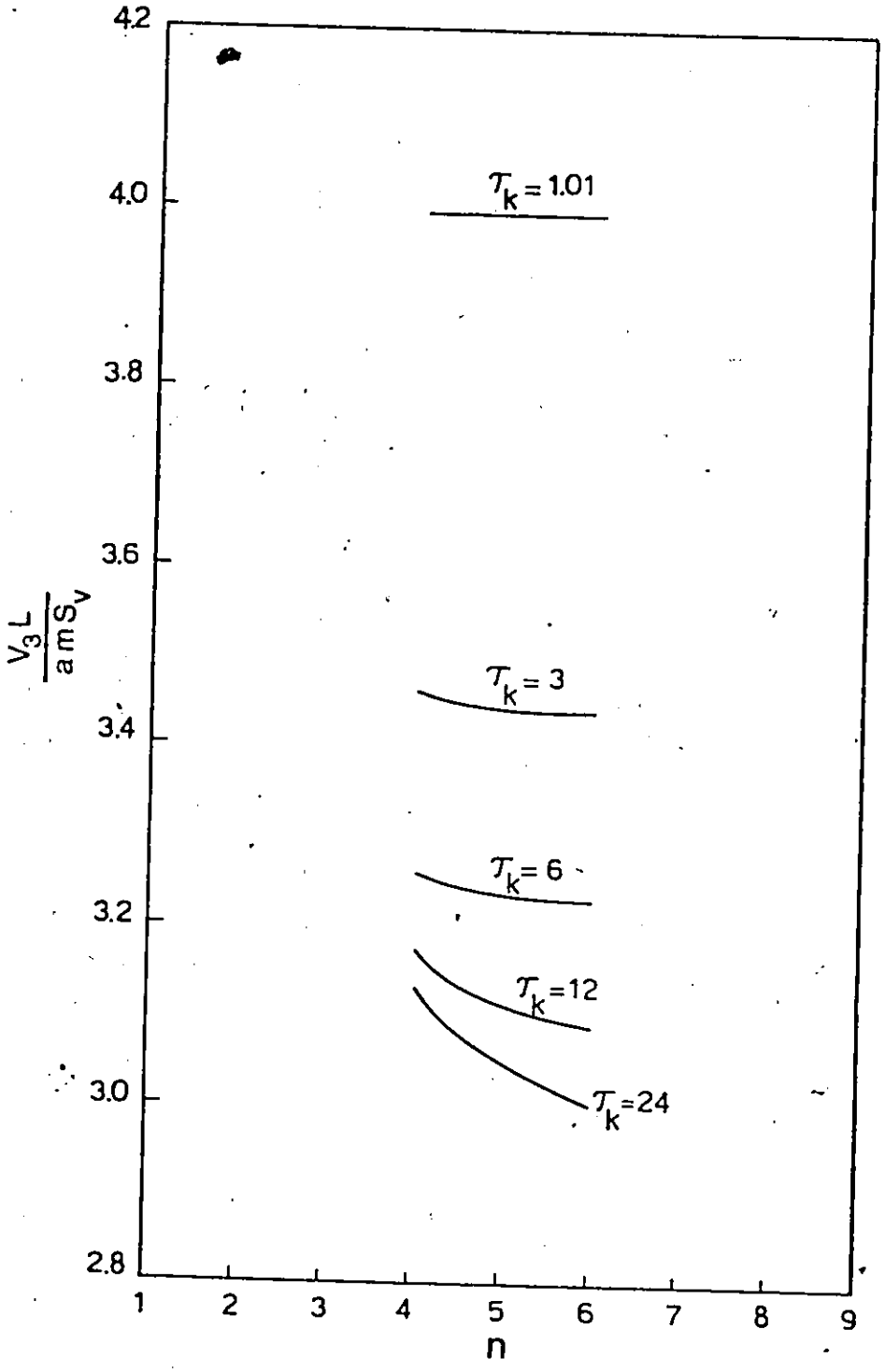

FIG. V1-13 RATE OF CONVERGENCE OF THIRD MODAL BASE SHEAR

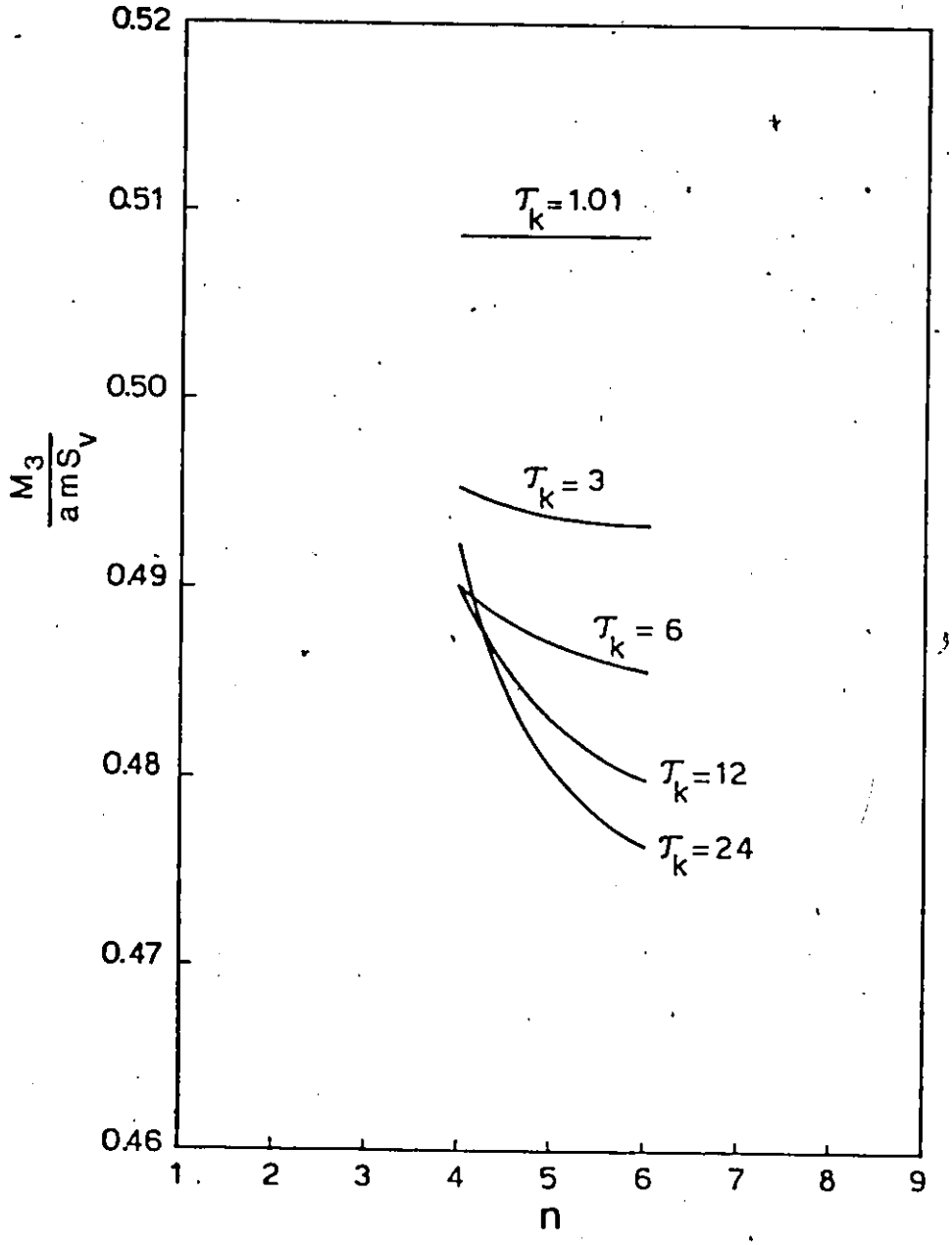

FIG. V1-14 RATE OF CONVERGENCE OF THIRD MODAL OVERTURNING MOMENT

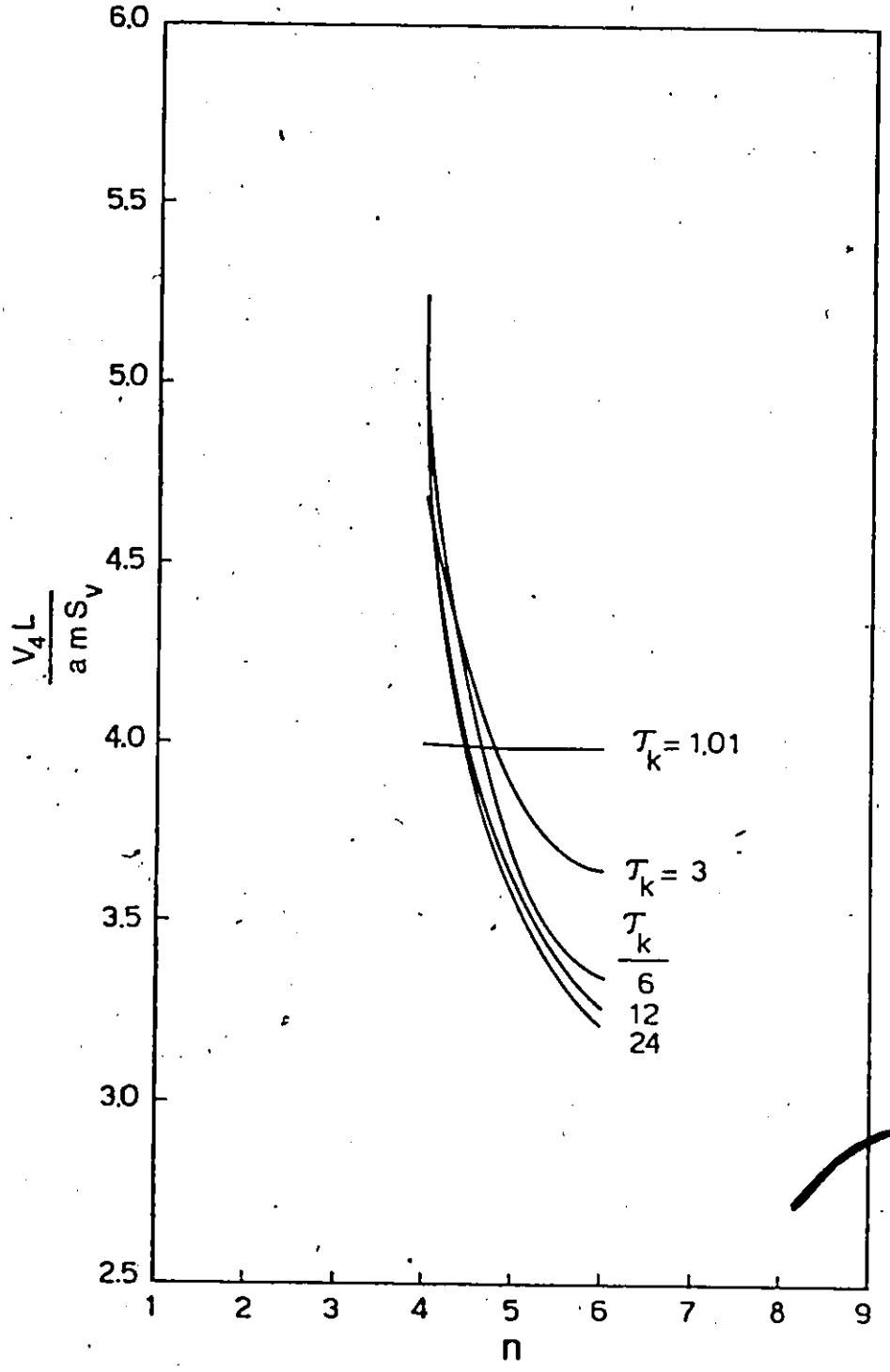

FIG. V1-15 RATE OF CONVERGENCE OF FOURTH MODAL BASE SHEAR

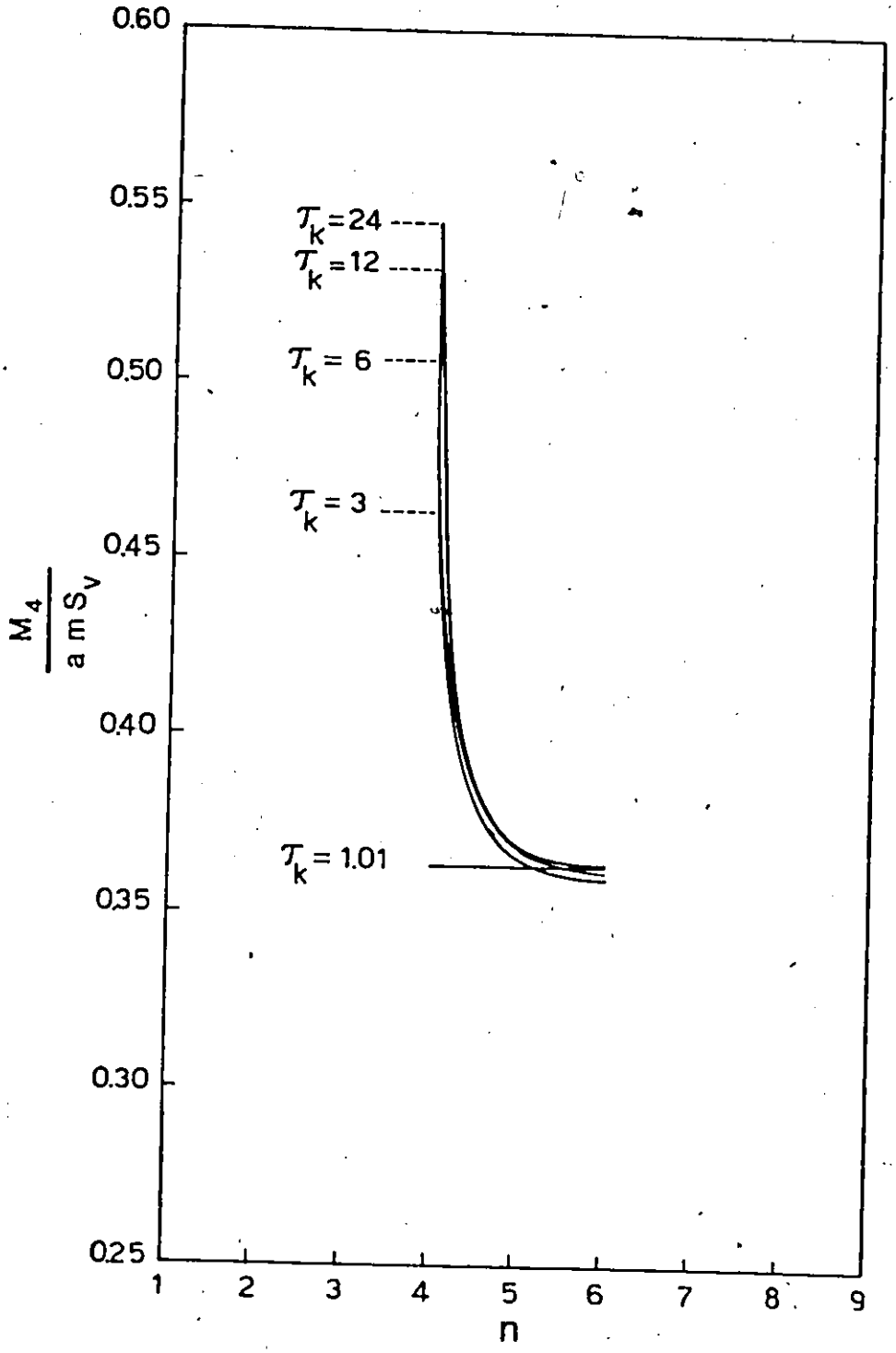

FIG. V1-16 RATE OF CONVERGENCE OF FOURTH MODAL OVERTURNING MOMENT